126p

GEMP-190f
(INFORMAL)

FACILITY FORM 602

N64-29789 (ACCESSION NUMBER)
(THRU)
126 (PAGES)
1 (CODE)
CR-52956 (NASA CR OR TMX OR AD NUMBER)
27 (CATEGORY)

Nuclear Materials & Propulsion Operation

INTRODUCTION TO NUCLEAR PROPULSION

Lectures 9 and 10 - REACTOR THERMAL DESIGN

C. W. Moon

[redacted]

OTS PRICE

XEROX $ 10.10 ph
MICROFILM $ ________

FLIGHT PROPULSION LABORATORY DEPARTMENT
GENERAL ELECTRIC

SQT-10563 f

GEMP-190f
(INFORMAL)

INTRODUCTION TO NUCLEAR PROPULSION

Lectures 9 and 10 - REACTOR THERMAL DESIGN

C. W. Moon refer

March 26, 27 and 28, 1963

Prepared for the George C. Marshall
Space Flight Center of the National
Aeronautics and Space Administration

Contract No. NAS8-5215

[redacted]

CONTENTS

CONTENTS (Cont.)

1. 0 INTRODUCTION TO REACTOR THERMAL DESIGN PROBLEMS

1. 1 THERMAL DESIGN OBJECTIVES

Nuclear reactors were described in the first lecture, and in subsequent lectures reactor physics and system design considerations were presented. Reactor thermal design involves the translation of system imposed flow, pressure and temperature constants, together with predicted power distribution characteristics, into requirements for the mechanical configuration of the reactor, and corresponding predictions of temperatures within the reactor. The specifications resulting from the thermal design include number, size, and location of coolant channels. In more detail they provide relationships between thermal and mechanical design parameters, e. g., temperatures versus fabrication tolerances, such that subsequent iterations make it possible to fix the final design configuration. Although we think of a sequence of system design, nuclear design, thermal design, and mechanical design, these are not mutually exclusive. To some extent the design must include iterative use of the above sequence. With experience and recognition of relative importance of the several design parameters the number of iterations is reduced.

Thermal design involves well established principles of fluid dynamics and heat transfer to arrive at specifications for heat transfer surface and flow channel configurations. A primary difference between nuclear and chemical systems is that the source of heat is distributed with solid materials, specifically the fuel elements and other components and structure. Distributed heat sources in solids also result from electrical resistive heating. An important consequence of the internal heat generation is that the materials may operate at temperatures above that of the hottest region of the working fluid whereas this does not occur in "internal combustion" systems. Nevertheless, for engineering purposes the basic heat transfer processes in reactors do not differ from those in other systems.

1. 2 INPUT FROM SYSTEMS DESIGN

To a first approximation, system design can view the reactor as a black box into which a specified fluid enters at a given rate, pressure, and temperature and from which it exits at a given elevated temperature and reduced pressure. The primary exception is that system weight is related to the size and weight of the black box, or reactor. That size and weight in turn is in part dependent upon the results of thermal design, primarily the coolant volume. Hence, system design will utilize relationships between coolant volume and reactor imposed conditions subject to later refinement.

To aid in the identification of other specifications and restraints that influence reactor thermal design we can review some configurations presented in Lecture 1. In the HTRE-3 reactor shield assembly, Figure 1. 1, the shield is liquid cooled and basically can be treated independently of the reactor thermal design problem. However, the end shields are pierced by annular ducts with relatively sharp turns and shallow plenums between reactor and end shields. Hence, radial pressure gradients across either end of the reactor may exist, with the result that flow maldistribution among the reactor tubes may be induced. Further flow maldistributions may persist at the reactor because flow is introduced at the upstream entrance to the annulus from two ducts instead of uniformly for all angular positions. Penetration of control rods through the front plenum potentially may cause further flow maldistribution in the reactor. With water cooled shields heat is transferred from the higher temperature air to the water across the separating wall with the result that a high temperature insulation requirement is imposed on the duct walls, particularly in the rear shield.

Number of sets of turbomachinery, or rocket engine nozzles, per reactor can influence the reactor flow distribution. For example, the XMA-1 power plant, Figure 1. 2, utilized two turbomachinery sets for one reactor with the result that shield ducts had to be designed such that the flow changed from two annular cross sections to a nearly uniform flow into the reactor. In the XNJ140E, Figure 1. 3, there is one turbomachinery set per reactor but with close coupling. Compressor induced swirl may persist to the reactor face if the front shield ducts are annular. In both of these configurations by-pass flow around the reactor core may be imposed by overall system design considerations. This flow might be used to cool shielding, structure, and turbomachinery components to temperatures appreciably lower than the reactor core. The result is that the reactor may have to heat the gas to a higher temperature than that entering the turbine if, as in the case of ANP systems, it is advantageous to reintroduce the gas upstream of the turbine. A similar introduction of cooler gases upstream of a rocket nozzle may also be deemed desirable or necessary.

1. 3 INPUT FROM NUCLEAR DESIGN

The thermal designer has to be concerned with the distribution of heat sources within the reactor shield assembly. Within the active core or fuel elements the heating is largely due to the fission process with a small fraction due to gamma and neutron absorption and scattering in nonfission reactions. A typical reactor configuration is the D141A-1, Figures 1. 4

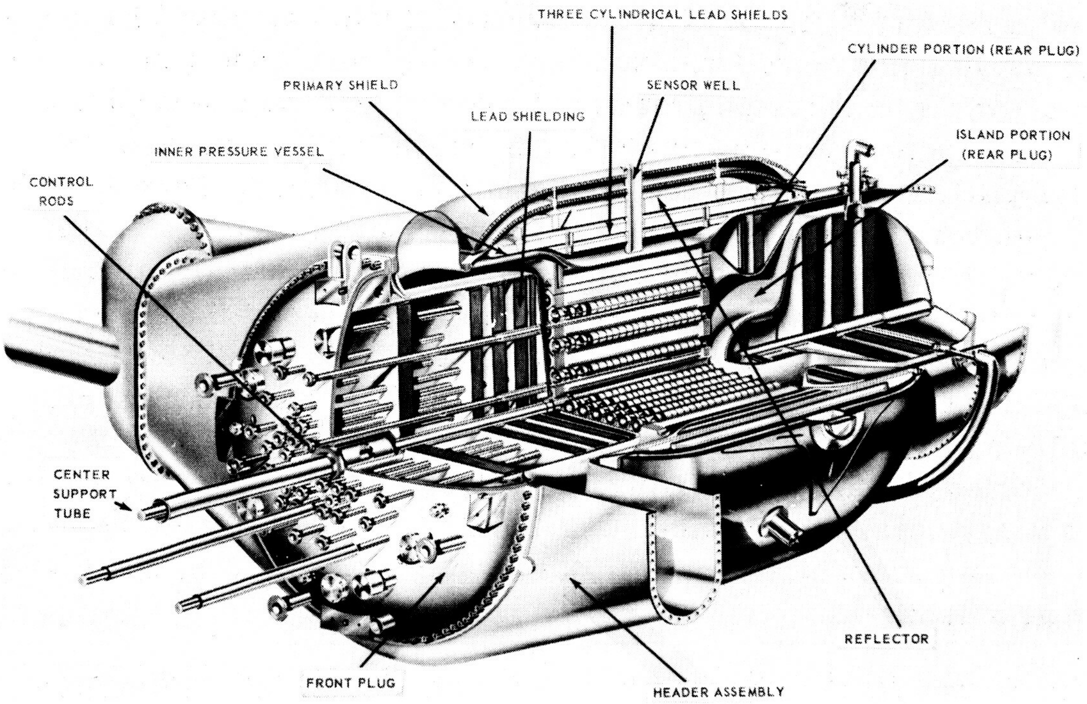

Fig. 1.1—HTRE-3 reactor-shield assembly

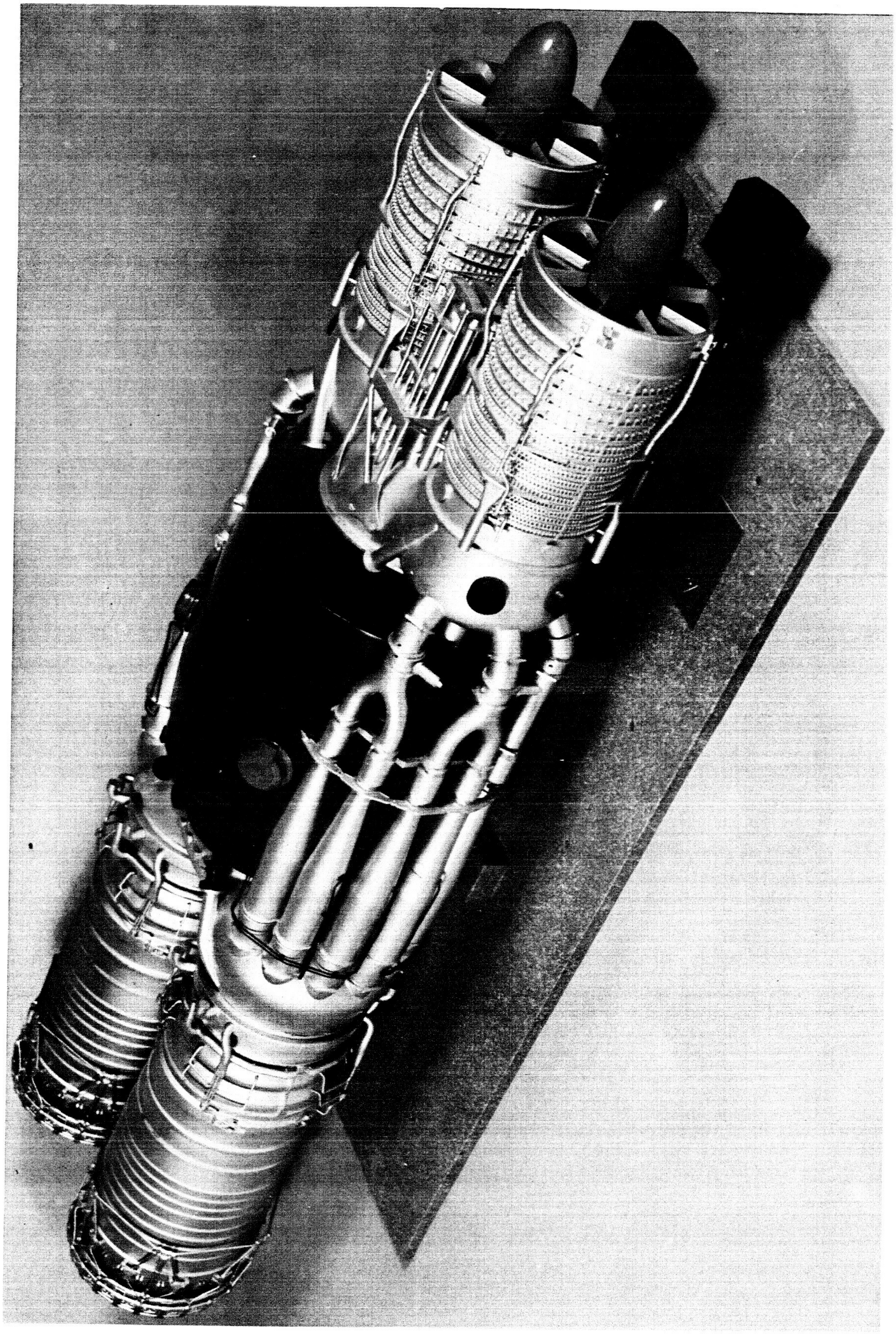

Fig. 1.2—Model of XMA-1 power plant (U-39336B)

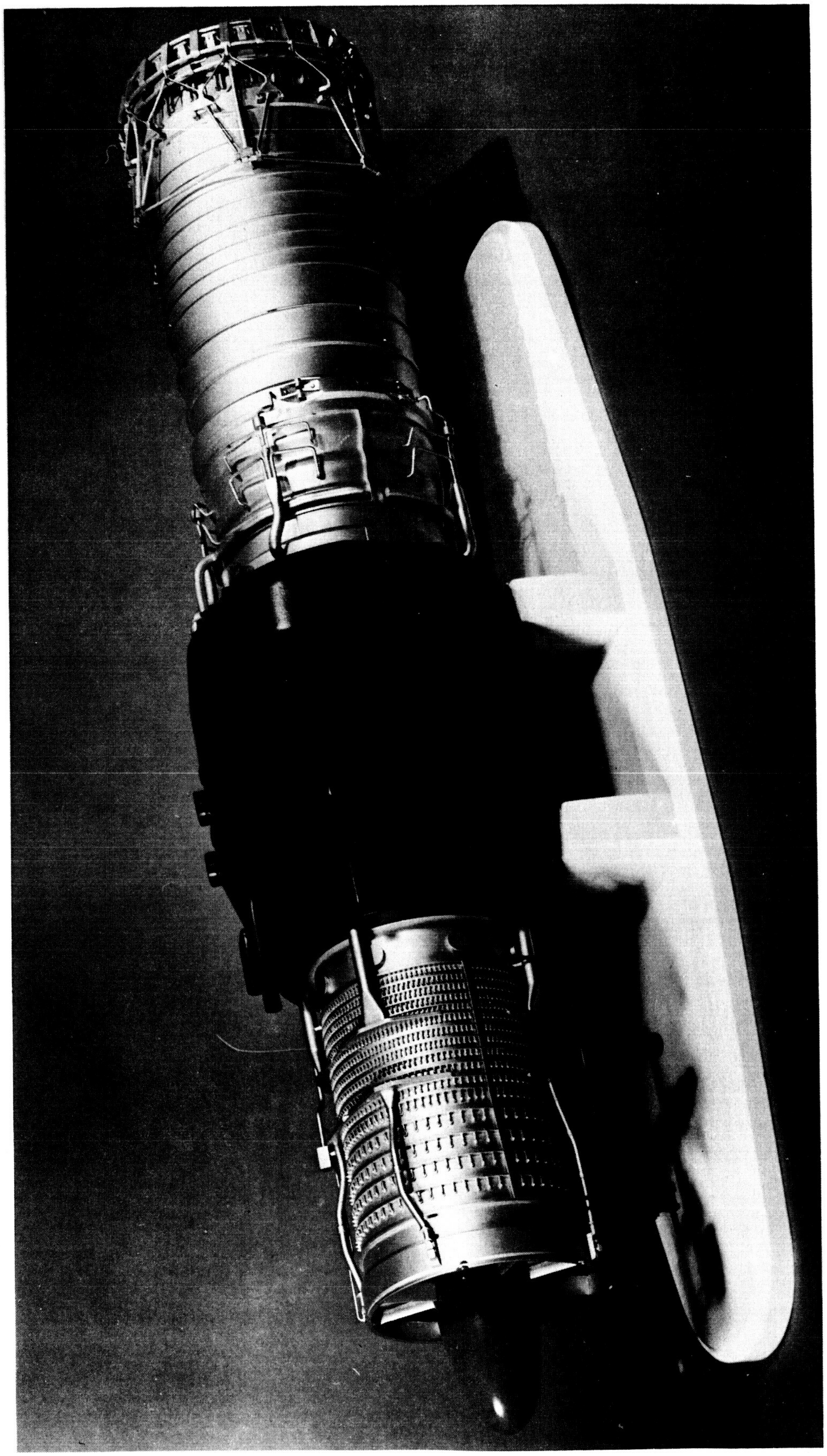

Fig. 1.3 – Model of XNJ140E nuclear turbojet engine

and 1. 5, wherein the reactor is a right cylinder surrounded by an annular reflector region. In such a system the power distribution tends to peak at an axial fractional distance of 0. 5 and to decrease symmetrically with distance from the midplane. A cosine distribution about the midplane is often used to represent the power distribution. Equally sized reflectors at either end may cause the power to "tip-up" at either end. Non-equal reflectors can cause a shift of power toward the more effective reflector.

Radially the power also decreases with radial distance. Use of a radial reflector can be used to reduce the reactor size or fuel requirements but in doing so the radial power is elevated adjacent to the reflector. An objective of the thermal design is the achievement of nearly radially uniform temperatures. This can be approached by radially varying hole sizes and spacing, i. e., the ratio of fueled volume to coolant volume, or by radially varying the fuel concentration. In reactors like the D141A-1, Figure 1. 4, both approaches were considered. However, variations cannot be continuous, but only in increments of a tube width. A power distribution resulting from radial variation of hole size is shown in Figure 1. 6. Typically, in this type of ANP reactor unbalanced end reflectors were used. Varying amounts of control rod insertion required over the lifetime of the reactor result in a variation of longitudinal power distribution as shown in Figure 1. 7.

More complex effects of control rod insertion on power distribution result if the control elements are placed in the radial reflector instead of within the active core. As with control rods in the active core, the longitudinal power distribution changes with amount of insertion. But the radial power distribution also changes as indicated in Figure 1. 8. In this particular example radial control of fuel element temperatures was by variation of fuel concentration while holding hole diameters and spacings constant. Accompanying changes in longitudinal power distribution are indicated in Figures 1. 9 to 1. 11. It is to be noted that because the large change in radial power near the reflector is localized, a power swing of about 15 percent, it is possible to limit the ratio of maximum to average power to about 1. 05.

Although the amount of heat in non-fueled components is relatively small the amount and distribution may need to be known quite accurately. Reasons are that those components may be thicker-walled and, because of lower temperatures, more coolant per unit of heat is required.

Finally, the distribution of heat after shutdown, i. e., afterheat, will need to be known because inherent changes are such that significant influence on the thermal design and on system provision for aftercooling may result.

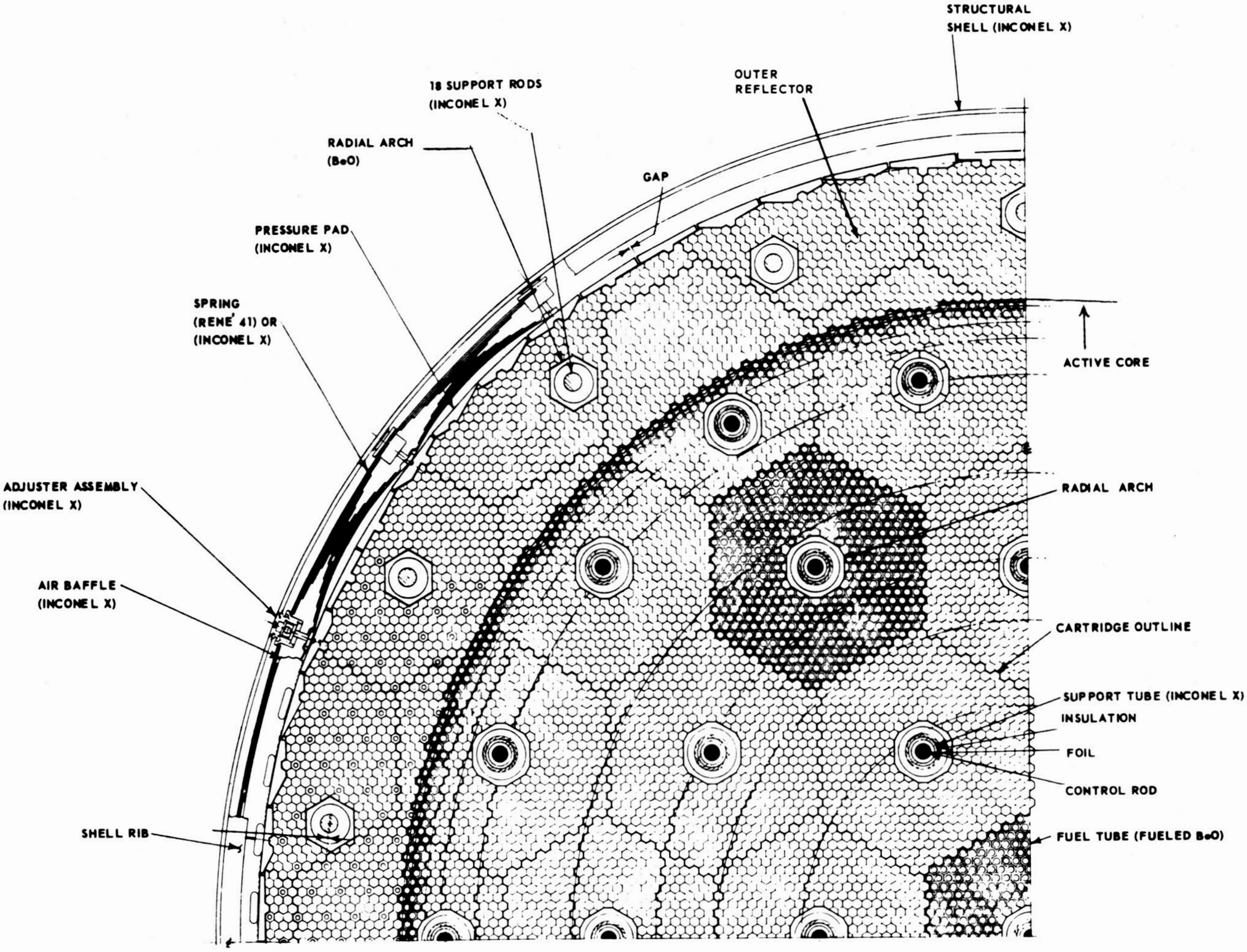

Fig. 1.4 – D141A-1 reactor

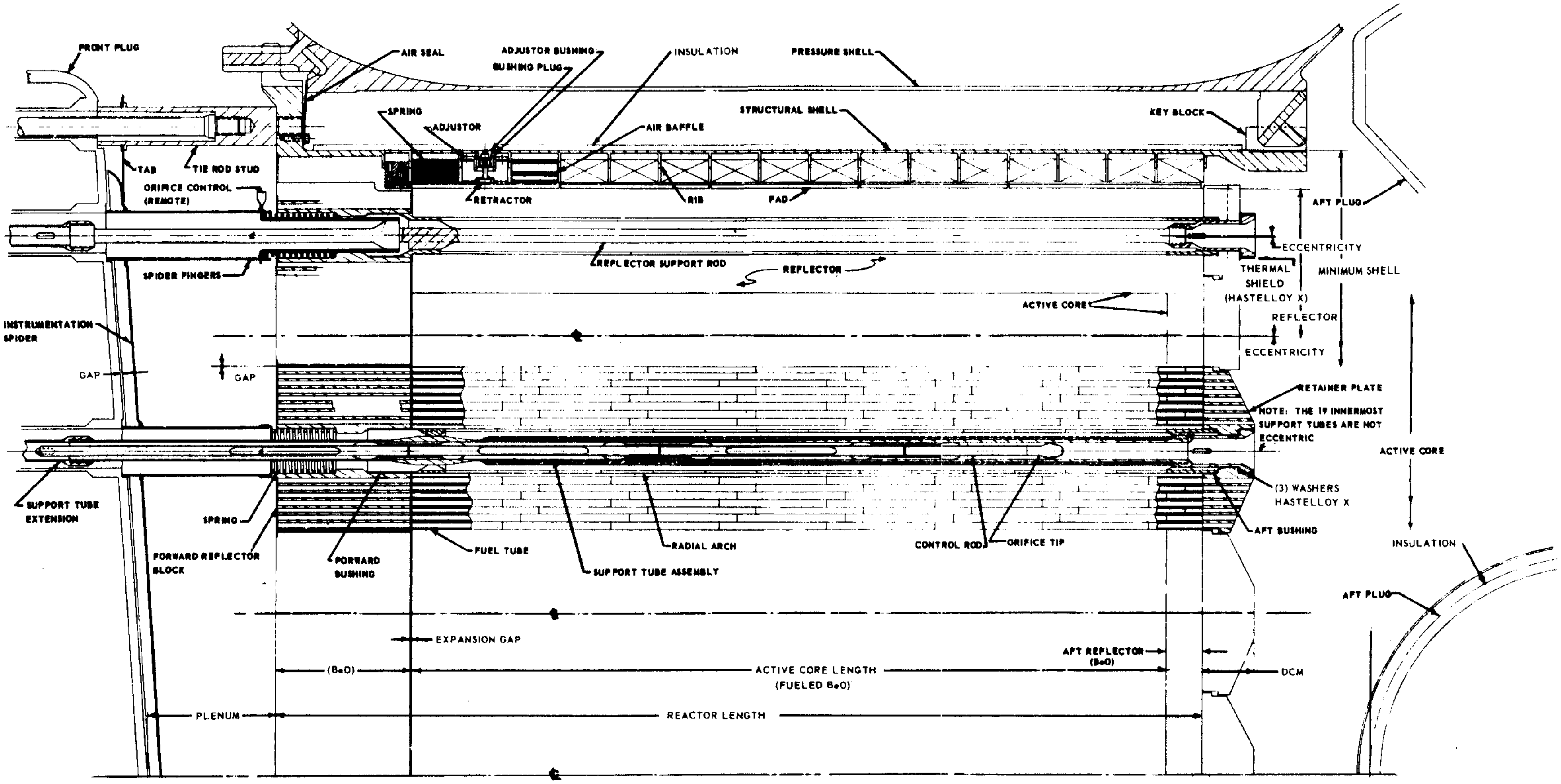

Fig. 1.5 – Longitudinal cross section of D141A-1 reactor

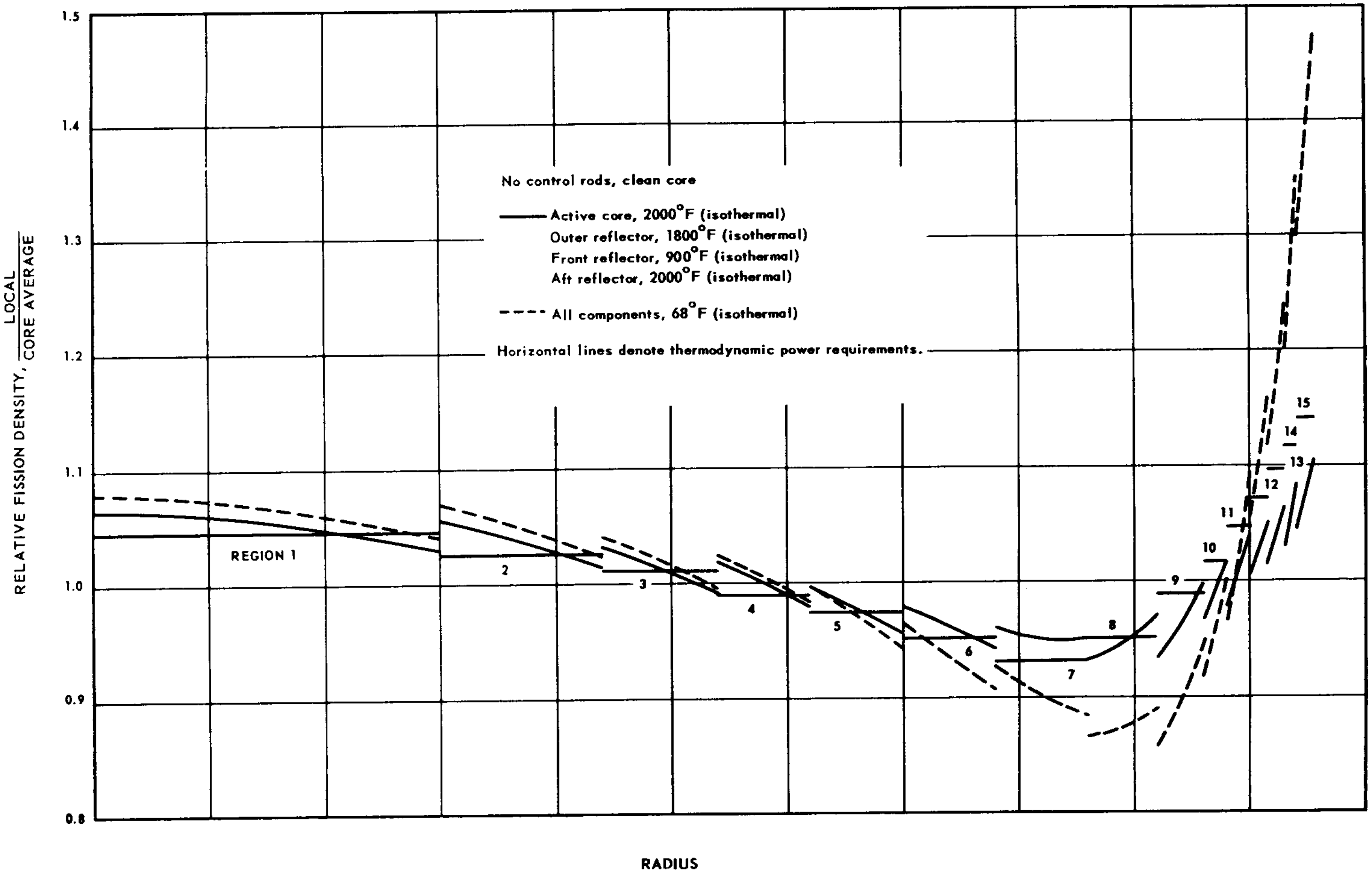

Fig. 1.6 – Radial power density, clean D141A-1 reactor

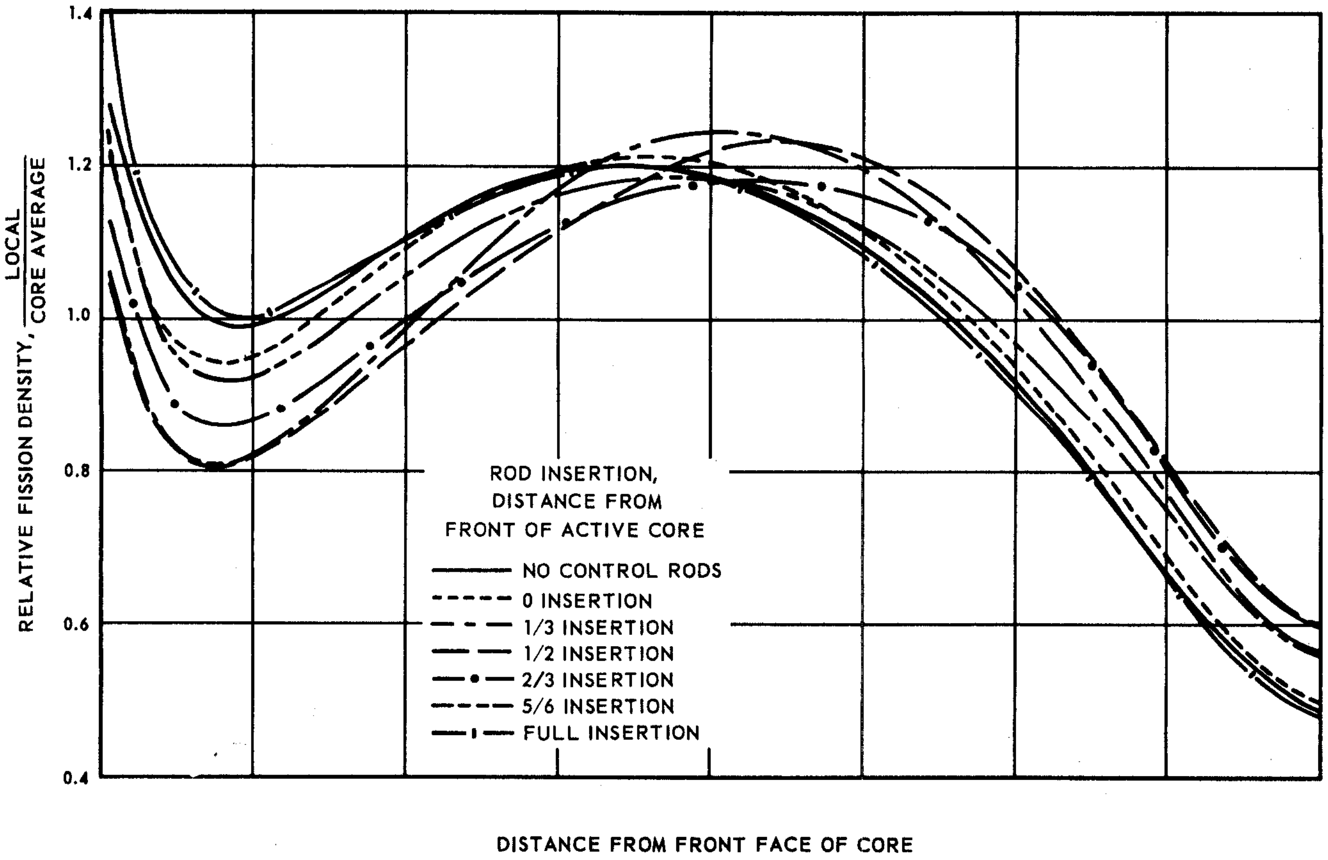

Fig. 1.7 – Longitudinal power distribution for various control rod insertions, clean D141A-1 reactor at 2000°F average temperature

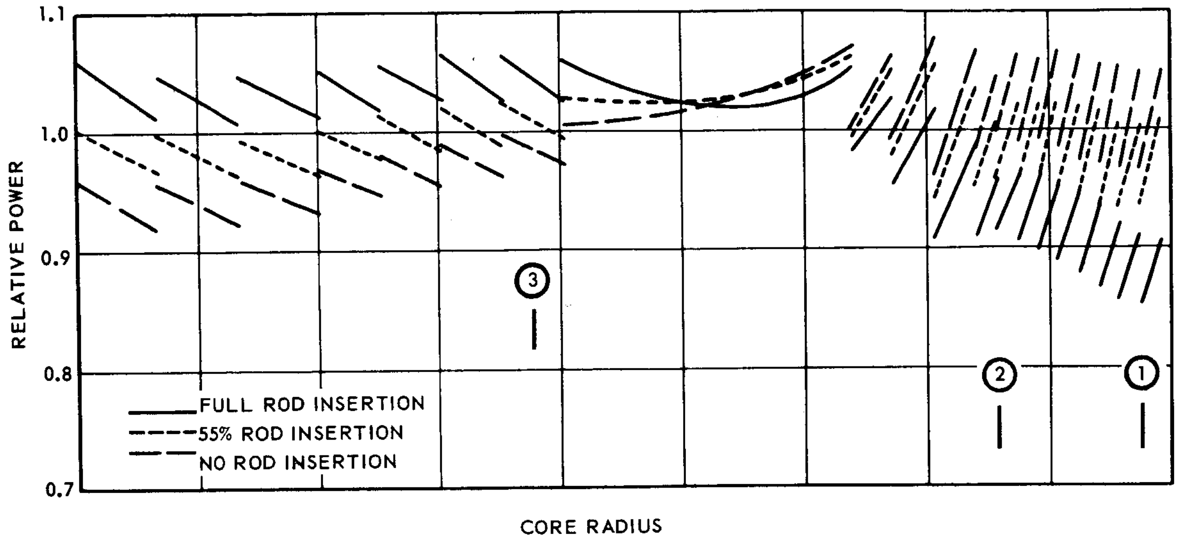

Fig. 1.8 — Gross radial power distribution for three rod-insertion depths in the XNJ140E-1 reactor

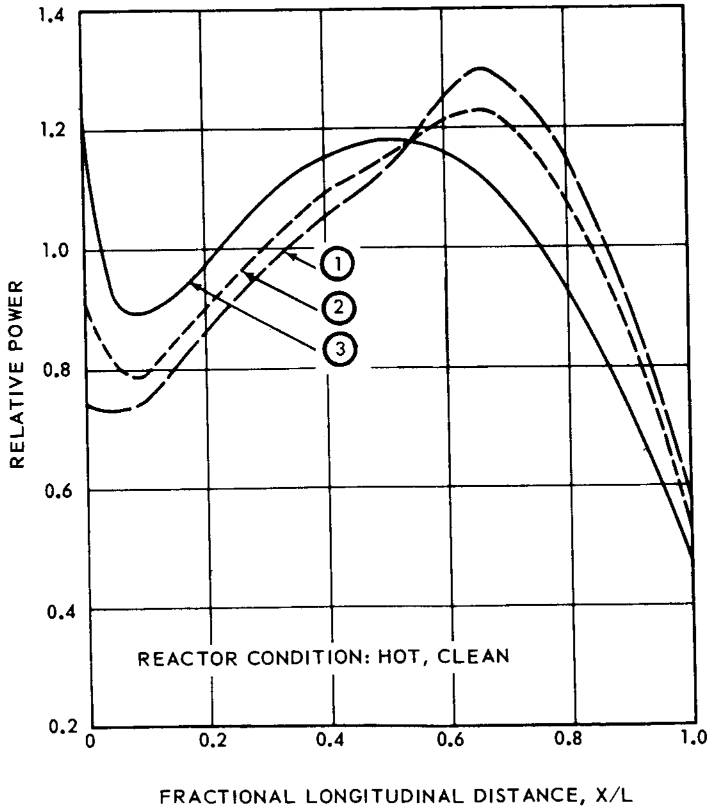

Fig. 1.9 — Relative longitudinal power distribution in the XNJ140E-1 reactor at three radial locations with control rods fully inserted

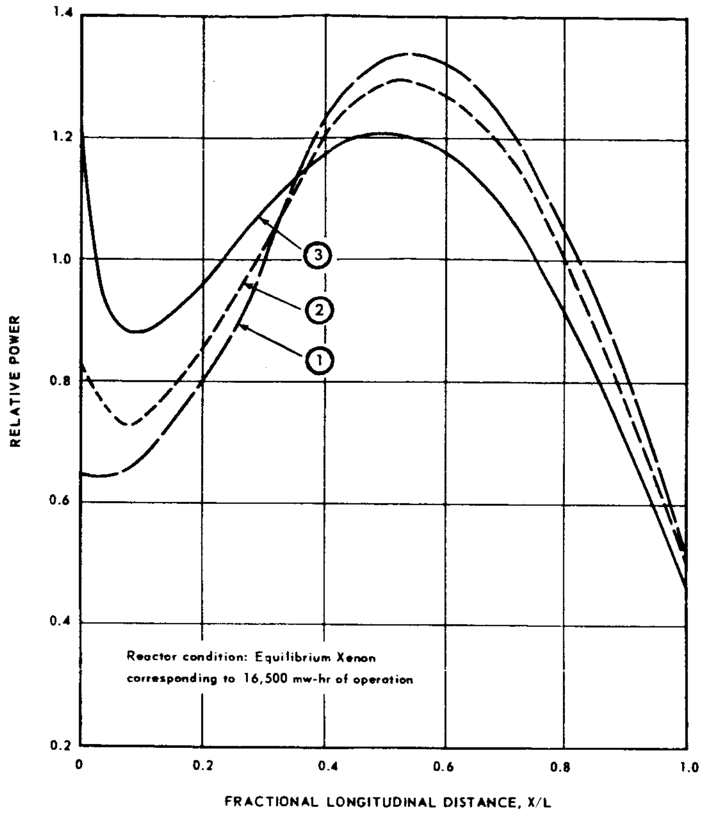

Fig. 1.10 – Relative longitudinal power distribution in the XNJ140E-1 reactor at three radial locations with control rods inserted 55 percent

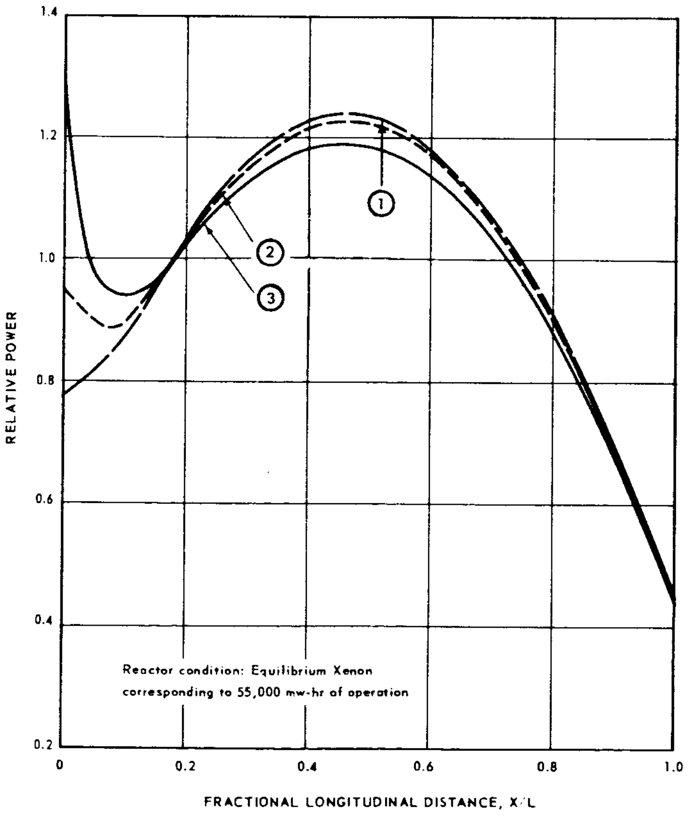

Fig. 1.11 – Relative longitudinal power distribution in the XNJ140E-1 reactor at three radial locations with control rods fully withdrawn

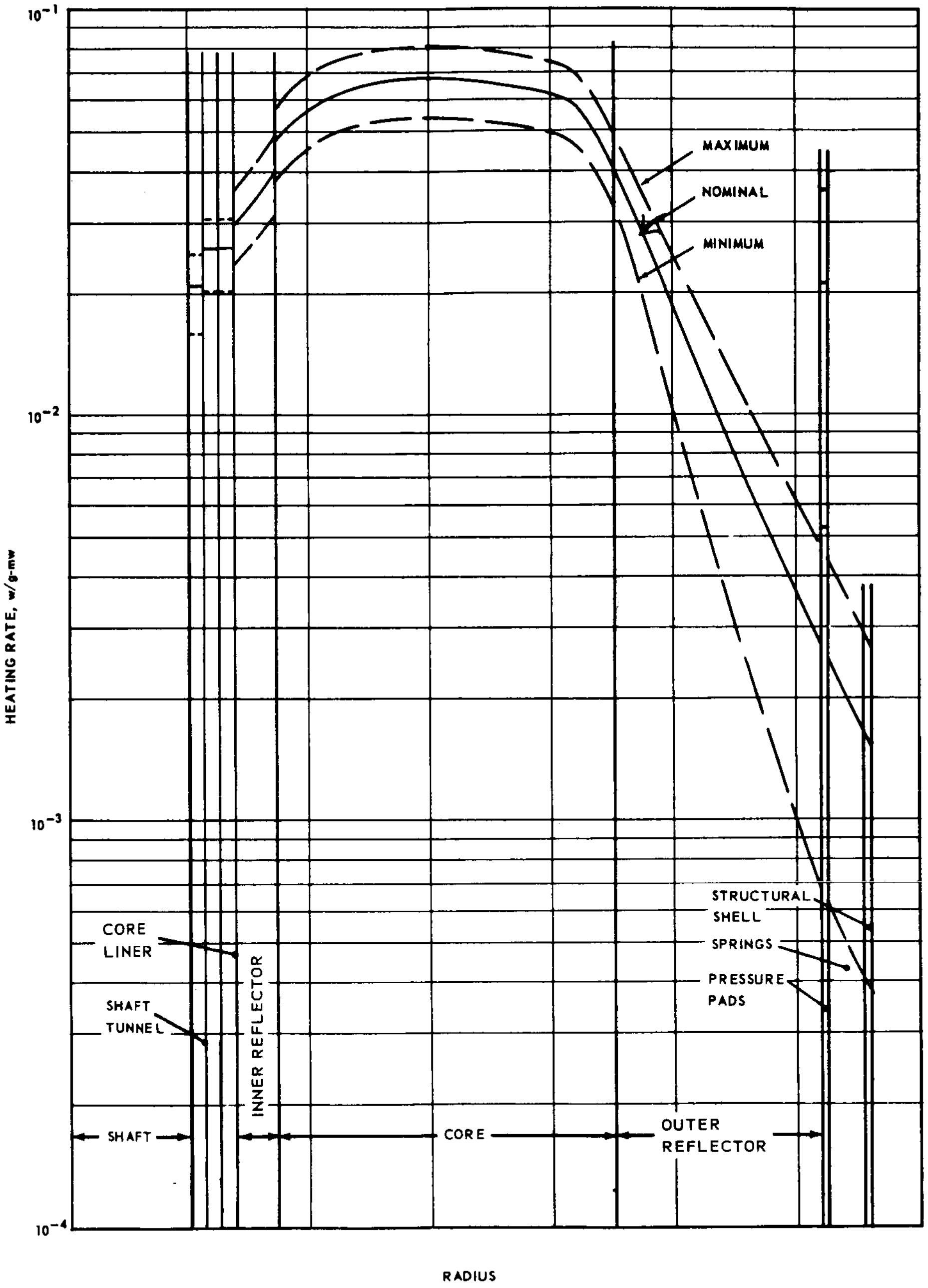

Fig. 1.12 – Gross radial secondary heating distribution, XNJ140E-1 reactor

A typical steady state distribution of heat among reactor components is shown in Table 1. 1 where the components identified are typical of those in a shaft-through-the-reactor configuration like the XNJ140E-1.

Typical radial and longitudinal distributions of heating are shown in Figures 1. 12 and 1. 13. Use of maximum, nominal, and minimum arises from analytical uncertainties in the nuclear design, i. e., at the time these curves were made experimental measurement of heating rates had not been made. Nominal corresponds to the best analytical estimate. Maximum and minimum bracket a range within which a high confidence exists that the range will include actual heating rates. Of interest in the thermal design is the fact that quite large variations of heating can exist across a single component, i. e., almost a factor of 10 across a thick reflector and almost a factor of 2 across a structural member like the rear support.

Another question in thermal design is that of sizing coolant passages in view of the uncertainties. If they are sized for less than maximum, over-temperature may result. If sized for maximum heating, significant under-temperature may result if the heating rates are in fact less than maximum. The concern is not so much that components are under-temperatured, but rather that excessive coolant will have been used. Since reactor size and weight are generally not sensitive to coolant volume in these components, one design approach is to size the coolant passages for maximum heating rate when the design is committed to hardware and provide adjustable or replaceable flow resistances or orifices, such that when an improved knowledge of heating rates becomes available or after temperatures are measured in an operating prototype, the flow rate can be changed for subsequent operation. Since the uncertainty for total heat in all components is generally much less than that for a single component, anticipation of total flow required for all non-fuel element components will normally be that corresponding to nominal heating rates or only slightly larger.

Problems of afterheat removal can be anticipated by observing the nature of the data in Table 1. 2.

As an example, observe that 100 seconds after shutdown the active core power has fallen to 3. 4 percent of the steady state value, while the outer reflector has only fallen to 18. 2 percent. This is due to the fact that the active core power is due mostly to fission product kinetic energy during reactor operation whereas the reflector power is due in large part to gamma energy absorption. A relatively high gamma level continues after shutdown due to radioactive decay, whereas the production of new fission products has, of course, stopped. Consequently, whereas during operation the outer reflector power was 2. 3 percent of fuel element power, it is now 12. 4

TABLE 1.1

TYPICAL FRACTIONAL ENERGY DEPOSITION

Region	Watts Deposited Per Watt Of Total Fission Energy[a]			
	Neutron	Total Gamma	Fission Fragment And Beta	Total
Core	0.0184	0.0614	0.8772	0.9570
Forward reflector and transition	0.00082	0.00168	-	0.0025
Aft transition, aft-retainer assembly	0.00027	0.00133	-	0.0016
Shaft, tunnel, liner, Be shaft inserts	0.00019	0.00261	-	0.0028
Inner reflector	0.00070	0.00420	-	0.0049
Outer reflector	0.00357	0.0187	-	0.0223
Pressure pads (n, α)	0.00310	0.00044	-	0.0035
Springs and shell	-	0.00081	-	0.0008
Reactor total	0.0270	0.0912	0.8772	0.9954
Estimated escape from reactor	0.0015	0.0031	-	0.0046

[a] Total fission energy does not include energy from neutron-induced reactions in the side shield or end shields.

TABLE 1.2

TYPICAL AFTER SHUTDOWN POWER

Component	Fraction Of Component Heating At Steady State								
	Time (t) After Shutdown, sec								
	0	1	5	10	50	10^2	10^3	10^4	10^5
Active core (includes fission)	1.0	0.290	0.173	0.123	0.0459	0.0344	0.0176	0.00970	0.00516
Be front reflector	1.0	0.547	0.368	0.308	0.214	0.162 ~~1.162~~	0.0855	0.0427	0.0256
BeO front reflector	1.0	0.572	0.387	0.323	0.226	0.169	0.0887	0.0484	0.0242
Rear reflector	1.0	0.577	0.392	0.330	0.237	0.175	0.0928	0.0515	0.0268
Rear grid plate	1.0	0.685	0.463	0.407	0.296	0.222	0.111	0.0556	0.0370
Shaft	1.0	0.629	0.426	0.361	0.268	0.204	0.102	0.0556	0.0278
Liner	1.0	0.667	0.454	0.388	0.285	0.218	0.109	0.0606	0.0303
Inner reflector	1.0	0.605	0.410	0.345	0.248	0.188	0.0976	0.0524	0.0286
Outer reflector	1.0	0.592	0.398	0.335	0.238	0.182	0.0932	0.0511	0.0268
Pads	1.0	0.297	0.177	0.126	0.0516	0.0387	0.0194	0.00968	0.00548

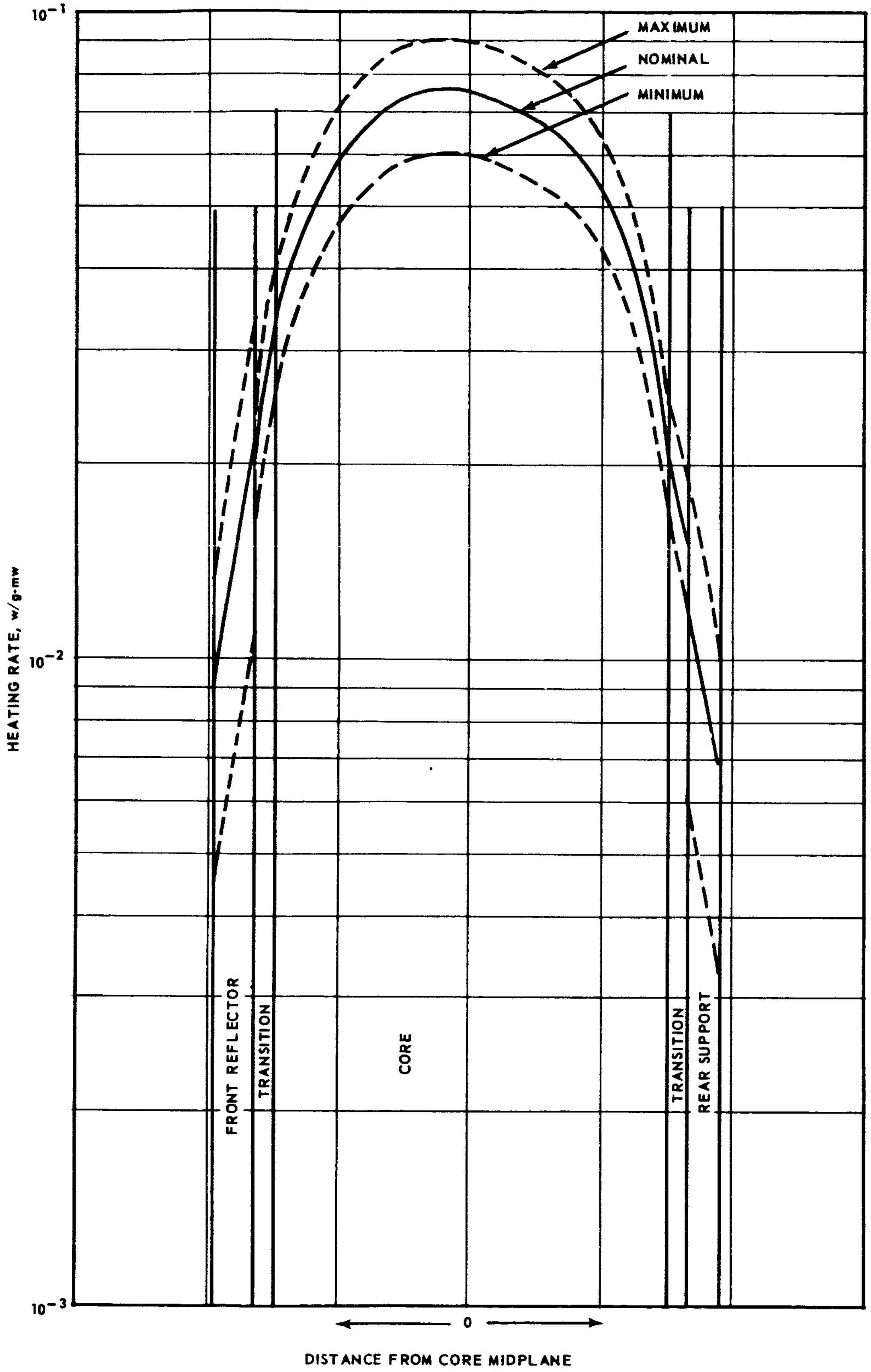

Fig. 1.13 — Longitudinal secondary heating rate, XNJ140E-1 reactor

percent. Since the flow passages are designed to provide a flow distribution to produce a desired steady state temperature distribution, control of flow rates after shutdown to maintain fuel element temperatures will result in a tendency for other components to increase in temperature. If alternately, temperatures of other components are maintained, excessive flow requirements will result, the fuel elements will cool rapidly, and large temperature gradients may result. Quite aside from the latter difficulties, per se, the high flow requirement can be a critical problem in nuclear rockets since, unlike air-breathing systems, the coolant supply is limited.

1. 4 THERMAL CHARACTERISTICS OF TYPICAL REACTORS

We can now display typical thermal characteristics of nuclear reactors by using ANP reactors as examples.

1. 4. 1 Flow Distribution

Typical flow distribution among the many components of a nuclear turbojet engine is shown in Figure 1. 14, in which it is noted that only 84 percent of the flow to the turbine is heated in the reactor. Non-fuel element reactor components require 8. 6 percent. The remaining 7. 4 percent is utilized to cool shield components, turbine components, chemical combustor components, and structure, and to provide for seal leakage, balance pistons, and by-pass bleed speed control. Because the 16. 0 percent of the flow not passing through the reactor active core was heated to a lower temperature, the average temperature for flow to the turbine was 13 percent less than the average temperature of the flow from the reactor, both temperatures expressed as the excess over the inlet temperature. The many interconnected flow passages result in a need for careful design of coolant channels such that the required flow distribution is assured. The flow circuitry is indicated in Figure 1. 15. Flows in each branch and pressures at the several branch junctions are shown in Table 1. 3.

Flow distribution within the reactor can be influenced by the plenum and header designs just upstream and just downstream from the reactor. Since such flow problems are complex and three-dimensional, experimental data will generally be required to evaluate the effects. Typical of annular ducts that can be utilized upstream and downstream of the reactor are those shown in Figure 1. 16. The HTRE-3 reactor (see Figure 1. 1) shield plans originally incorporated ducts like those in the upper sketch of Figure 1. 16, but as finally designed, used ducts like those in the second sketch. Further refinement to make the ducts more tortuous and hence allow less radiation leakage may result in configurations as shown in the third sketch. Reverse

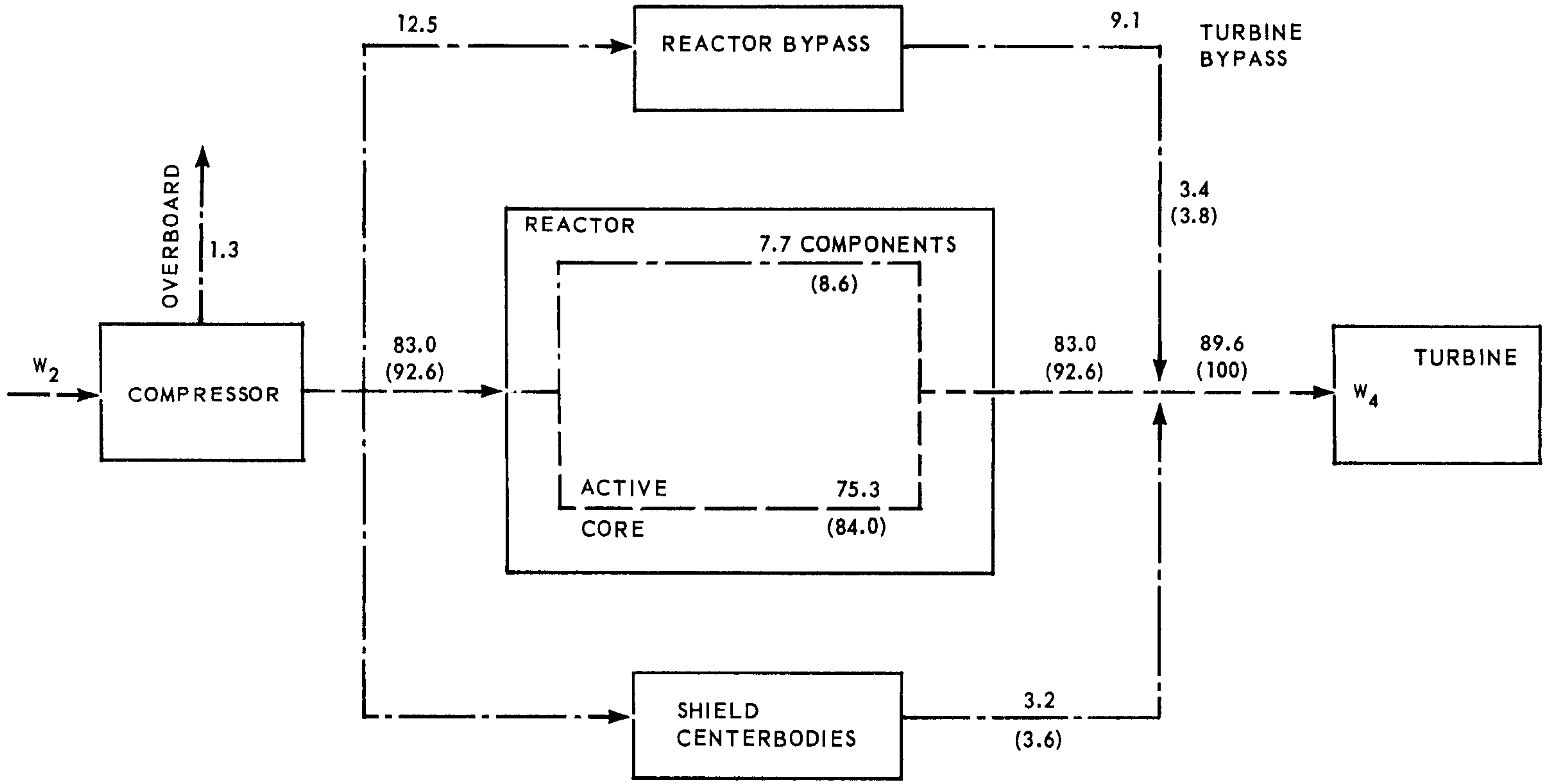

1. Numbers enclosed in parentheses are flows expressed as a percentage of W_4
2. Numbers not enclosed in parentheses are flows expressed as a percentage of W_2

Fig. 1.14 – Airflow distribution in the XNJ140E engine

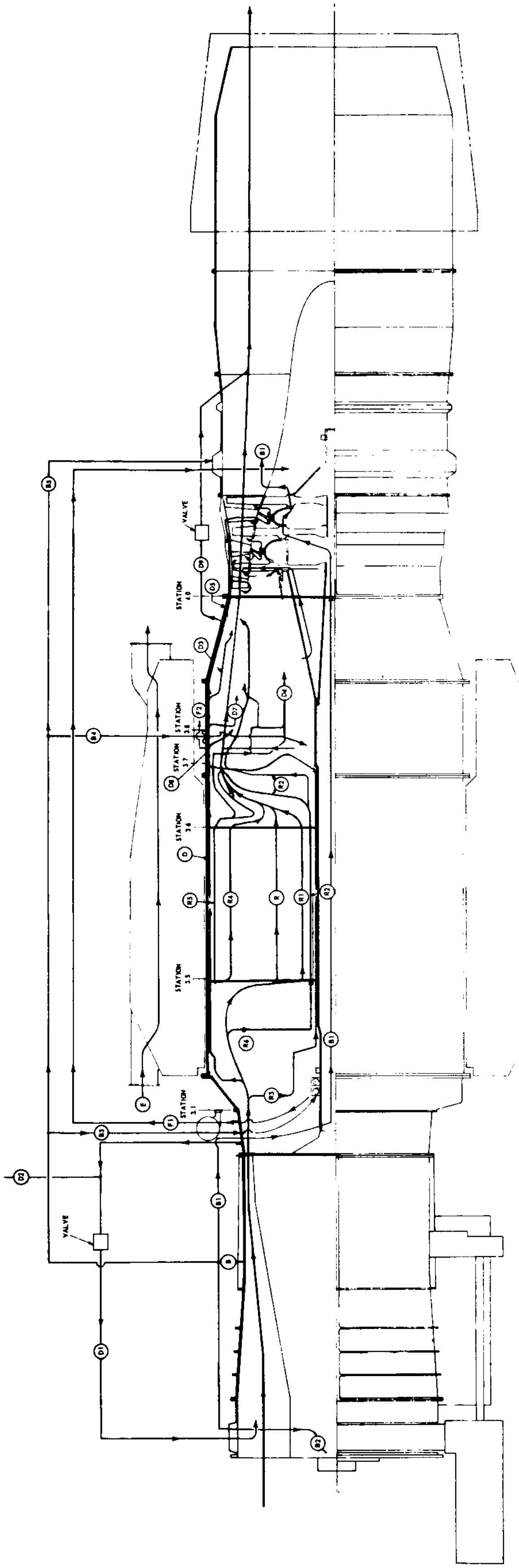

Fig. 1.15 – Cooling airflow paths and pressure stations, XNJ140E engine

TABLE 1.3

STATIC AND TOTAL PRESSURES AND FLOW QUANTITIES FOR COOLING AIRFLOW PATHS

Path	Purpose	Location	Condition 1[a]	Condition 2[b]	Location	Condition 1	Condition 2	Location	Condition 1	Condition 2	Location	Condition 1	Condition 2	Location	Condition 1	Condition 2	Location	Condition 1	Condition 2	Location	Condition 1	Condition 2	Location	Condition 1	Condition 2	Location	Condition 1	Condition 2
			P_s P_t	P_s P_t		P_s P_t	P_s P_t		P_s P_t	P_s P_t		P_s P_t	P_s P_t		P_s P_t	P_s P_t		P_s P_t	P_s P_t		P_s P_t	P_s P_t		P_s P_t	P_s P_t		P_s P_t	P_s P_t
R	Primary flow	Station 3.000	69.9 72.8	220 230	39	70.0 71.2	220 225	Station 3.500	68.8 69.5	215.7 218.2	Station[e] 3.600	59.3 59.6	185.0 189.6	11[f]	56.5 58.1	176 183	12	52.9 54.6	166.8 172	13			14	59.3 59.6	186.0 189.6	42	57.6 60.0	179.5 185.7
R1	Center reflector[c]	Station 3.600	57.7 ~59.6	185.6 ~189																								
R2	Front and rear shield centerbody	Station 3.500	70.3 71.4	213 216	Station 3.550	66.9 69.6	202.5 210.7	Station 3.600	65 67.8	197 206.5	15	67.3 67.8	204 206.5	16	64 64.4	193.5 199	18	61.8 61.8	187 187									
R3	Shaft tunnel purge flow	Station 3.500	74.3 74.5	223 225	Station 3.600	74.2 74.4	222.9 224.9	43	74 74.2	222.7 224.7	17	72.4 72.8	220 221															
R4	Outer reflector	Station 3.500	69.2 69.2	216.2 216.2																								
R5	Outer front and rear shields and radial springs	Station 3.600	69.2 69.2	216.2 218.2	Station 3.600	60 to 65 60 to 65	190 to 205 190 to 205	41	67.2 67.2	212 212																		
R6	Control rods[d]	Station 3.500	69.2/65.8 69.8/66.8	218/208 220/211																								
B1	Shaft cooling	Station 3.500			Station 3.600																							
B2 B3 B4 B5	Seal pressurization																											
D	Speed bleed	Station 3.500	75.5 75.8	219.5 221	Station 3.600	~67 ~67	212 212																					
D1	Anti-icing																											
D2	Control and flange leakage																											
D3	Hot-duct-wall cooling																											
D4	Turbine rotor, balance piston seals, and rear-shield centerbody	20			44			30	63.8	208																		
D5	Turbine stator cooling	21			23			24			25																	
D7 D8	Burner injector cooling																											
D9	Speed-control bypass																											
F1 F2	Seal leakage (sump pressure)	26			40																							
Z	Side-shield cooling																											

Point	Location	Condition 1 P_s P_t	Condition 2 P_s P_t
27	12th-Stage Rotor Discharge Root	64.5	204
28	CRF Cavity	13.6 to 17	43.6 to 53.7
29	CRF Shaft Cooling Cavity	20.2	63.8
31	Turbine Balance Piston Pressure		
32	Turbine Balance Piston Pressure		
33	P4.1 Root	32.3	102
34	P4.2 Root	29.8	94.2
35	P4.3 Root	18.8	59.4
36	P4.4 Root	17.3	54.7
37	P4.5 Root	11.8	37.3
38	P5.0 Root	11.5	36.3

COOLING AIR QUANTITIES

Path	Percent of W_2
R	75.3
R1	0.8
R2	3.2
R3	0.3
R4	4.1
R5	1.2
R6	1.6
B1	1.0
B2-B5	0.2
D	D1-D9[g]
D1	0.3[h]
D2	0.6
D3	1.5
D4	2.5[i]
D5	3.0
D7	1.0
D8	0.9
D9	2.0[j]
F1-F2	0.4

NOTES:

[a] Condition 1: Objective power plant, cruise flight condition.

[b] Condition 2: Objective power plant, maximum sea-level acceleration. This condition is more severe than any ACT test condition.

[c] Pressures are given in psia.

[d] Varies as function of control rod position.

[e] At retainer plate discharge.

[f] Upstream of 10 strut fairings.

[g] Flow path "D" is origin of D1 through D9.

[h] Intermittent.

[i] This value is for the cooled turbine. For XNJ140E-1, D4 = 1 percent.

[j] Maximum steady-state bleed-speed control above 90 percent N.

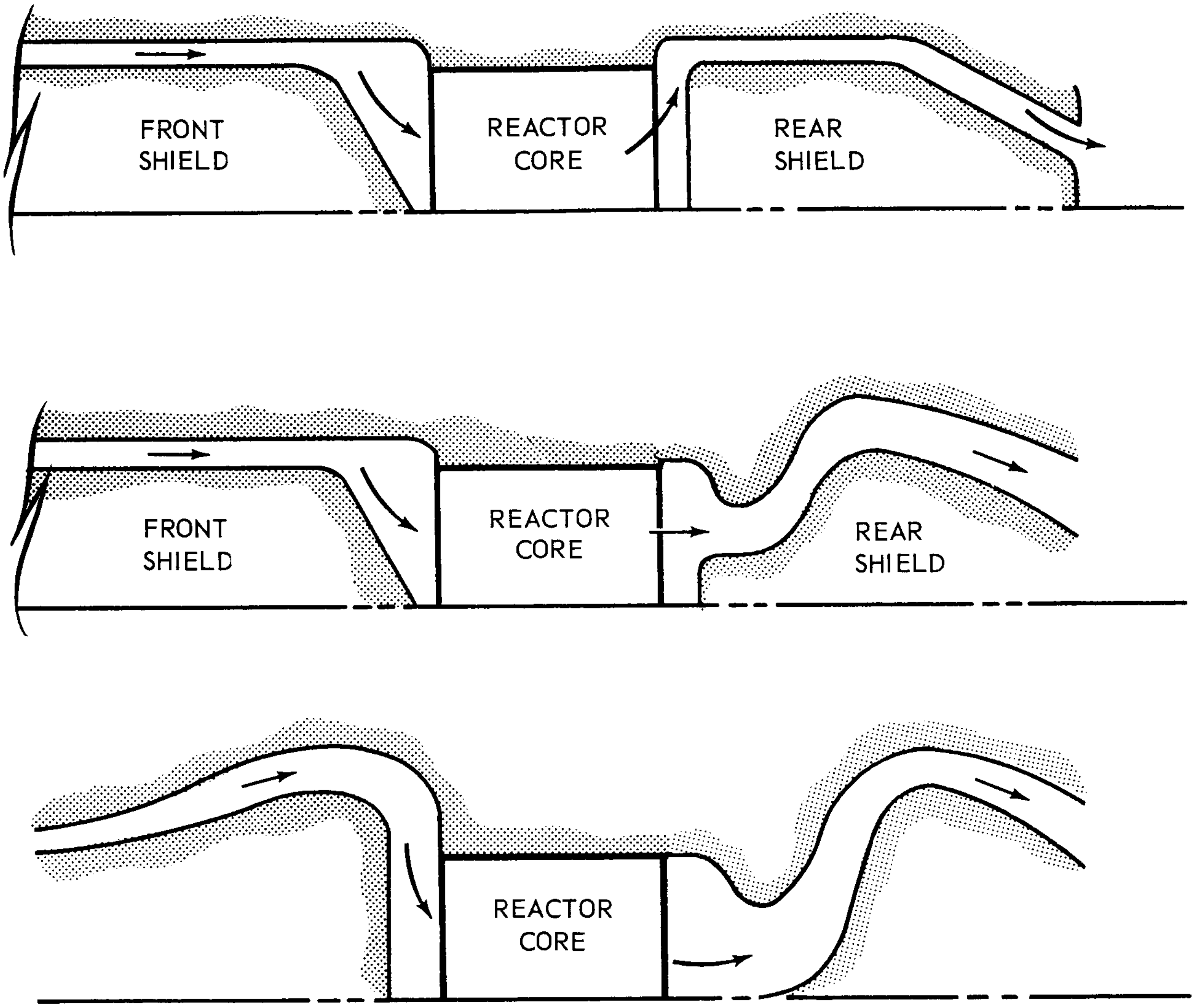

AXIAL FLOW DUCTS

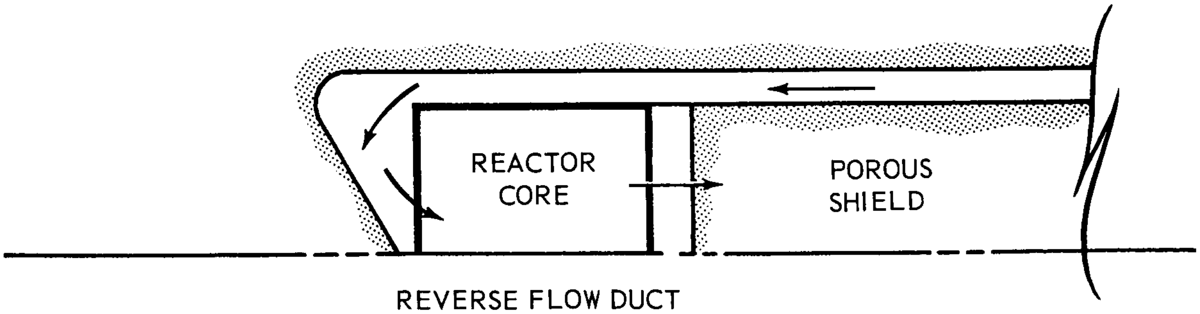

REVERSE FLOW DUCT

Fig. 1.16 – Typical single annulus shield ducts

flow ducts like that shown in the lower sketch have been included in design studies and, except for the rear shield region, may be a logical choice for nuclear rocket engine.

All ducting arrangements shown in Figure 1. 16 have the potential of inducing flow maldistributions within the reactor. Flow experiments using a 1/4 scale mockup during the HTRE-3 reactor shield development program utilized the configurations shown in Figure 1. 17. Initial tests with the front shield only resulted in the flow distributions shown in Figure 1. 18. Subsequent testing with simulations of both front and rear shield plugs yielded the data shown in Figure 1. 19. Rear shield plugs as originally conceived, i. e., with a flat face next to the reactor, yielded flow local reductions of 4 to 6 percent. Since these were deemed unacceptable and further increase of spacing could not be tolerated from a shielding consideration, the final, or "HTRE No. 3 Current Design," was developed and did reduce the maximum flow reduction to about 2. 5 percent. If a general conclusion can be drawn from the ANP experience it is that unless large plenums are permitted by the system design, experimental duct development will be required, flow maldistributions of ±2 percent can be achieved, and that uncertainties in the experiment will be on the order of 1/2 to 1 percent. The measured distribution will, of course, be accounted for in the temperature levelling aspects of the reactor design.

1. 4. 2 Reactor Sizing

With inlet pressures, inlet and exit temperatures, flow rates specified by the system design, and with a longitudinal power distribution provided by the nuclear design, coolant channels can be sized. Fuel element temperatures versus fuel element flow area are shown in Figure 1. 20 for the D141A-1 reactor with tube hydraulic diameter, D_H, and core pressure ratio as parameters. It can be observed that the required surface temperature is quite sensitive to the choice of D_H and only moderately sensitive to the choice of flow area. Conversely, the core pressure ratio is a strong function of flow area and a weaker function of hydraulic diameter. If a maximum fuel element temperature is imposed the hydraulic diameter is fixed within fairly small limits. Combination of flow area and pressure ratio can only be chosen in conjunction with system studies wherein such parameters as thrust-to-weight ratio will be maximized. Further restraints on permissible choices may also be provided by thermal and mechanical stress considerations.

1. 4. 3 Fuel Element Calculated Temperatures

After setting the basic fuel element dimensions the fuel element temperatures can be examined in more detail utilizing power distributions from

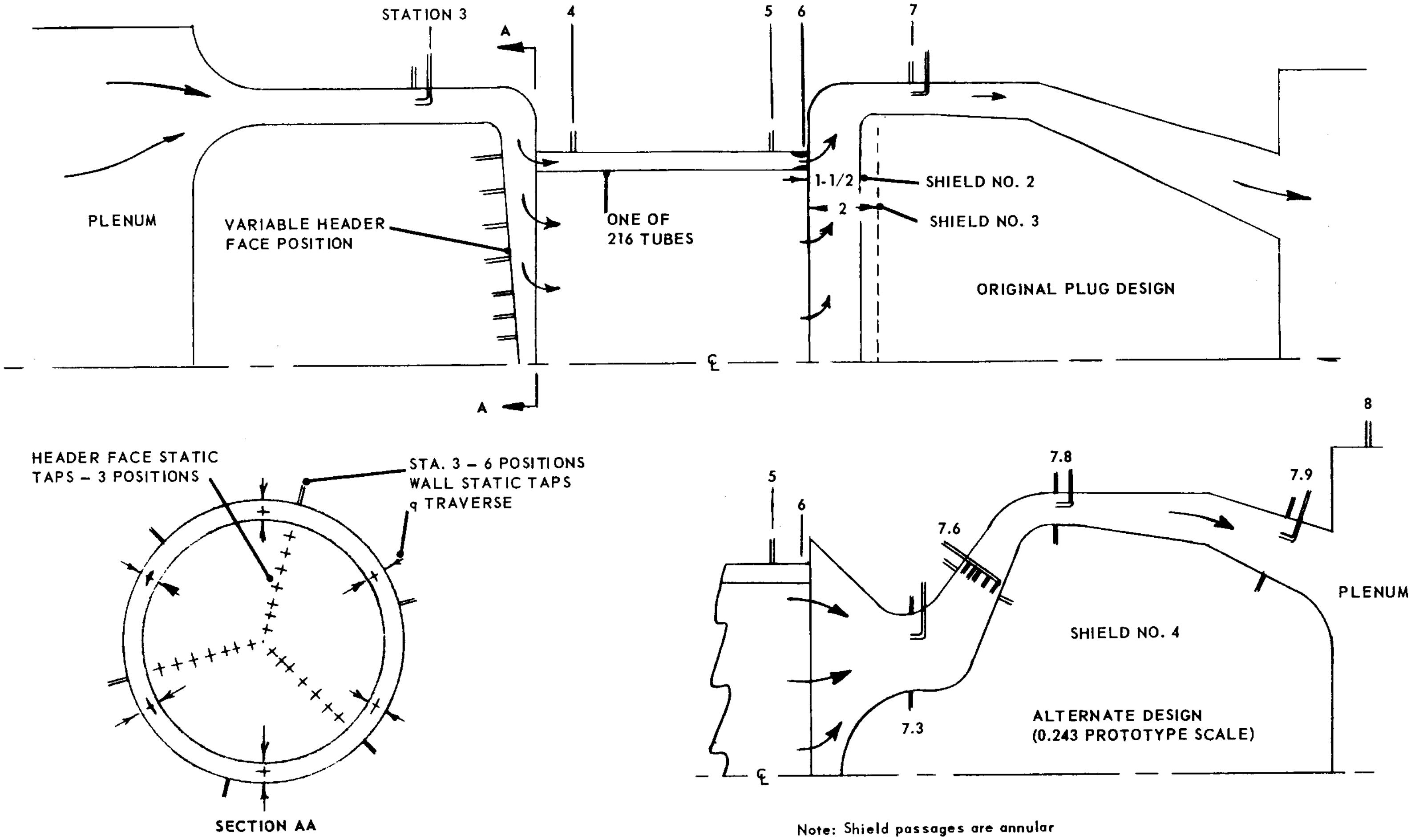

Note: Shield passages are annular

Fig. 1.17 – Model configuration for tests of various front and rear header shields

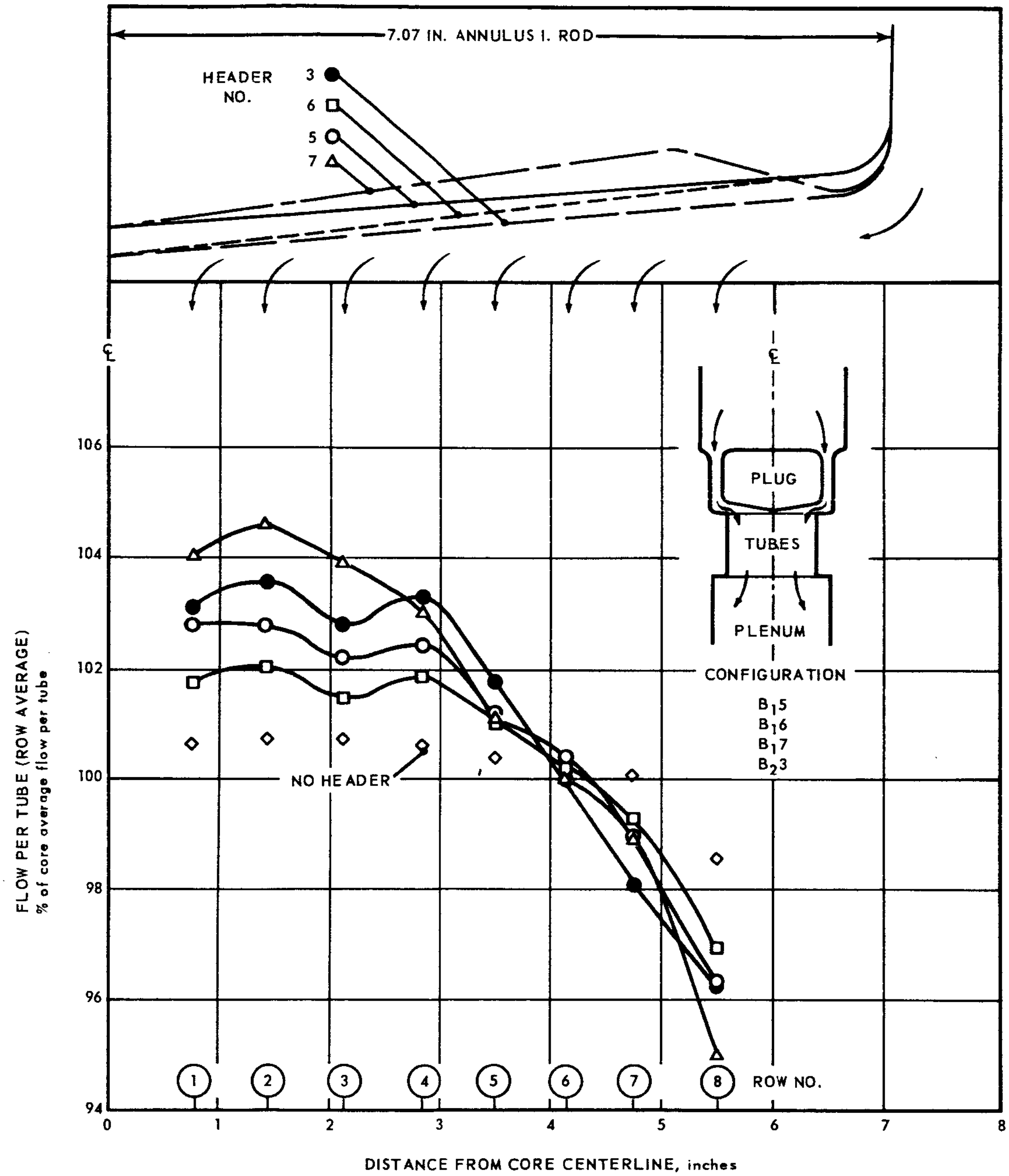

Fig. 1.18 – Weight flow distribution radially in core for various front header shapes

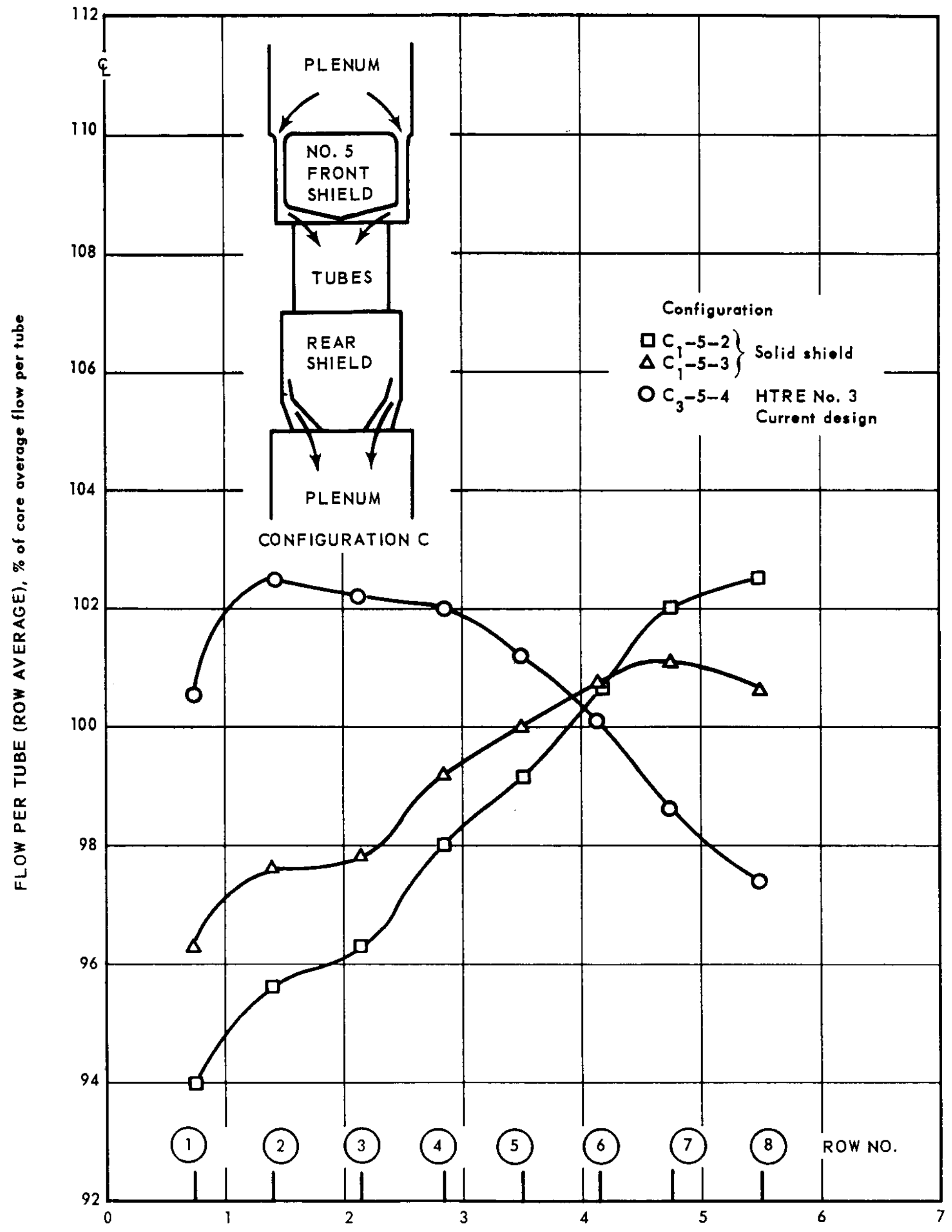

Fig. 1.19 – Weight flow distribution radially in core for various rear plugs

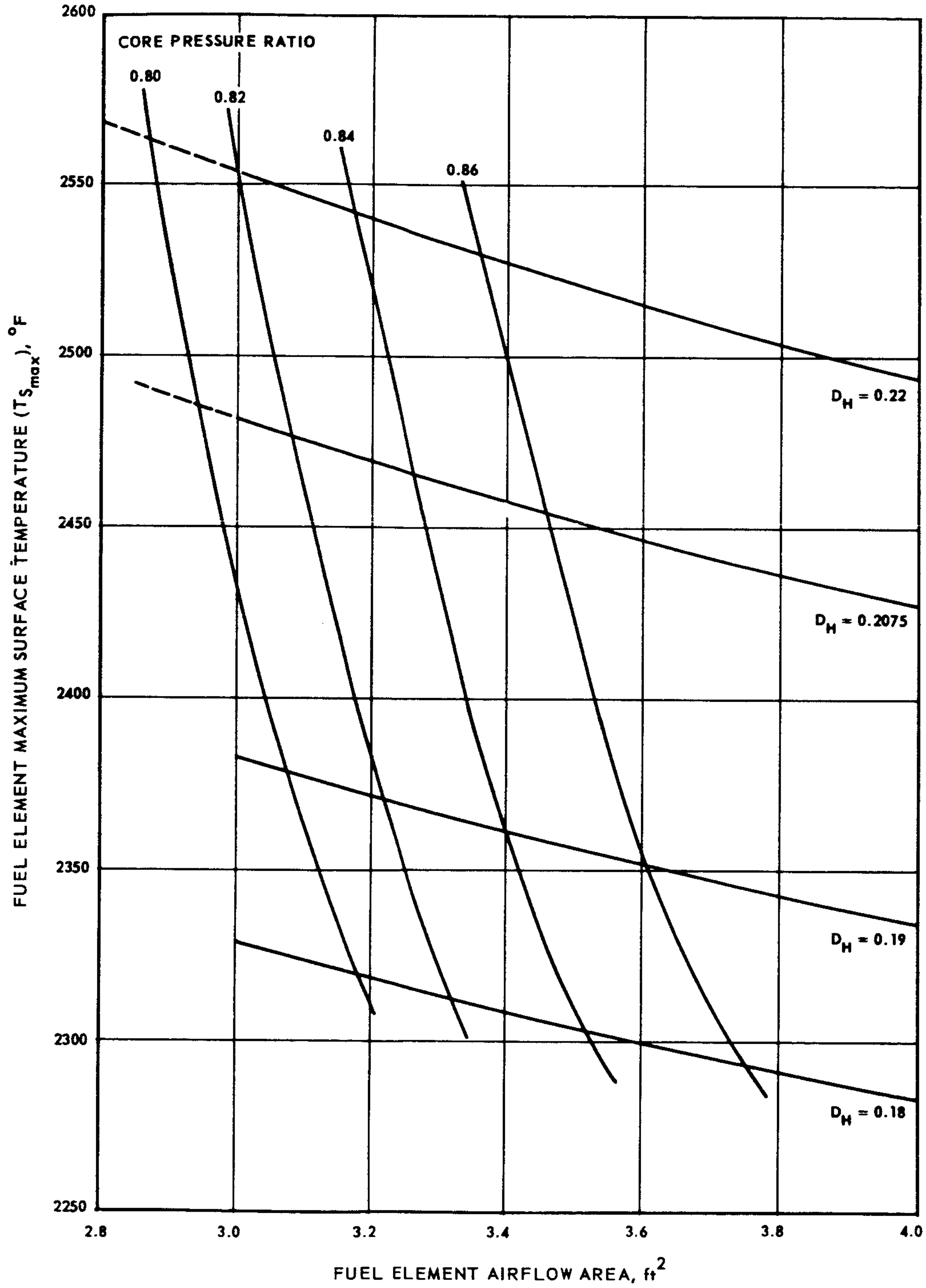

Fig. 1.20 – Aerothermal parametric data for D141A-1 reactor

the nuclear design. Axial surface temperature of the fuel element channel and the associated gas temperature for the D141A-1 reactor vary as shown in Figure 1. 21. If radial temperature flattening is achieved by variation of fuel concentration and the control rods are placed in the reflector, the radial variation of maximum temperatures in the axial direction will tend to be as shown in Figure 1. 22.

The data in Figure 1. 22 have to be considered further. A temperature shown is the temperature a tube would assume if it were located at the corresponding distance and somehow uniformly subjected to the corresponding relative power. Actually, the power varies across the thickness of a single tube, such as is indicated in Figure 1. 23 (here temperature flattening is by hydraulic diameter variation). Computational models, like the one shown in Figure 1. 24, have been used to evaluate the effect of heat transmission between adjacent tubes on fuel element temperatures. Results of such computations are shown in Figure 1. 25 where it is to be noted that internal conduction within a tube, in the absence of heat transmission between adjacent tubes, results in a temperature gradient within the tube that is small compared to the power gradient. However, the temperature levels in adjacent tubes vary by magnitudes similar to those for the tube powers. Allowance for heat flow between adjacent tubes with realistic resistances causes the temperature difference for adjacent tubes to be reduced by 50 to 75 percent.

The net result of radial temperature flattening design effort is that maximum calculated temperatures are normally determined by maximum values of average tube power. As we have seen in ANP reactors this value may be 5 to 7 percent above average, and the resulting maximum temperature less the inlet gas temperature may be 5 to 7 plus percent higher than for the average tube. Thus, in ANP reactors where the fuel elements nominally operate about 1000°F above the inlet gas temperatures, local tubes will be at temperatures about 100°F higher than the average temperature.

1. 4. 4 Fuel Element Maximum Temperatures

Because of random effects, local temperatures may exceed maximum temperatures calculated utilizing known reactor characteristics by significant amounts. These temperatures are at various times referred to as maximum temperatures, hot channel temperatures, and hot spot temperatures. Factors to be accounted for include uncertainties in experimental data and design computations plus statistical accounting of effects of fabrication tolerances.

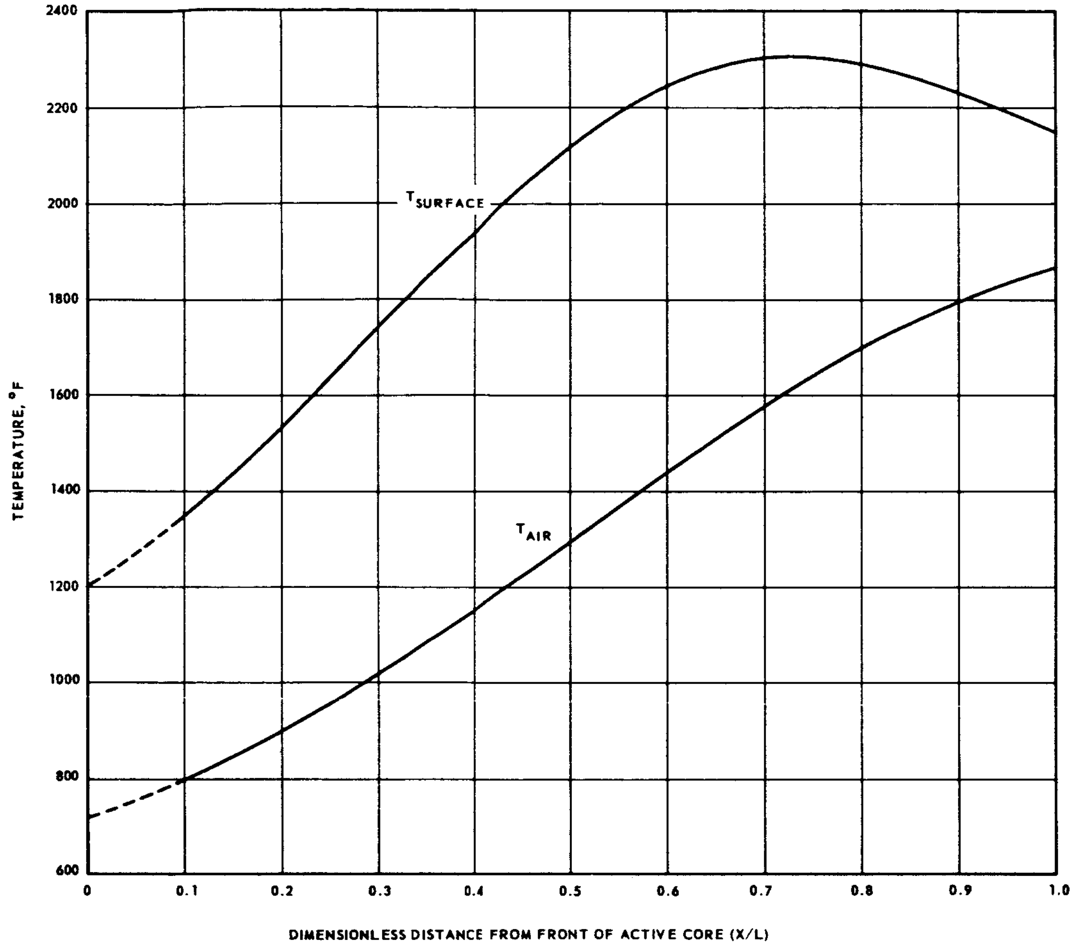

Fig. 1.21 – Fuel element average-channel longitudinal temperature profiles, D141A-1 reactor

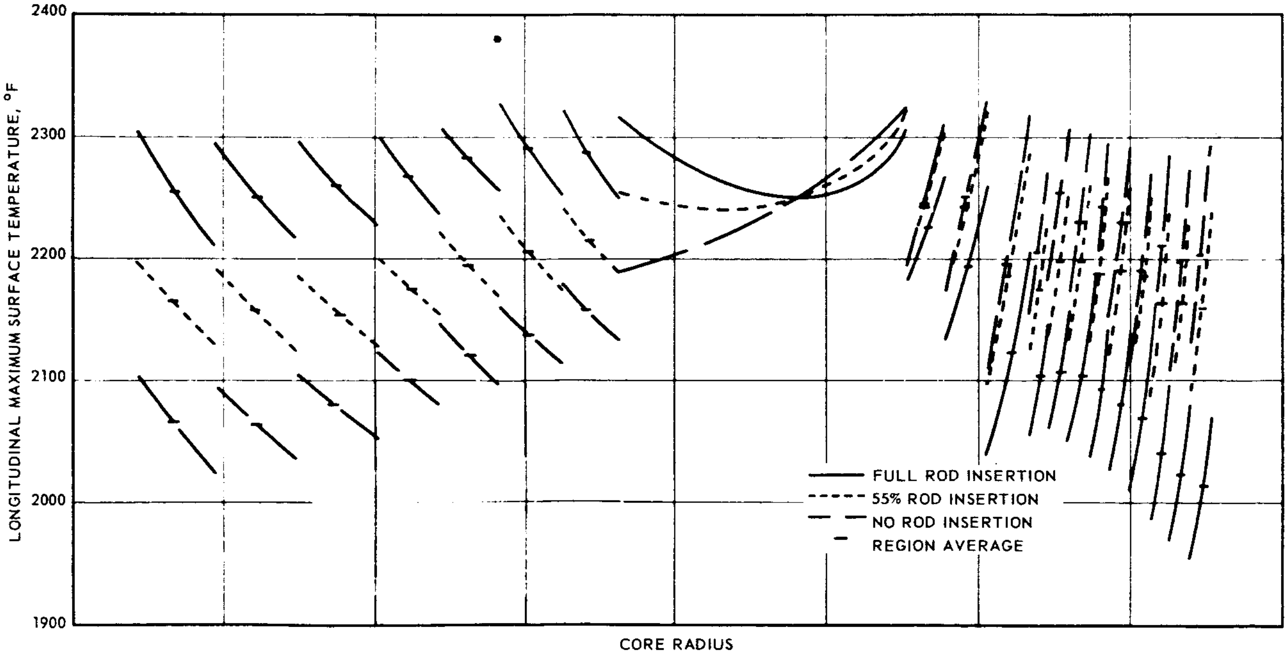

Fig. 1.22 – Surface temperature in XNJ140E-1 fuel elements

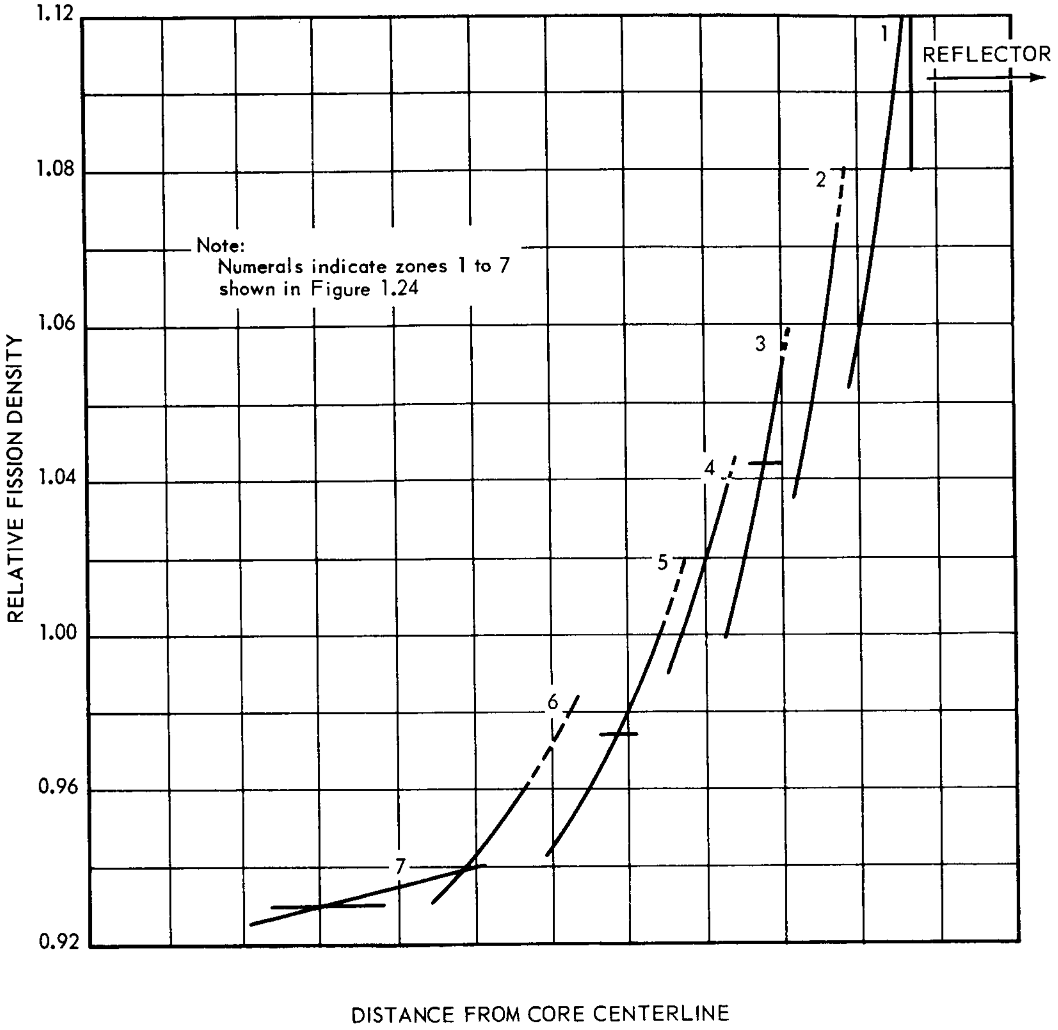

Fig. 1.23 – Radial power distribution in temperature alleviation study

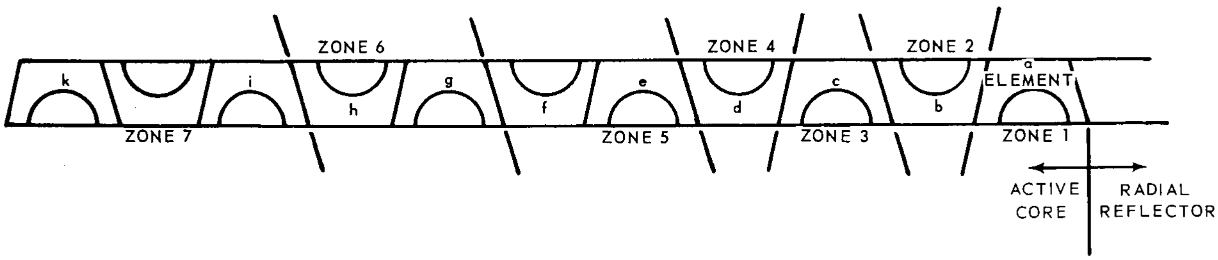

Fig. 1.24 – Geometric model used in temperature alleviation study

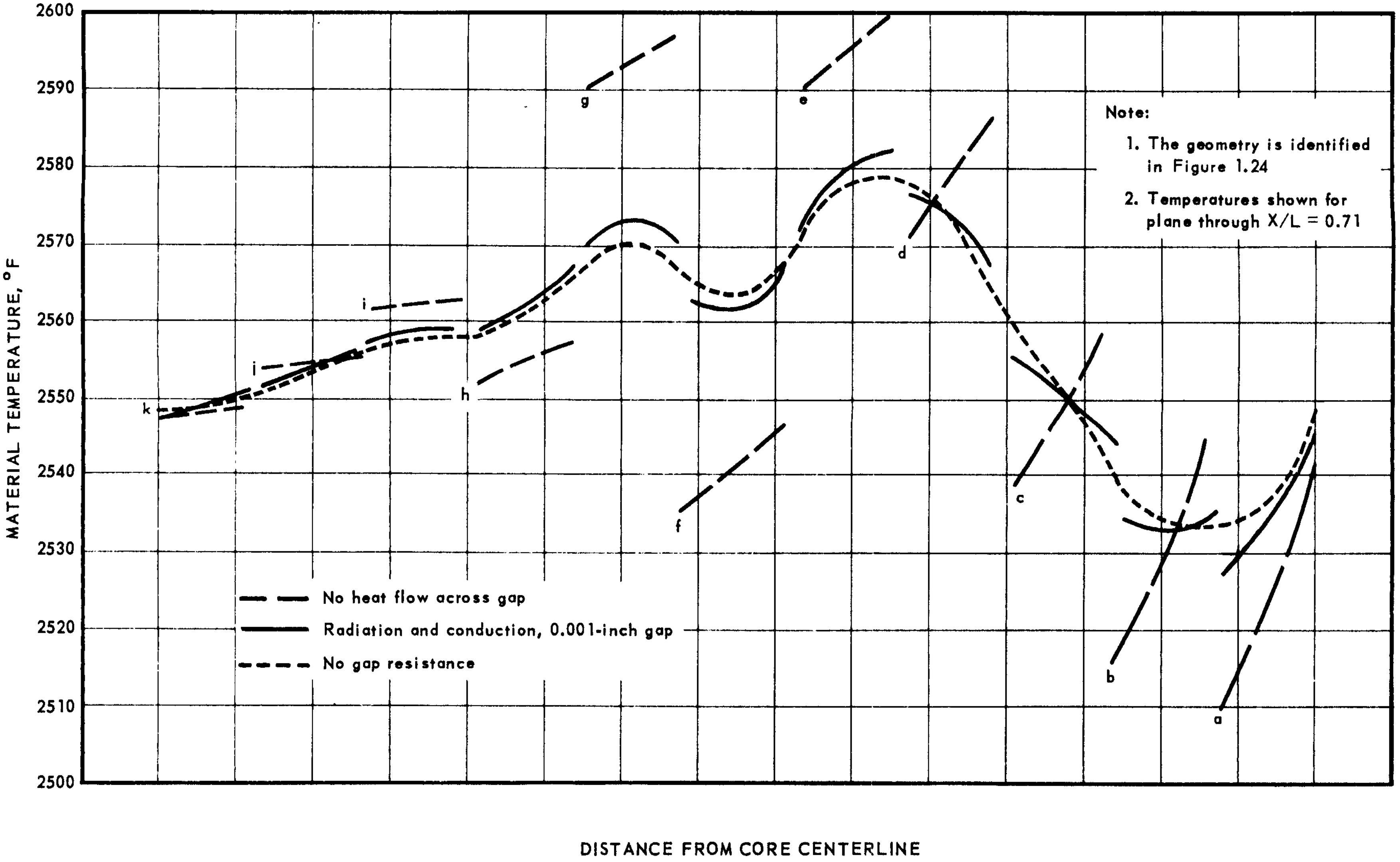

Note:

1. The geometry is identified in Figure 1.24
2. Temperatures shown for plane through X/L = 0.71

Fig. 1.25 – Temperature distribution results from temperature alleviation study

As we have indicated, experimental evaluations of externally induced flow distributions may be in the order of 1 percent. Even with carefully controlled critical experiments, power distribution measurements may have associated uncertainties of 1 to 2 percent. Fabrication tolerances, i. e., dimensional and fuel concentration, will normally be based on a reasonable balance between inspectional acceptance, or yield, percentages and achievable reactor performance. Parts accepted as being within tolerance will generally not be identical but will have characteristics, e. g., a dimension, that varies within the tolerance range. This distribution can be determined by sampling or can be assumed to follow a normal distribution centered about the nominal value. General procedure in the ANP program was to relate effects of individual tolerance limits to a temperature effect and then to statistically sum the individual temperature effects. Examples of individual temperature effects are shown in Table 1. 4. A simple sum of those temperature effects will result in a temperature increment significantly larger than that due to measured effects of flow and power distribution. However, a statistical sum will be of the same magnitude as the calculated effects. A typical result of such temperature studies is shown in Table 1. 5. Built-in temperature deviations were computed to be 120^{O}F based on best evaluation of experimental data and use of analytical procedures. Allowance for fabrication tolerances and uncertainties was somewhat greater, i. e., 170^{O}F. Finally, an internal temperature rise of 30^{O}F is added. One of the dilemmas here is that only a very small percentage of the active core is at or exceeds the "maximum fuel element temperature." This is indicated by the temperature frequency distribution shown in Figure 1. 26. Only one or, at most, a few tubes out of many thousands equal or exceed the maximum temperature of 2530^{O}F, and then only at a particular axial location. Actually, only a small percent of the total volume is within 100^{O}F of the maximum temperature. Such a situation tends to be unavoidable and hence careful consideration of permissible maximum temperature in a few localized regions becomes a critical aspect of reactor design. This picture of course has led to the use of the expression "hot spot" temperature.

1. 4. 5 Other Reactor Components

Thermal design of other reactor components is fundamentally the same as for fuel elements. The objectives may be different, e. g., in some components, instead of a uniform temperature, the objective may be to obtain and maintain a significant but constant temperature gradient across a thickness. Only a few of the many examples from the ANP program will be cited. It should be noted that although discussions of fuel element or active core design tend to be popular, the ramifications associated with other components can lead to an even greater and more demanding effort.

TABLE 1.4

CONTRIBUTIONS TO FUEL ELEMENT AND EXIT-AIR TEMPERATURE DEVIATIONS

		Temperature Deviation, °F	
		Fuel Element	Exit-Air
Power Distribution			
Reference-to-region average temperature deviation		80	70
Local deviation from region average		40	30
Fabrication Tolerances			
Hydraulic diameter	-0. 001 in.	20	15
Flats dimension	+0. 001 in.	15	10
Eccentricity	0. 0025 in.	10	0
Fuel loading	+1% of value	10	8
Coating thickness	-0. 001 in.	15	10
Measurement Uncertainties			
Radial power		60	50
Longitudinal power		20	0
Thermal conductivity		3	0
Channel axis misalignment		6	4
Tube dimension measurement		15	10
Flow measurement		20	15
Configuration			
Cladding		12	0
Fuel element		13	0
Hexagonal shape (outer corners)		5	0

TABLE 1.5

MAXIMUM FUEL ELEMENT TEMPERATURE

	Temperature, °F
Average Maximum Surface Temperature (reference)	2210
Plus Built-in Temperature Deviations	120
Maximum Calculated Surface Temperature	2330
Plus Allowances	
Fabrication tolerance	100
Measurement uncertainty	70
Total	170
Maximum Estimated Surface Temperature	2500
Plus Internal Temperature Rise	30
Maximum Fuel Element Temperature	2530

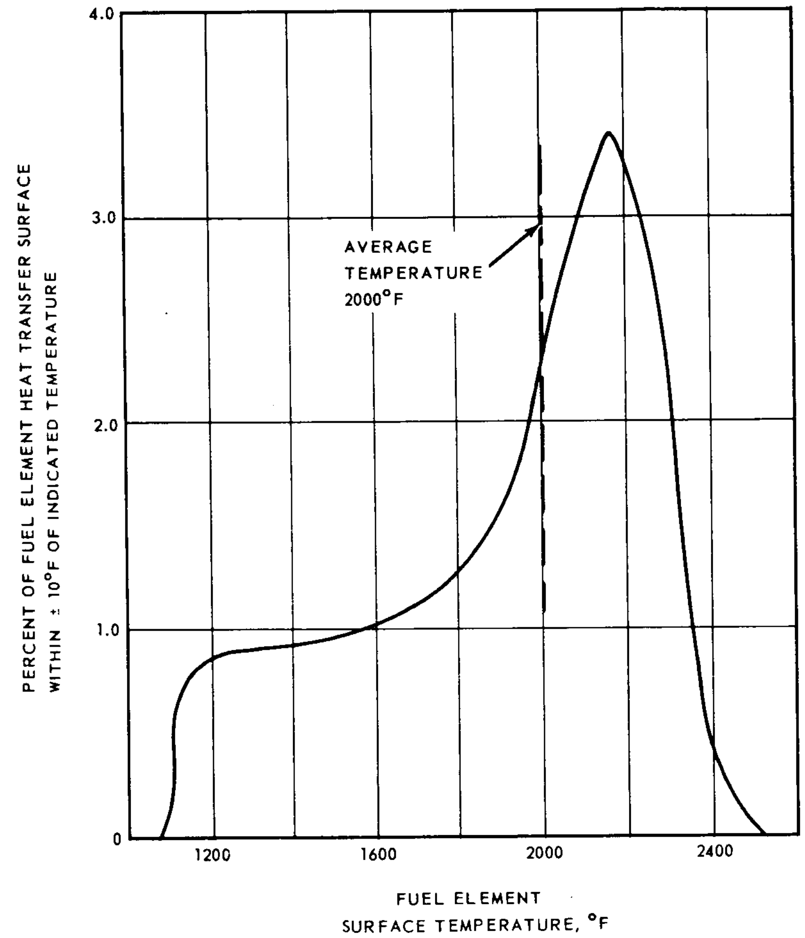

Fig. 1.26 – Percentage of total fuel tubes with heat transfer area operating at indicated temperature

A typical component is the radial reflector. Heating rates may vary as indicated earlier and as again shown in Figure 1. 27. In addition to the heating variation, the design objective is for the temperature to decrease linearly from the inner face next to the active core by about 1000°F to the temperature of structural materials in contact with the outer surface of the reflector. The problem of sizing and spacing coolant holes becomes quite complex. If the reflector is comprised of many small elements the assumptions regarding assembled conditions become significant, i. e., are adjacent elements in good thermal contact or are they separated by an air gap. Such effects are indicated in Figure 1. 28 in which an over-all or gross conductance is shown to be very significantly affected by air gap assumptions. The complexity requires use of numerical approximations for solution of the temperature equations and involves node models such as shown in Figure 1. 29. Typical results obtained by using digital computers for actual computations are shown in Figures 1. 30 and 1. 31. Data are shown for different axial positions. Also, the effect of a 0. 001-inch gap between elements is demonstrated. With perfect contact, i. e., zero thermal resistance, more heat is conducted from the active core.

Nature of temperature distribution problems after reactor shutdown that were earlier indicated are shown in Figure 1. 32. Note that the fuel element temperatures decrease continuously, whereas regions of the reflector a short distance away from the inner surface and adjacent to the outer surface at first increase and later decrease. The time response as a function of axial distance for a particular radial location is shown in Figure 1. 33.

Some problems involve questions of controlling heat flow between gases flowing at markedly different temperature levels. These problems are then like conventional heat exchanger problems, but complicated by internal heat generation. In one ANP ceramic reactor a metallic aft support for the active core was required to operate at temperatures several hundred degrees F less than the active core. In the design that evolved, Figure 1. 34, air from the active core passed axially through tubes integrally connected to transverse plates. Coolant air flowed radially inward between the transverse plates and over the outside of the connecting tubes. Hence, the configuration is somewhat like a short cross flow heat exchanger. Again, numerical approximations were used to compute temperatures as shown in Figure 1. 35. Also, because of differences in heating rates, difficulty is experienced in maintaining the two transverse plates at equal temperatures.

In the aft retainer, in addition to the heating rate uncertainties, uncertainties in predicting the local air temperature enter into an uncertainty

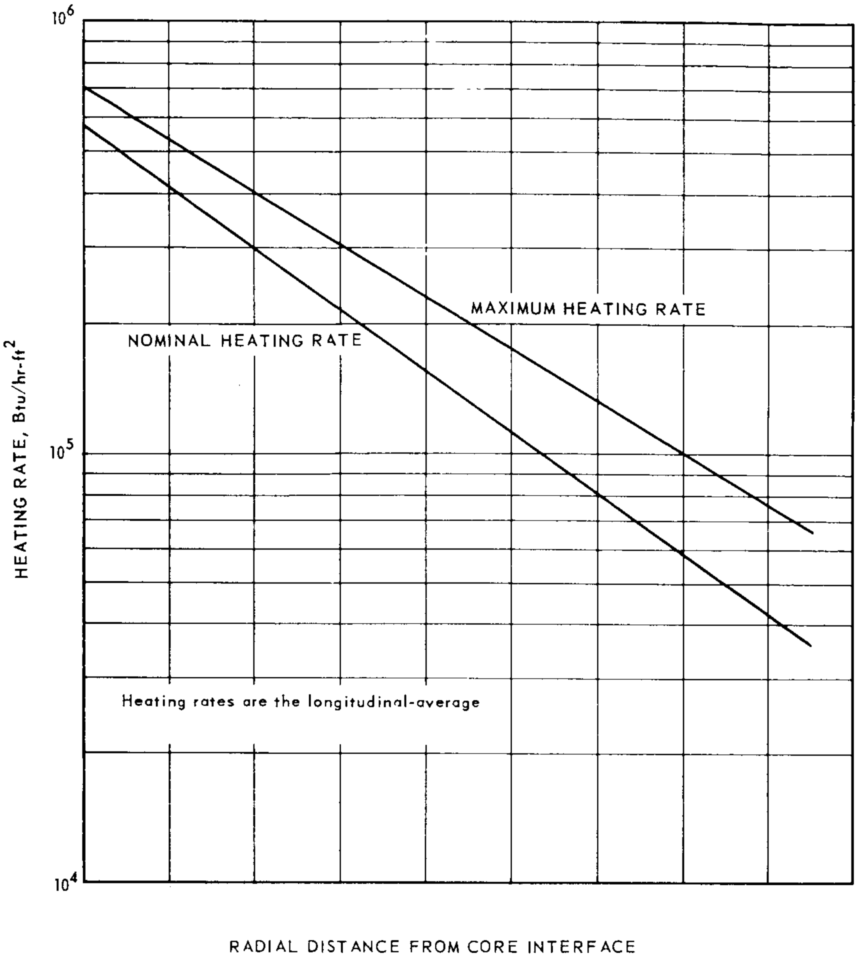

Fig. 1.27 – Secondary heating rates in the outer-reflector

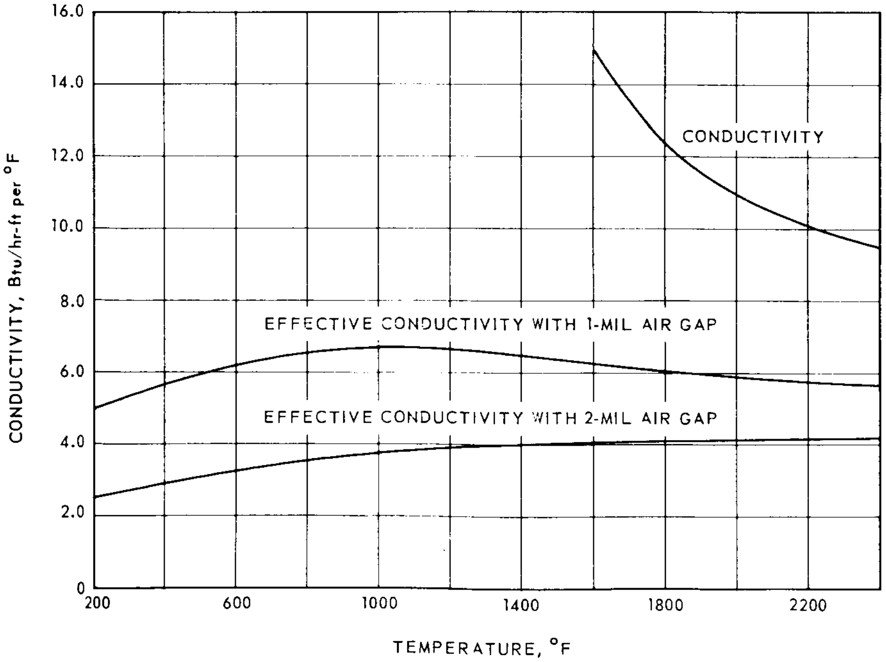

Fig. 1.28 – Effect of contact resistance on conductivity of BeO hexagonal tubes

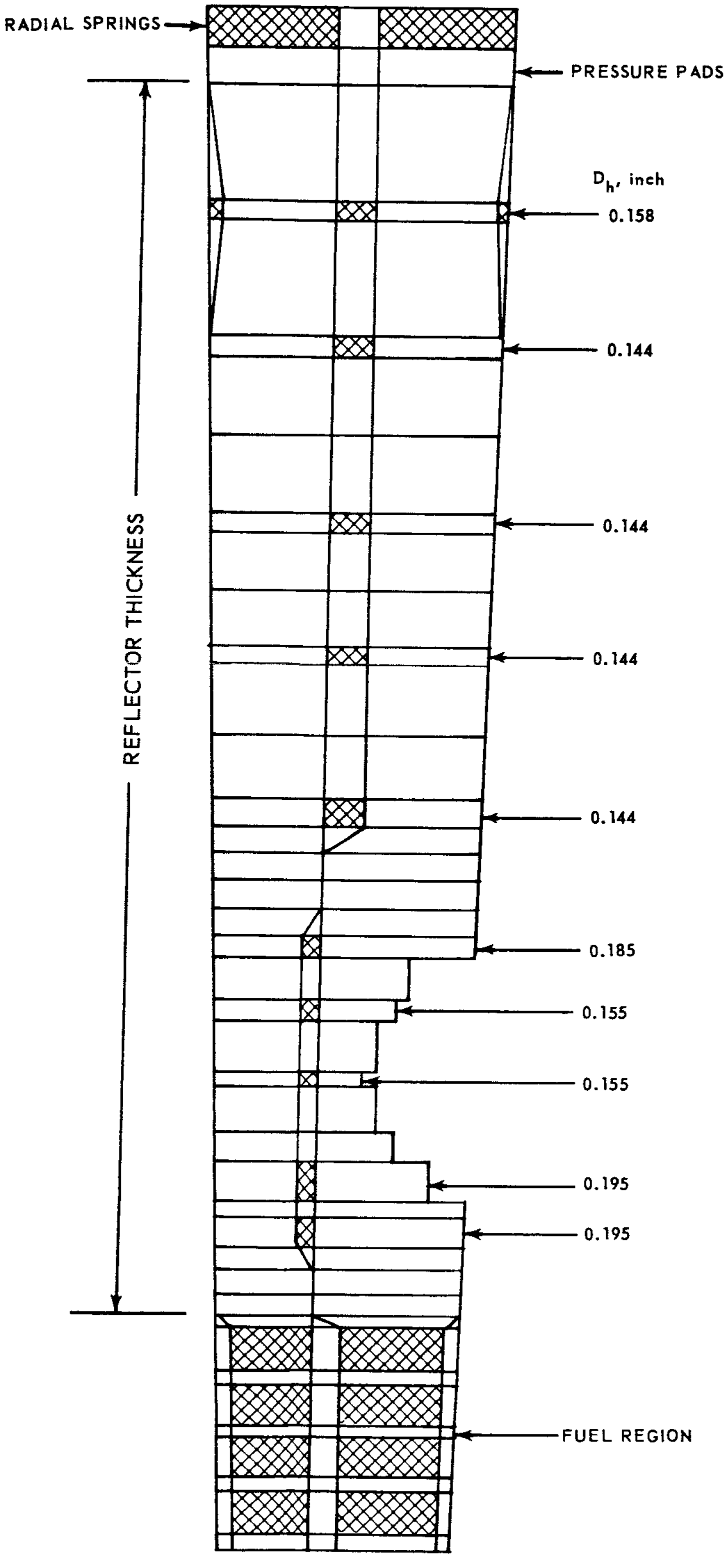

Fig. 1.29 – Outer reflector nodes used in FANTAN analysis

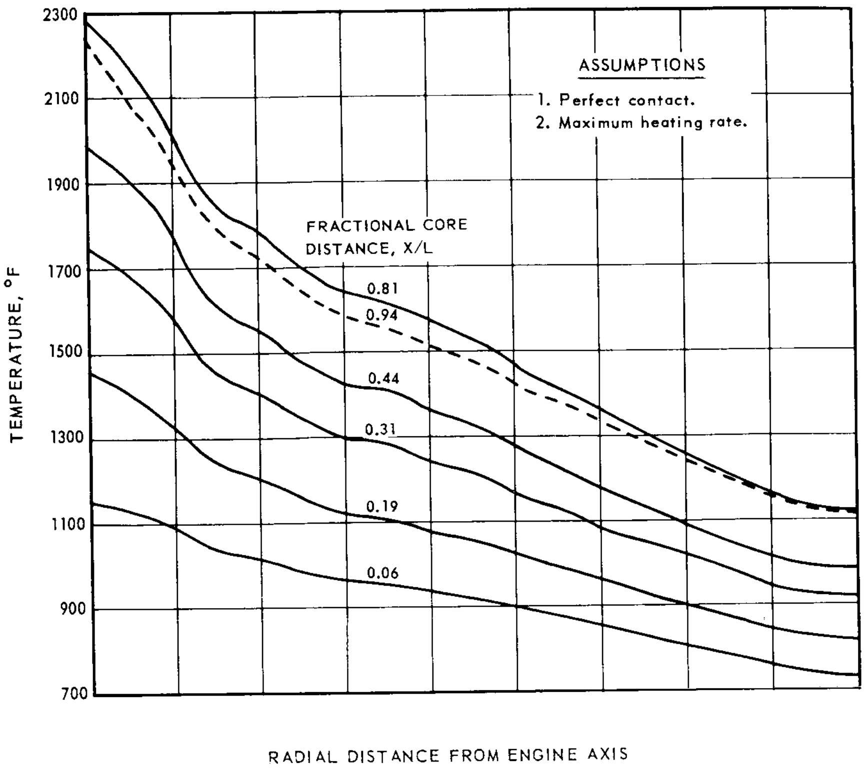

Fig. 1.30 – Typical radial temperature distribution in the outer reflector

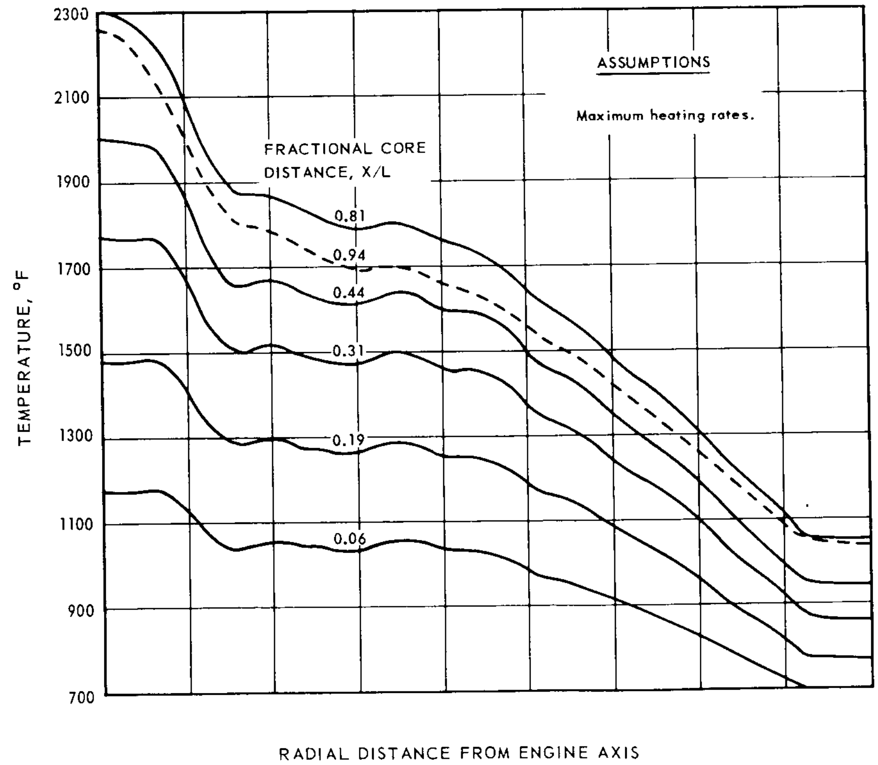

Fig. 1.31 – Effect of 0.001-inch air gap on radial temperature distribution in outer reflector

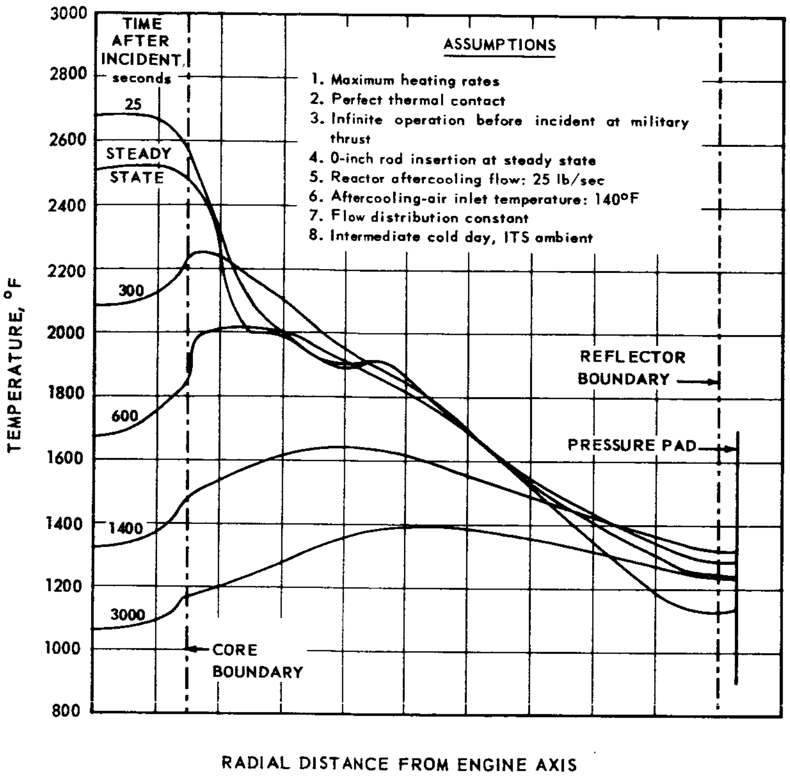

ASSUMPTIONS

1. Maximum heating rates
2. Perfect thermal contact
3. Infinite operation before incident at military thrust
4. 0-inch rod insertion at steady state
5. Reactor aftercooling flow: 25 lb/sec
6. Aftercooling-air inlet temperature: 140°F
7. Flow distribution constant
8. Intermediate cold day, ITS ambient

Fig. 1.32 – Outer reflector radial temperature distribution following locked rotor scram

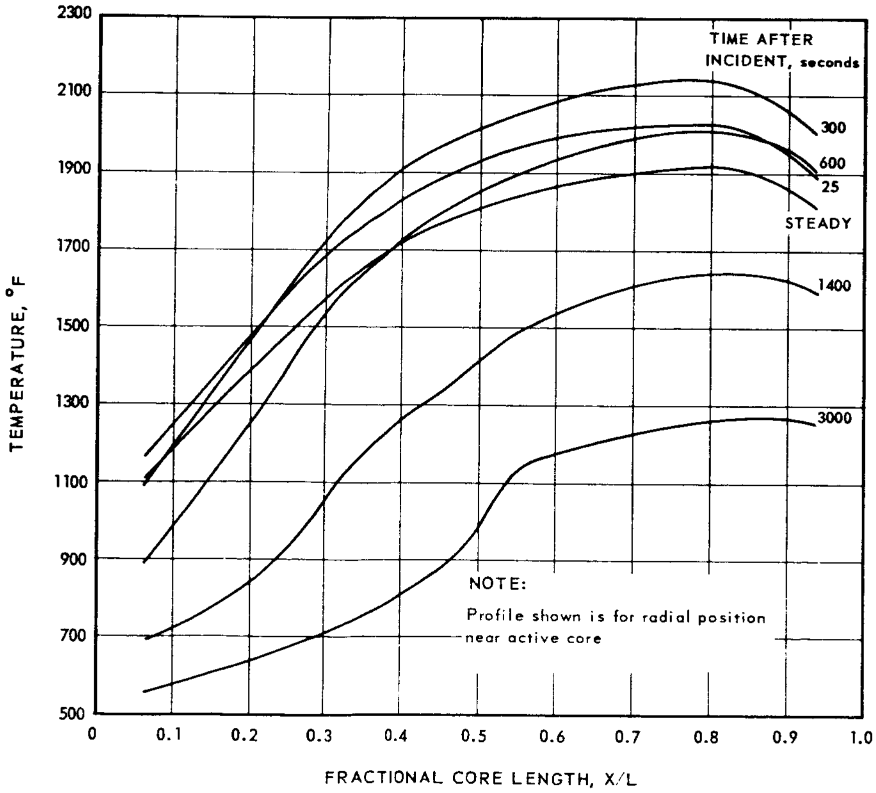

NOTE:

Profile shown is for radial position near active core

Fig. 1.33 – Outer reflector longitudinal temperature profile following locked rotor scram

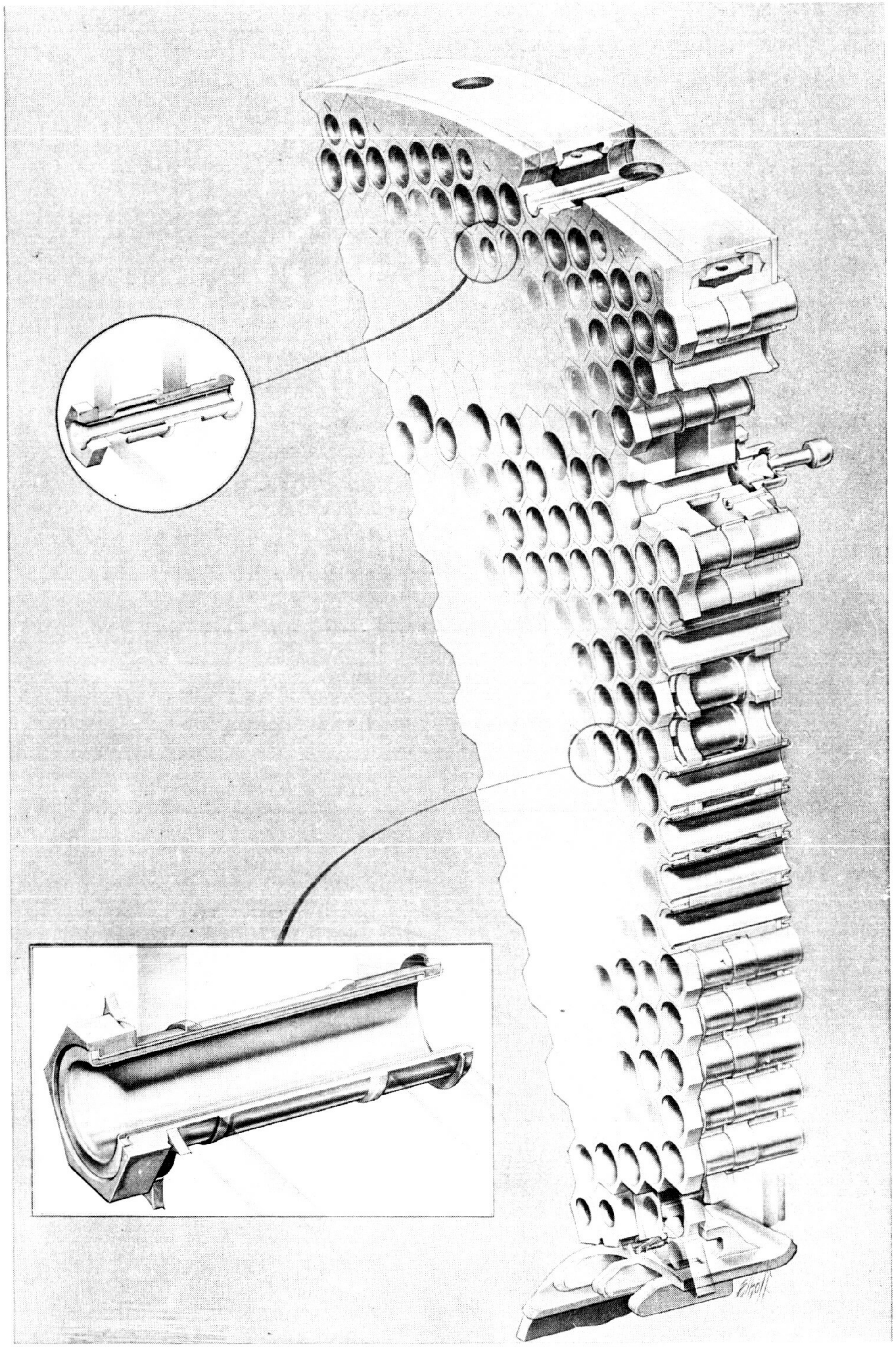

Fig. 1.34 – Sector of 140E aft-retainer assembly (Neg. DI-533)

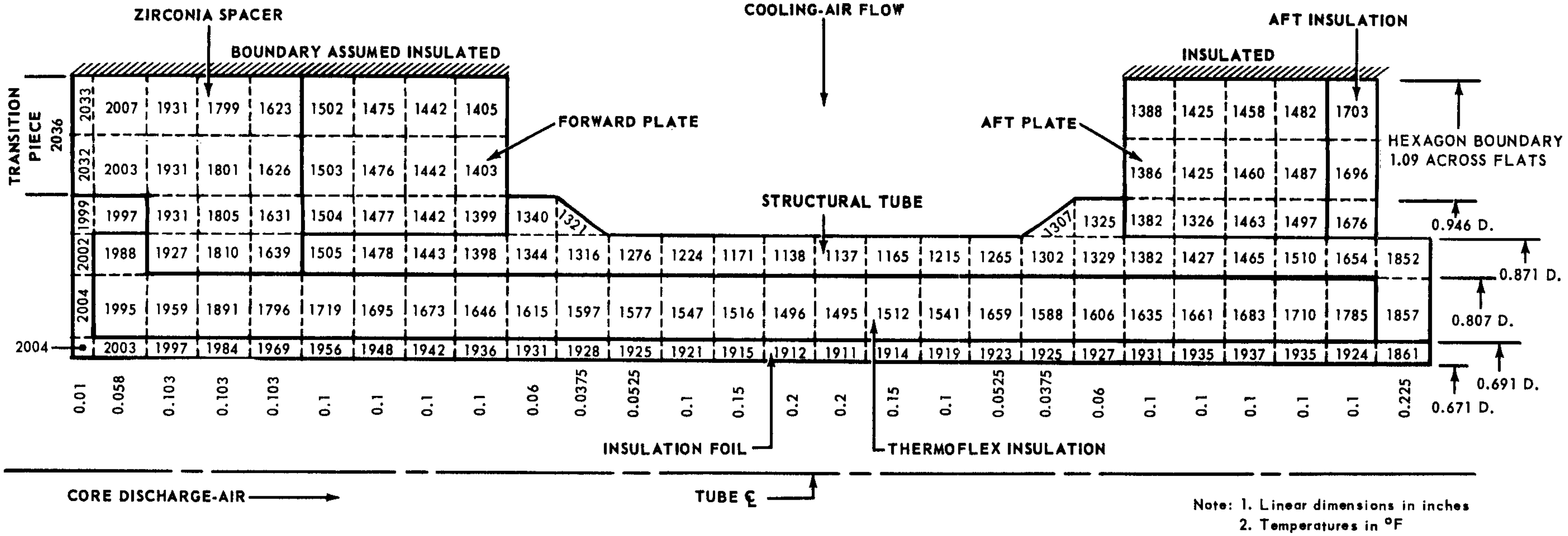

Fig. 1.35 – Temperature distribution surrounding the hottest tube of the aft-retainer assembly.

in predicting the component temperature. This is illustrated in Figure 1.36.

Many additional examples are included in ANP reports. Included are such reactor components as springs, end reflectors, pressure shells, and control rods, and other power plant components such as shield and structure.

1.4.6 Temperatures After Shutdown

We have already indicated temperature responses in the outer reflector following a reactor scram. Here, we will identify the nature of fuel element time-temperature relationships to indicate some of the interdependence among thermal, system, and control design.

If the reactor is shut down suddenly, i.e., scrammed, and simultaneously, flow is cause to cease, the afterheat that we identified earlier will cause components to increase in temperature - rapidly at first and then at decreasing rate - as shown in Figure 1.37. In going from ANP reactors to nuclear rocket engines, the power per unit of heat capacity will generally increase several fold and the temperature time curves will become significantly steeper. Common practice in the ANP designs was to provide an auxiliary source of coolant to be used for afterheat removal in case of sudden cessation of flow from the primary source. As shown in Figures 1.38 and 1.39, the temperature increases shown in Figure 1.37 are terminated by this flow at levels which are fairly sensitive to the flow rate. For flows in the order of 10 percent of primary flow, i.e., 35 or more, the temperature increase is limited to a few hundred degrees F. If the flow is limited to in the order of 1 percent the temperature increase is in the order of 1000°F.

Actually, with a turbojet the normal situation is that flow is provided at a decreasing rate during an engine coastdown that extends in time until the afterheat in the fuel elements has decayed appreciably. If the auxiliary system has been sized for the abnormal situation of no engine coastdown, and as indicated in Figure 1.40, engine coastdown will reduce the temperature in a minute or two to a fraction of the steady state value after which the auxiliary system easily maintains that low temperature. Actually, as indicated in Figure 1.41, the auxiliary system can be operated at a fraction of its capacity if the temperature after engine coastdown is allowed to rise back to its original value.

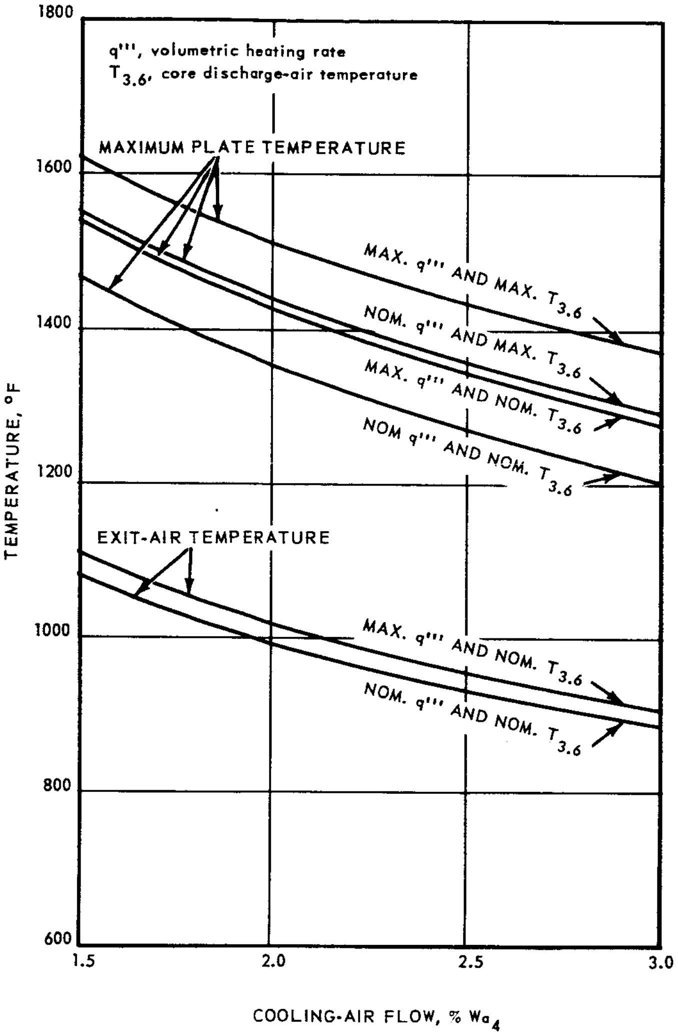

Fig. 1.36 – Parametric study of thermal performance, aft-retainer assembly

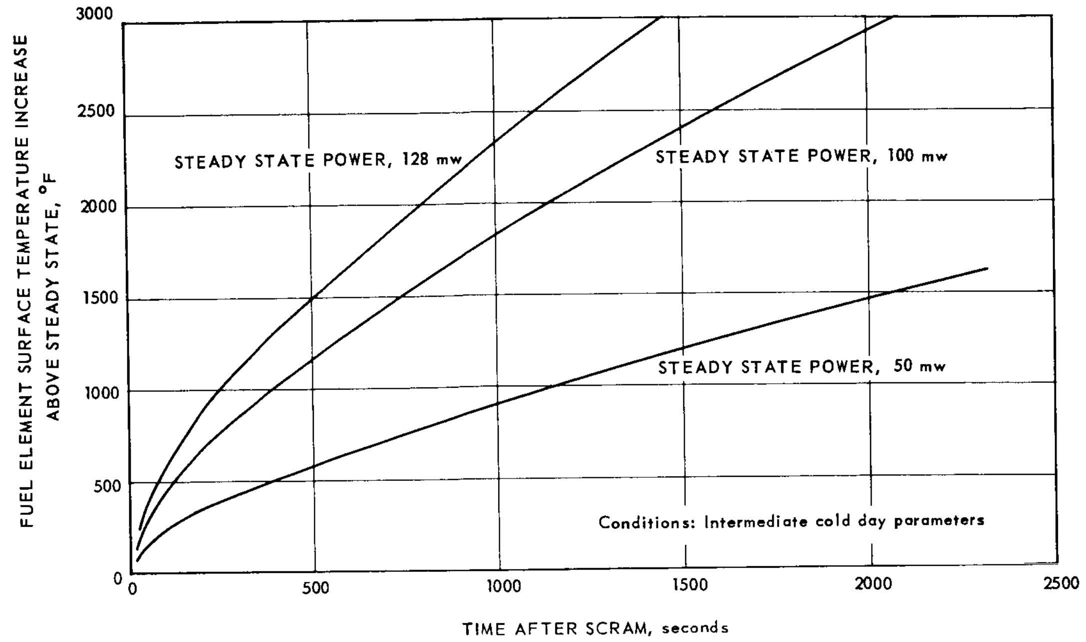

Fig. 1.37 – Increase in fuel element average-channel maximum surface temperature in absence of aftercooling air

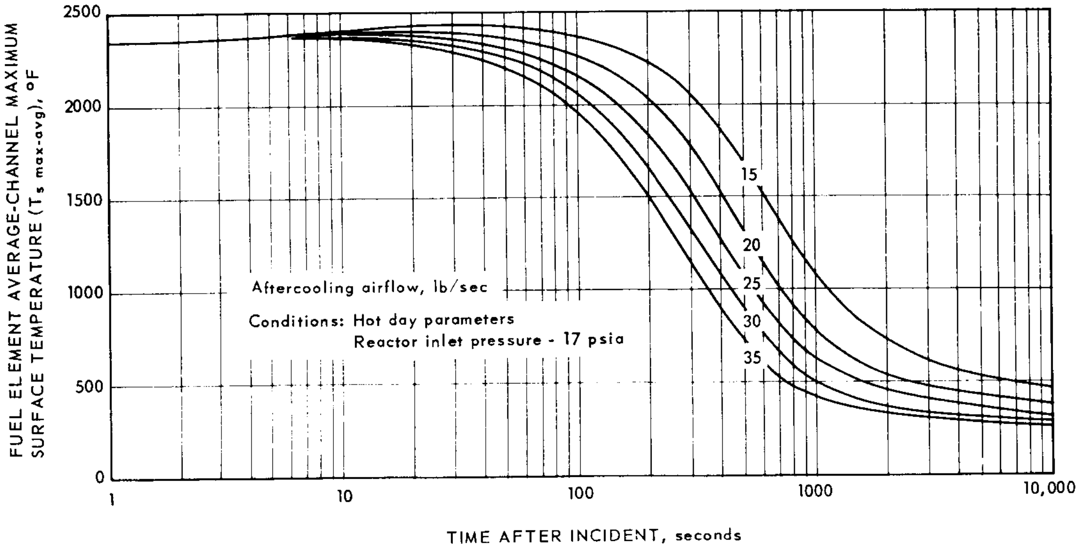

Fig. 1.38 – Fuel element average-channel maximum surface temperature following scram caused by rotor seizure

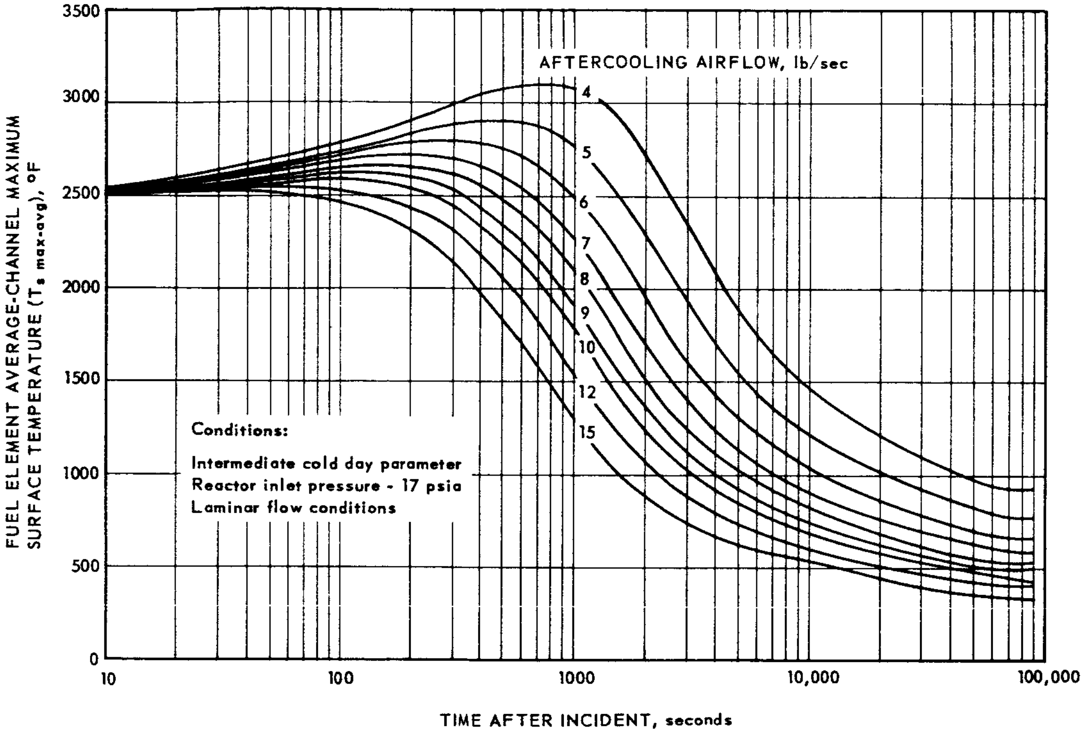

Conditions:
Intermediate cold day parameter
Reactor inlet pressure - 17 psia
Laminar flow conditions

Fig. 1.39 – Fuel element average-channel maximum surface temperature following scram caused by rotor seizure (low airflows)

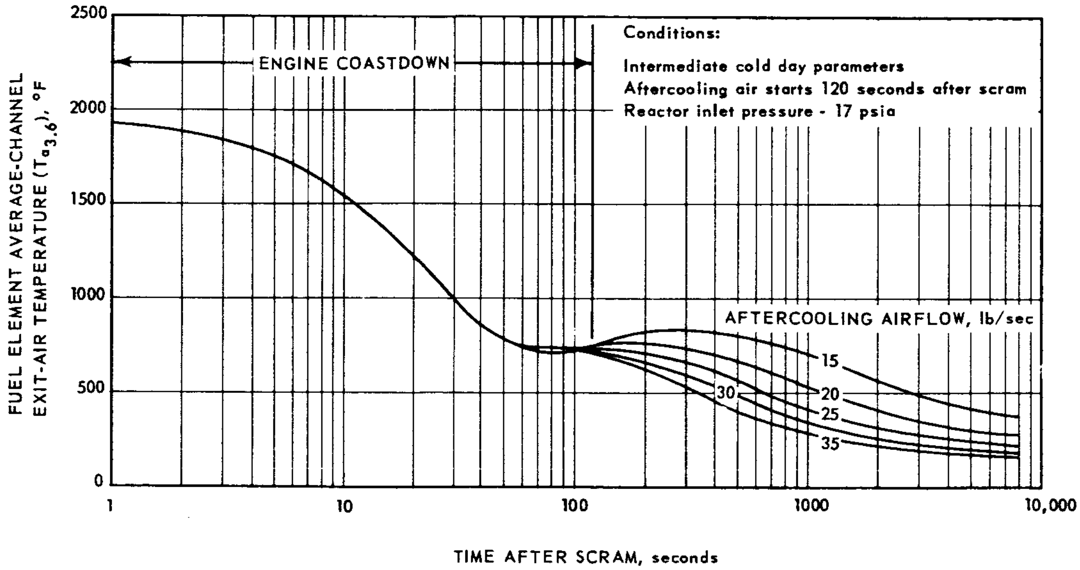

Conditions:
Intermediate cold day parameters
Aftercooling air starts 120 seconds after scram
Reactor inlet pressure - 17 psia

Fig. 1.40 – Fuel element discharge air temperature following scram followed by engine coastdown

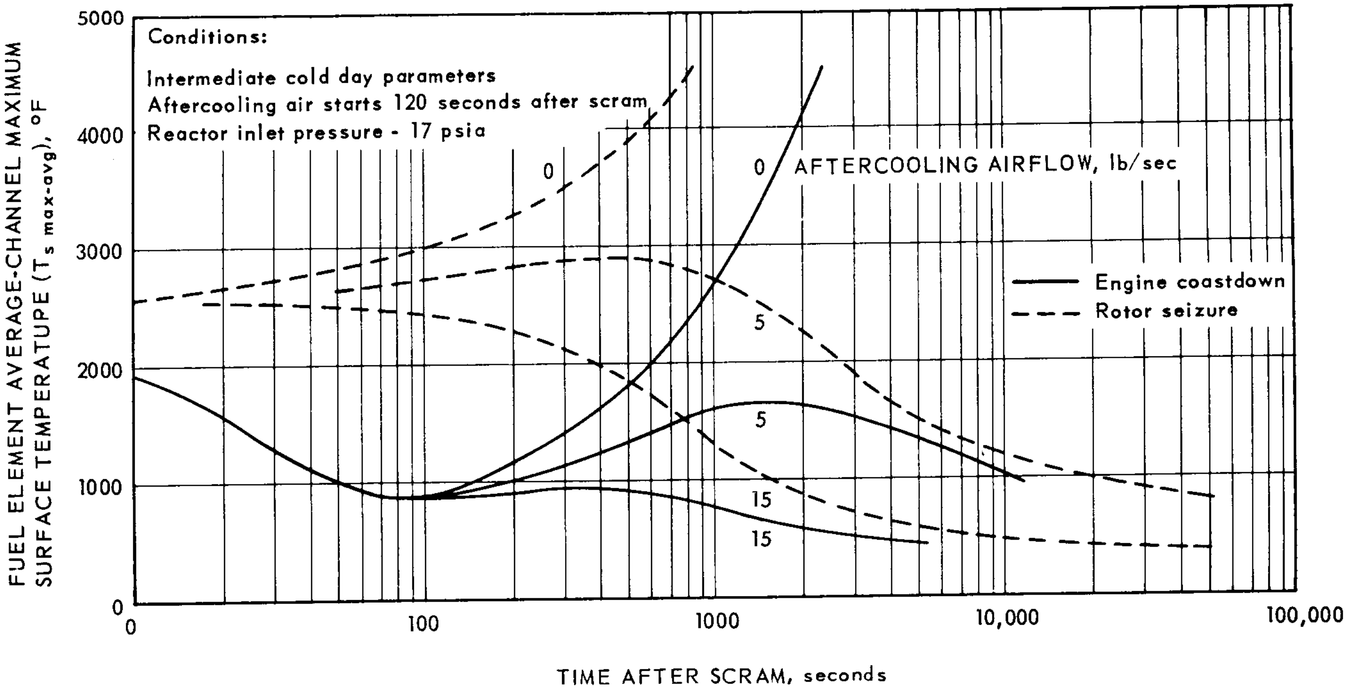

Fig. 1.41 – Fuel element average-channel maximum surface temperature following scram with low aftercooling airflow rates

2. 0 HEAT TRANSFER AND FLUID DYNAMICS

2. 1 INTRODUCTION

Heat is normally defined thermodynamically as that energy which is in transit by virtue of a temperature difference. Heat thus defined cannot be "stored" and should not be confused with internal energy, enthalpy, etc. The study of heat transmission is concerned with temperature as a function of time and with heat transfer rates as a function of time.

Heat transfer is by three different mechanisms, each described by its own rate equation. Solution of heat transfer problems requires utilization of those rate equations in combination with an energy balance.

2. 1. 1 Heat Conduction

Heat conduction includes processes in both solids, and liquids and gases. In solids, conduction is thought of in terms of transfer of thermal energy from one molecule to another. There is no macroscopic flow of material. In gases, even in a state of rest, molecules are in constant motion and heat conduction may be thought of as due to elastic impacts.

The basic law of heat conduction, known as Fourier's Law, is

$$q = k \frac{A}{L} \Delta T \qquad (1)$$

where

q is heat transfer rate, e. g., $\frac{\text{Btu}}{\text{hr}}$

ΔT is a temperature difference, e. g., $^{\circ}$F

L is a length in the direction of heat flow, e. g., ft.

A is the area perpendicular to the direction of heat transfer through which q is transferred, e. g., ft^2

k is thermal conductivity; to satisfy the equation, k has units of (Btu) / (hr) - (ft^2/ft) - ($^{\circ}$F)

The law of heat conduction is analagous to the law of electrical conduction

$$I = \frac{E}{R} \qquad (2)$$

Hence, q is analagous to electrical current I, T to voltage E, and the thermal resistance $\frac{L}{kA}$ to electrical resistance R.

2. 1. 2 Convection

The second mode of heat transfer, convection, occurs in liquids and gases wherein the normal concern is the transfer of heat from the surface of a solid to the fluid. In 1701 Newton recommended the following equation for heat convection

$$q = hA\Delta T = hA\,[T_s - T_b] \quad (3)$$

Although this equation is often known as "Newton's cooling law," it actually is a definition of h, the coefficient of heat transfer, or unit convection conductance. Units for h are the same as for k/L, e. g., (Btu)/(hr)(ft)(^{o}F).

Convection is the transfer of heat from one point to another within a fluid due to the motion of the fluid. Convection is generally thought of as a macroscopic molecular process while conduction is a microscopic process.

2. 1. 3 Heat Radiation

The third and last mode of heat transfer is that of radiation. Solid bodies, as well as liquids and gases, are capable of radiating thermal energy in the form of electromagnetic photons (e. g., "infrared" heat), and of picking up radiant energy by absorption of photons. Heat transfer by radiation in the case of a black body, i. e., a perfect radiator, is according to

$$q = \sigma A T^4 \quad (4)$$

where σ is a natural constant known as the Stephan-Boltzmann Constant. In engineering calculations for radiation between bodies it is necessary to account for both departure of the bodies from perfect radiators and the angle by which surfaces "see" each other. The equation normally utilized is

$$q = \sigma A F_A F_\epsilon\,[T_1^4 - T_2^4] \quad (5)$$

where

A = area of one of the two surfaces, ft^2

F_A = the angle coefficient by which surface "A" sees the other surface

F_ϵ = the emissivity coefficient which takes into account the departure of both surfaces from perfect blackness

T = absolute temperature, ^{o}R

q = total energy transferred, Btu/hr

$\sigma = 0.173 \times 10^{-8}$ Btu/ft^2 - hr - ^{o}R^4

2. 1. 4 Resistance Concept - Thermal Circuit

The resistance concept and associated thermal circuits may be helpful, and are based on the fact that all three rate equations can be manipulated to the form of

$$q = \frac{\Delta T}{R} \qquad (6)$$

where R equals

for conduction $\frac{L}{kA}$

for convection $\frac{1}{hA}$

for radiation $\frac{1}{h_r A}$

The unit conductance for radiation, h_r, is derived by letting

$$q = h_r A\,[T_1 - T_2] = \sigma\ A\ F_A F_\epsilon\,[T_1^4 - T_2^4] \qquad (7)$$

$$h_r = \sigma\ F_A\ F_\epsilon\,[T_1^2 + T_2^2]\ [T_1 + T_2] \qquad (8)$$

$$\text{if } T_1 \rightarrow T_2 = T_{avg}$$

$$h_r \rightarrow 4\ \sigma\ F_A F_\epsilon\ T_{avg}^3 \qquad (9)$$

Analagously to electrical circuits, thermal circuits can be drawn and similar equations written, For purely resistive circuits, both electrical and thermal

$$q = \frac{\Delta T_{total}}{R_{overall}} \qquad (10)$$

where $R_{overall}$ will be of the form

$$R_{overall} = R_1 + R_2 + \frac{1}{\frac{1}{R_3} + \frac{1}{R_4}} \qquad (11)$$

or more generally

$$R_{overall} = \sum_{series} R + \frac{1}{\sum_{parallel} \frac{1}{R}} \qquad (12)$$

In heat transfer $1/R_{\text{overall}}$ is known as overall conductance, U, and the overall rate equation is $q = U A \Delta T_{\text{total}}$ where, if several areas are involved, A may be selected arbitrarily but the product UA will be the same for any selection of A. If transient conditions are imposed, just as in electrical circuits, capacitances must be added, i. e., temperature build-up in a material is analagous to the voltage buildup in an electrical capacitor. Generation of heat within a body due to electrical resistance heating or to nuclear fission in a reactor corresponds to a current source in an electrical circuit.

2. 2 CONDUCTION

2. 2. 1 Differential Equations

The general heat conduction equation is derived by writing an energy balance on a differential volume followed by a substitution of appropriate rate equations. The energy balance is

$$dq_{\text{in}} + dq_{\text{generated}} = dq_{\text{energy storage}} + dq_{\text{out}} \tag{13}$$

In x, y, z coordinates, dq_{in} in the x direction is

$$dq_x = -\,k\,[dy \cdot dx]\,\frac{\partial T}{\partial x} \tag{14}$$

dq_{out} in the x direction at the opposite face will be

$$dq_{x+dx} = -\,k\,[dy \cdot dx]\left[\frac{\partial T}{\partial x} + \frac{\partial}{\partial x}\,\frac{\partial T}{\partial x}\,dx\right] \tag{15}$$

$$dq_{\text{generated}} = q''' \,dx\,dy\,dz \tag{16}$$

where q''' = heat generated per unit volume.
The energy storage term will be

$$dq_{\substack{\text{energy}\\ \text{storage}}} = \rho\, C_p\, dx\,dy\,dz\,\frac{\partial T}{\partial \tau} \tag{17}$$

where ρ is density
C_p is specific heat
τ is time

When all rate equations are substituted into the energy balance equation the following general conduction equation results

$$\frac{\partial^2 T}{\partial x^2} + \frac{\partial^2 T}{\partial y^2} + \frac{\partial^2 T}{\partial y^2} + \frac{q'''}{k} = \frac{1}{\alpha}\,\frac{\partial T}{\partial \tau} \tag{18}$$

where $$\alpha = \frac{k}{C_p \rho} \qquad \frac{ft^2}{hr} \tag{19}$$

and k is assumed constant.

The term σ is called thermal diffusivity.

Using the operator form

$$\nabla^2 = \frac{\partial^2}{\partial x^2} + \frac{\partial^2}{\partial y^2} + \frac{\partial^2}{\partial z^2} \tag{20}$$

the general equation is sometimes written

$$\frac{\partial T}{\partial \tau} = \alpha \, \nabla^2 T + \frac{q'''}{\rho \, C_p} \tag{21}$$

If there is no internal generation of heat the resulting equation, Fourier's equation, is

$$\frac{\partial T}{\partial \tau} = \alpha \, \nabla^2 T \tag{22}$$

Further, for steady state the equation reduces to Laplace's equation

$$\nabla^2 T = 0 \tag{23}$$

With internal heating and steady-state heat transfer, the general equation reduces to Poisson's equation

$$\nabla^2 T = -\frac{q'''}{k} \tag{24}$$

The generalized equation has few practical solutions for problems in three dimensions. Solutions to three dimensional problems can be approximated by simplifications and solution of circuit equations. By using analogous electrical circuits, wherein electrical elements simulate "lumped" values of thermal characteristics, temperatures can be determined by measuring analogous voltages. If a fine subdivision is desired, i. e., computation of temperatures at many locations, finite difference approximations to the differential equations can be made and numerical solutions obtained. Frequently, digital computers will be used and make possible numerical solutions for complex problems with a high degree of accuracy.

One-dimensional transient heat flow problems and two-dimensional steady-state problems have long been popular in mathematics and heat-transfer textbooks. But even here application to reactor thermal design, because of configuration and boundary condition complexities, may result in approximations because of a necessity to approximate the actual problem.

2.2.2 One-Dimensional Conduction With Internal Heating

Problems of heat flow in plate type fuel elements and other reactor components sometimes can be closely approximated by a simple plate model with uniform internal heating.

2.2.2.1 Slab

Consider a plate with thickness L that is perfectly insulated on the surface at x = L. The differential equation is

$$\frac{d^2T}{dx^2} = -\frac{q'''}{k} \tag{25}$$

Integration yields

$$\frac{dT}{dx} = -\frac{q'''}{k}\, x + C_1 \tag{26}$$

$$T = -\frac{q'''}{k}\,\frac{x^2}{2} + C_1 x + C_2 \tag{27}$$

Applying boundary conditions

1. $$\left[\frac{dT}{dx}\right]_L = 0 = -\frac{q'''L}{k} + C_1 \tag{28}$$

$$C_1 = \frac{q'''L}{k} \tag{28a}$$

2. $$T_0 = T_1 = +C_2 \tag{29}$$

we find that

$$T - T_1 = -\frac{q'''}{2k}\, x^2 + \frac{q'''L}{k}\, x = \frac{q'''L^2}{2k}\left[2\,\frac{x}{L} - \frac{x^2}{L}\right] \tag{30}$$

and

$$T_2 - T_1 = \frac{q'''L^2}{2k} = 2\,\Delta T_1 \tag{31}$$

Sometimes dimensionless groupings are used

$$\frac{k\,\Delta T}{q'''L^2} = \frac{1}{2}\,; \tag{32}$$

$$\frac{k(T - T_1)}{q'''L^2} = 2\left[\frac{x}{L}\right] - \left[\frac{x}{L}\right]^2 \tag{33}$$

A straightforward exercise that may provide additional feel for conduction problems in reactor components is to again consider a slab, but allow q''' to be a function of x. Cylindrical shells, e.g., pressure vessels and shield components, can often be studied with a flat slab approximation because the thickness is small compared to the mean diameter. The volumetric heating rate decreases with distance from the active core and can be approximated by an exponential function. The slab approximation becomes

$$\frac{d^2T}{dx^2} = -\frac{q_0'''}{k}\,e^{-\mu x} \quad (\mu = \text{constant}) \tag{34}$$

where q_0''' occurs at x = 0. Three sets of boundary conditions that can be considered are

1. All heat flow to surface at x = 0
2. All heat flow to surface at x = L
3. Equal heat flow to both surfaces.

Items of interest for comparison are the maximum temperatures and mean, or volumetric average, temperatures. As we observed earlier, ratios of q_0'''/q_L''' are commonly as great as two and may be in the order of ten.

2.2.2.2 Rod

Next consider a circular rod of radius R. In cylindrical coordinates the differential equation is

$$\frac{d^2T}{dr^2} + \frac{1}{r}\frac{dT}{dr} = -\frac{q'''}{k} \tag{35}$$

By introducing a new variable, T'

$$T' = T + \frac{q'''r^2}{4k} \quad \text{or} \quad T = T' - \frac{q'''r^2}{4k} \tag{36}$$

we obtain

$$\frac{d^2T'}{dr^2} - \frac{q'''}{2k} + \frac{1}{r}\left[\frac{dT'}{dr} - \frac{q'''r}{2k}\right] = - \frac{q'''}{k}$$

$$\frac{d^2T'}{dr^2} + \frac{1}{r}\,\frac{dT'}{dr} = 0 \qquad (37)$$

A general solution of this equation is

$$T' = M \ln r + N \qquad (38)$$

which can be derived by introducing $W = dT'/dr$

In applying boundary conditions we recognize that for T and hence T' at r = 0 to be finite M must be equal to zero. Hence,

$$T' = N = T + \frac{q'''r^2}{4k}$$

and

$$T = N - \frac{q'''r^2}{4k} \quad ; \quad N = T_R + \frac{q'''R^2}{4k} \qquad (39)$$

$$T - T_R = \frac{q'''R^2}{4k}\left[1 - \frac{r^2}{R^2}\right] \qquad (40)$$

$$T_0 - T_R = \frac{q'''R^2}{4k} \qquad (41)$$

In nuclear reactor fuel element studies a criterion for comparing configurations may be internal temperature differences for equal surface heat fluxes. For energy to be conserved at the surface this means equal internal temperature gradients at the surface. A comparison of a slab with a rod is as follows.

$$\frac{dT}{dx} = - \frac{q'''}{k}\,x + \frac{q'''L}{k} \qquad \text{Slab} \qquad (42)$$

$$\left.\frac{dT}{dx}\right]_{x=0} = \frac{q'''L}{k} \qquad (43)$$

$$\frac{dT}{dr} = \left[\frac{q'''R^2}{4k}\right]\left[-\frac{2r}{R^2}\right] \qquad \text{Rod} \qquad (44)$$

$$\left.\frac{dT}{dr}\right]_{r=R} = \frac{q'''R}{2k} \tag{45}$$

$$\left.\frac{dT}{dx}\right]_{o} = -\left.\frac{dT}{dr}\right]_{R} = \frac{q'''L}{k} = \frac{q'''R}{2k} \tag{46}$$

$$R = 2L \tag{46a}$$

$$\frac{\left[T_o - T_R\right]_{\text{rod}}}{\left[T_2 - T_1\right]_{\text{slab}}} = \frac{\left[\frac{q'''L^2}{2k}\right]}{\left[\frac{q'''R^2}{4k}\right]} = \frac{\left[\frac{L^2}{2}\right]}{\left[\frac{R^2}{4}\right]} = 2\,\frac{L^2}{R^2} \tag{47}$$

$$\frac{\left[T_o - T_R\right]_{\text{rod}}}{\left[T_2 - T_1\right]_{\text{slab}}} = \frac{1}{2} \qquad \text{for equal surface heat fluxes} \tag{48}$$

Even though for this criterion a rod appears to have an advantage, it may not be chosen because of difficulties of providing a flow passage for convection from the surface to the fluid without undue complication of the reactor design.

2. 2. 2. 3 Thick-Wall Cylinder

Thick wall cylinders are also common configurations, perhaps even more so than slabs and rods. Consider a cylinder with uniform volumetric heating with inner radius r_1 and outer radius r_2. The general solution derived in cylindrical coordinates is applicable

$$T' = M \ln r + N \tag{37}$$

$$T' = T + \frac{q'''r^2}{4k} \tag{36}$$

$$T = M \ln r + N - \frac{q'''r^2}{4k} \tag{49}$$

Because the heat is normally removed from the inner surface only, we will consider as boundary conditions

$$T = T_1 \quad \text{at} \quad r = r_1$$

$$\frac{dT}{dr} = 0 \quad \text{at} \quad r = r_2$$

$$\frac{dT}{dr} = \frac{M}{r} - \frac{q'''r}{2k} \tag{50}$$

$$\left.\frac{dT}{dr}\right]_{r_2} = \frac{M}{r_2} + \frac{q'''r_2}{2k} \tag{51}$$

$$M = \frac{q'''{r_2}^2}{2k} \tag{51a}$$

$$T_1 = \frac{q'''{r_2}^2}{2k} \ln r_1 + N - \frac{q'''{r_1}^2}{4k} \tag{52}$$

$$N = T_1 - \frac{q'''{r_2}^2}{2k} \ln r_1 + \frac{q'''{r_1}^2}{4k} \tag{52a}$$

$$T - T_1 = \frac{q'''{r_2}^2}{2k} \ln r - \frac{q'''{r_2}^2}{2k} \ln r_1 + \frac{q'''{r_1}^2}{4k} - \frac{q'''r^2}{4k}$$

$$= \frac{q'''}{4k} \left[{r_1}^2 - r^2 + {r_2}^2 (\ln r - \ln r_1)\right] \tag{53}$$

$$T - T_1 = \frac{q'''{r_1}^2}{4k} \left[1 - \frac{r^2}{{r_1}^2} + \frac{{r_2}^2}{{r_1}^2} \ln \frac{r^2}{{r_1}^2}\right]$$

$$T_2 - T_1 = \frac{q'''{r_1}^2}{4k} \left[1 - \frac{{r_2}^2}{{r_1}^2} + \frac{{r_2}^2}{{r_1}^2} \ln \frac{{r_2}^2}{{r_1}^2}\right] \tag{54}$$

Another exercise of interest that may provide useful background for thermal stress considerations in Lectures 13 and 14, Mechanical Design, is to derive an expression for the mean temperature, T_m.

2. 2. 3 Transient Heat Conduction

2. 2. 3. 1 General Comment

Even for the simplest of bodies, i. e., plates, cylinders, and spheres, solutions of transient condition equations in the absence of internal heating are series solutions, e. g., series involving Bessel and trigonometric functions.

Beginning courses in heat transfer and textbooks usually show the derivation of such solutions and tabulate or plot numerical results using dimensionless groupings. Also, finite difference equations are stated and numerical and graphical methods introduced.

In thermal design of nuclear reactors complications of configuration, internal heating, and boundary conditions are such that numerical methods are utilized almost exclusively. Finite difference equations are either derived by applying an energy balance with appropriate rate equations to a finite volume instead of to a differential volume, or by directly writing the finite difference equation corresponding to the differential equation. The result is a set of algebraic equations, one for each temperature to be computed, that must be solved simultaneously for each point in time. Quite commonly, digital computer programs are written for solution of the equations.

2. 2. 3. 2 Dimensionless Groupings

In the solutions of transient conduction problems in simple bodies four,, dimensionless groups normally evolve. These are

$$Y = \frac{T_f - T}{T_f - T_o}$$ the "relative temperature ratio" (55)

$$\frac{x}{L}$$ the "relative position ratio" (56)

$$\frac{k}{hL}$$ the "internal-external thermal conductance ratio" (57)

$$N_{F_o} = \frac{\alpha \tau}{L^2}$$ the "relative time-material-and-size ratio" (Fourier's number) (58)

where

T_f is the temperature of the fluid surrounding the body

T_o is the temperature of body, originally uniform at start, time $\tau = 0$

T is the temperature of the body at any time τ at distance x

L is a typical dimension of the body, generally measured from the center of the body to surface, in the direction of the path of heat flow, as radius or thickness

x is distance from the center of the body in the direction of heat flow

It is to be noted that y can also be expressed as

$$Y = 1 - \frac{T - T_o}{T_f - T_o} = 1 - \frac{\text{temperature rise of body at time } \tau}{\text{ultimate temperature change}} \qquad (55a)$$

2.2.3.3 Physical Interpretation of Dimensionless Groupings

The grouping k/hL is a measure of the ability of the body to transfer heat within itself compared to its ability to transfer heat to its surroundings. It then becomes a criterion for the method of solution of transient temperature problems. If k/hL is very large, say over 5, the temperatures within the body will tend to be uniform, and simplified solutions obtained by eliminating the dependence of temperature on x will be fairly accurate. If the k/hL is very small, say less than 0.1, the temperature difference between the surface and the surroundings is relatively small and fairly accurate solutions may be obtained by considering h to be infinite, i.e., by imposing boundary conditions in terms of surface temperature equal to the fluid temperature. For intermediate values the problem is general and either approximation may be inadequate.

2.2.3.4 Dimensionless Groupings Related To Reactor Design

In gas-cooled reactors large heat transfer areas are required and k/hL may tend to be large. For heteorogeneous reactors in particular, the fuel element volume may be small so that k/hL becomes large, both because of the large surface area and the small volume. Computer programs used to analyze concentric ring fuel element transient temperatures, such as for the HTRE-3 reactor, do in fact characterize the ring by a single temperature (across the thickness). In homogeneous reactors the wall becomes appreciably thicker and this simplification may no longer be valid, and generally can not be permitted in predicting temperature distributions for use in thermal stress calculations.

The grouping $\alpha\tau/L^2$ provides an indication of the time that it takes for a body to approach within a given fraction of its ultimate value. Often a time constant is defined as the time required to reach 63.2 percent of the final value, where 0.632 is the numerical value of $[1 - 1/e]$. Holding the other groupings constant, $\alpha\tau/L^2$ becomes the dominate criterion for relative temperature ratio. For fuel elements like those in HTRE-3, L will be small and the time constant will be small. However, for homogeneous ceramic reactors like the D141A-1 and the XNJ140E-1, L will be large and the time constant will be larger. Further effects are produced by effects of differences in physical properties. ANP homogeneous ceramic reactors generally had time constants several times those for heterogeneous metallic reactors with the result that in some cases different philosophies were required in design of power plant controls.

2.2.3.5 Axial Effects-Convection Is Fluid Thermal Capacity

Finally, solution of transient heat flow in nuclear reactors is further complicated by large changes in temperature of the gas coolant along the length of the reactor. Corresponding to the curves of surface temperature versus time after reactor shutdown that were viewed earlier are curves of exit gas temperature that closely parallel those of surface temperature, even though the inlet gas temperature is held constant at a low value. Hence, we can anticipate another parameter that will be a criterion for the temperature-time response of the reactor. It will be in the nature of the ratio of convective heat transfer capability to the capability of the fluid to carry thermal energy along the length of the reactor.

2.3 FLUID DYNAMICS

Our interest in fluid dynamics has two motivations. First the laws of fluid dynamics govern the reactor pressure drop, which is of concern in thermal sizing of the reactor, reactor structural design and in system design studies. Secondly, heat convection processes are intimately related to fluid flow characteristics.

2.3.1 Pressure Drop

2.3.1.1 Incompressible

Pressure loss relationships are derived in many standard references. For example, McAdams* presents essentially the following development.

Equating forces on a differential length of fluid flowing in a duct gives

$$- v\,dp = \frac{V\,dV}{\alpha g_c} + \frac{\tau_w v\,dL}{r_h} + dz\,\frac{g}{g_c} \tag{56}$$

where

v = specific volume
p = pressure
V = velocity
τ_w = tractive force at wall due to fluid friction, sometimes called wall shear stress
L = duct length
r_h = hydraulic radius = $D_h/4$
z = vertical distance above arbitrary datum
g_c = conversion factor in Newton's law of motion
g = gravitational acceleration, local
α = term to allow for variations in local velocity with radius

τ_w is conventionally eliminated by an arbitrary definition of a friction factor

$$f \equiv \frac{\tau_w}{\rho V_m^2/2\,g_c} \tag{57}$$

---

*McAdams, W. H., "Heat Transmission," McGraw-Hill Book Company, Inc., Third Edition, 1954.

then

$$- dp = \frac{G\,dV}{\alpha g_c} + \frac{f\,G^2 v\,dL}{2 g_c r_h} + \frac{dz}{v}\,\frac{g}{g_c} \tag{58}$$

$$= - dp_a - dp_f - dp_z \tag{58a}$$

where subscripts a, f, z refer to acceleration, friction and lift and $G = \rho V$

$$- dp_f = \frac{f\,G^2 v\,dL}{2 g_c\,r_h} = \frac{4\,f\,G^2 v\,dL}{2 g_c\,D_h} \tag{59}$$

is commonly called the Fanning equation.

First consider computation with incompressible flow and neglecting dp_z

$$p_1 - p_2 = \frac{1}{2}\,\frac{\rho V^2}{g_c}\,4\,f_m\,\frac{L}{D} \tag{60}$$

McAdams then recommends other approximation for gases and vapors.

for v_2/v_1 less than 2:1

$$p_1 - p_2 = \frac{G^2 (v_2 - v_1)}{\alpha\,g_c} + \frac{G^2 v_m}{2\,g_c}\,4\,f_m\,\frac{L}{D} \tag{61}$$

or alternately using perfect gas law.

$v = \dfrac{R_G T}{p}$ and letting R_G = constant

use T_m as an approximation

$$\frac{p_1^2 - p_2^2}{2 R_G T_m} = \frac{G^2}{\alpha\,g_c}\ln\frac{v_2}{v_1} + \frac{G^2}{2\,g_c}\,4\,f_m\,\frac{L}{D} \tag{62}$$

2.3.1.2 Compressible

In general we will want more accuracy and so resort to compressible flow relationships. Again standard references develop equations starting from a force balance on an incremental length of fluid. For friction without drag of stationary bodies immersed within the stream

$$\frac{dp_o}{p_o} = - \frac{\gamma M^2}{2}\left[\frac{dT_o}{T_o} + 4\,f\,\frac{dx}{D}\right] \tag{63}$$

where

M = ratio of local velocity to velocity of sound c
γ = ratio of specific heats, C_p/c_v
Subscript o refers to stagnation state, sometimes p_o, for example, is called total pressure.

If γM^2 is assumed to be a constant, this equation can be readily integrated to give

$$\ln \frac{P_{o2}}{P_{o1}} = -\frac{\gamma M^2}{2}\left[\ln \frac{T_{o2}}{T_{o1}} + 4f\frac{L}{D}\right] \tag{64}$$

Since the variation of γM^2 over the length of the reactor core generally is large enough that γM^2 cannot realistically be assumed constant, one can replace L with ΔL and compute the pressure ratio and loss over the first incremental length. By repeating the computation for all successive increments the pressure loss across the reactor core can be obtained by summing the incremental losses. This procedure was used extensively in the ANP program both for hand calculations and in programs for digital computers. Experience has shown that 10 to 15 increments give excellent accuracy. This procedure is advantageous in that fluid property variations with temperature can be approximated and that both the flow area and the hydraulic diameter can be allowed to vary from increment to increment. The latter was particularly useful for the concentric ring fuel element wherein the number of rings per fuel cell was different for different axial increments or stages. Thermal expansion can also be accounted for in the calculation by this procedure.

2.3.1.2 Compressible - Related to End Conditions

Even with the above procedure incorporated into digital computer programs, a relationship that relates pressure loss to reactor core inlet and exit conditions is desirable for illustrative purposes and, more particularly, for preliminary and parametric studies. Of several derivations available for constant flow area and hydraulic diameter, one by Fox* is of particular interest in reactor calculations.

$$\left[\frac{p_1}{p_2}\right]^2 = 1 + \frac{2\gamma_2 M_2^2}{T_2}\{T_{o2}(1+bz_2) + T_{o1}[z_2(1-b) - 1]\} + 2M_2^2 \ln[p_1/p_2] \tag{65}$$

*Fox, R. H., "An Accurate Expression for Gas Pressure Drop in High-Speed Subsonic Flow With Friction and Heating," Transactions of the ASME, Journal of Applied Mechanics, Series E, Number 4, December 1960.

where

$$b = \int_0^1 d\epsilon \int_0^{\epsilon} g(\epsilon')\, d\epsilon' \qquad (66)$$

$$z_2 = \frac{f_2 L}{a} = 4\left[\frac{f_2}{2}\right]\frac{L}{D} \qquad (67)$$

$\epsilon = x/L$

f = friction factor

$g(\epsilon)$ is the normalized power distribution function

L = tube length

a = tube radius

D = tube diameter

P = gas free stream pressure

γ = gas specific heat ratio

M = Mach number

T_o = gas stagnation temperature

By utilizing the relationship

$$\frac{T_{o2}}{T_2} = 1 + \frac{\gamma_2 - 1}{2} M_2^2$$

The above equation can be written

$$\left(\frac{p_1}{p_2}\right)^2 = 1 + 2\,\gamma_2 M_2^2 \left[\left(1 + \frac{\gamma_2 - 1}{2} M_2^2\right)\left\{(1 + bz_2) + \frac{T_{o1}}{T_{o2}}\left[z_2(1 - b) - 1\right]\right\} + \frac{1}{\gamma_2} \ln \frac{P_1}{P_2}\right]$$

This relationship both relates pressure drop to inlet and exit conditions and accounts for an arbitrary axial variation of wall heat flux. For flow through a constant area, even though the parameter z is evaluated at exit conditions only, accurate results are obtainable.

2.3.2 Fluid Dynamics Concepts

As in the case of the defining equation for the heat transfer coefficient, h, our definition of the friction factor, f, appears to be simple. However, f or the wall shear stress, is a complex function governed by the laws of fluid dynamics and fluid properties. Values of f depend on the configuration of walls that confine the fluid.

2.3.2.1 Laminar Versus Turbulent Flow

Flow of fluids is generally characterized as laminar or turbulent. In laminar flow individual particles follow smooth parallel paths determined by the shape of the physical boundaries. Turbulent flow occurs when fluid particles follow erratic paths, but the fluid mass as a whole has an average velocity in a direction determined by physical boundaries. Characteristics of the two types of flow differ markedly.

After observations that increases in flow velocity above certain magnitudes resulted in changes from laminar to turbulent flow, Osborne Reynolds in 1883 demonstrated that the criterion for transition from laminar to turbulent flow depended only on the dimensionless parameter,

$$\frac{DV\rho}{\mu} = N_{re} \text{ or } Re \tag{68}$$

where

N_{re} = Reynold's Number, dimensionless
D = Diameter, e.g., ft.
V = Velocity, e.g., ft./sec.
ρ = Density, e.g., lb./ft.^{3}
μ = Absolute viscosity, e.g., lb./sec. ft.

For laminar flow in a circular tube the radial velocity profile is parabolic, being a maximum at the axis and decreasing to zero at the walls. For turbulent flow the profile is generally flat over a large part of the diameter and then drops steeply to a value of zero at the wall. Most of the fluid dynamics literature for turbulent flow is premised on a model of the velocity profile that is subdivided into three regions. Next to the wall, within the laminar sub layer, the velocity is approximately proportional to the distance y from the wall. The central region, sometimes called the "turbulent core" the velocity profile is fairly flat and is approximately proportional to log y. The intermediate region is characterized by a rapidly decreasing slope with distance y, and is called the transition region, or buffer layer.

2.3.2.2 Velocity Profile in Circular Tube-Laminar

Typical derivations of the velocity profile in a circular tube of radius r_o start with a differential cylindrical volume of radius r and length dx. The assumption is made that pressure is a function of x only. A force balance on the element is

$$P \pi r^2 = (P + dP) \pi r^2 + \tau \, 2\pi r \, dx \tag{69}$$

or

$$\tau = - \frac{r}{2} \frac{dP}{dx} \tag{69a}$$

where τ is the shear force at radius r. Definition of absolute viscosity yields

$$\tau = - \mu \frac{dV}{dr} \tag{70}$$

hence

$$\mu \frac{dV}{dr} = \frac{r}{2} \frac{dP}{dx} \tag{71}$$

$$\int_{V_o}^{V} dV = \frac{1}{2\mu} \left[\frac{dP}{dx}\right] \int_{o}^{r} r \, dr \tag{72}$$

$$V - V_o = \frac{1}{2\mu} \left[\frac{dP}{dx}\right] \frac{r^2}{2} \tag{72a}$$

if $V = 0$ at $r = r_o$

$$\frac{dP}{dx} = - \frac{4 \mu V_o}{r_o^2} \tag{73}$$

$$V - V_o = - \frac{r^2}{r_o^2} V_o \tag{74}$$

or

$$V = V_o \left[1 - \frac{r^2}{r_o^2}\right] \tag{74a}$$

The mean velocity, V_m, can be defined in terms of the continuity equation

$$W = A_c V_m \rho \tag{75}$$

where W is mass flow and A_c is cross sectional area. Also

$$W = \int_0^{r_o} [2 \pi r\, dr] V \rho \tag{76}$$

Straightforward integration and substitution yields

$$V_m = \frac{V_o}{2} \tag{77}$$

Recall that friction factor is defined in terms of wall shear stress, τ_o, i. e.

$$\tau_w = f \frac{\rho V_m^2}{2g_c} \tag{57}$$

$$\tau_w = - \mu \left[\frac{dV}{dr}\right]_{r=r_o} = [-\mu] \left[-\frac{4V_m}{r_o}\right] \tag{78}$$

$$f \frac{\rho V_m^2}{2g_c} = \frac{4 V_m \mu}{r_o} \tag{79}$$

$$f = \frac{4\mu \cdot 2g_c}{r_o \rho V_m} \tag{79a}$$

$$= \frac{4\mu \cdot 2g_c}{\frac{D}{2} \rho V_m} = \frac{16}{\left(\frac{DV_m \rho}{\mu g_c}\right)} \tag{79b}$$

$$= \frac{16}{Re} \tag{79c}$$

Reynolds number is a ratio of inertia forces to viscous forces. Friction factor as derived here is applicable only to circular tubes. Other duct shapes require separate derivation.

2. 4 CONVECTIVE HEAT TRANSFER

2. 4. 1 Circular Tube - Laminar Flow

In a manner similar to that for velocity distribution, equations for temperature distribution can be derived. Here, typically a stationary differential volume bounded by r and r + dr, and dx in length, is utilized for an energy balance. The energy balance is $E_x + q_r = E_{x+dx} + q_{r+dr}$

where

E_x and q_r are energies into the volume at x and r respectively

E_{x+dx} and q_{r+dr} are energies out of the volume at x + dx and r + dr respectively.

The rate equations can be formulated. For example, for a perfect gas

$$E_x = 2\pi r \, dr \, V\rho \, C_p T \tag{80}$$

where several assumptions included are that

flow work is neglected
pressure is constant
dissipative effects of viscous forces are neglected

$$q_r = - k \, (2\pi r \, dx) \frac{\partial T}{\partial r} \tag{81}$$

After formulating the other two rate equations and substitution in the energy equation there results

$$\frac{\partial^2 T}{\partial r^2} + \frac{1}{r} \frac{\partial T}{\partial r} = \frac{V\rho C_p}{k} \frac{\partial T}{\partial x} = \frac{V}{\alpha} \frac{\partial T}{\partial x} \tag{82}$$

where $k/\rho C_p = \alpha$, the diffusivity and the equation is restricted to laminar flow in a circular tube with a fully established velocity profile and constant fluid properties.

Although we won't go through the mathematics here, variables can be separated and certain solutions obtained. In doing so, the heat transfer coefficient is introduced and the problem of choosing a fluid temperature must be made arbitrarily. Typically, the choice is

$$T_m = \frac{1}{A V_m} \int_A V T \, d A \tag{83}$$

Finally a solution for conditions of constant heat input is derived

$$\frac{hD}{k} = \frac{48}{11} = 4.364 \tag{84}$$

which is the Nusselt number. Dimensional reasoning gives as an identify

$$\mathrm{Nu} \equiv \mathrm{St\ Pr\ Re} \tag{85}$$

Hence

$$\mathrm{St\,Pr} = \frac{\overset{4.364}{\cancel{3.364}}}{\mathrm{Re}} \tag{85a}$$

which is in a form analagous to that for the friction factor.

The constant wall temperature solution is

$$\mathrm{Nu} = 3.658 \tag{86}$$

Other solutions with boundary conditions such that the Nusselt number varies with flow distance x, i.e., velocity and temperature profiles vary with x, are obtainable and typically involve the dimensionless grouping.

$$\frac{\mathrm{Re\ Pr}}{x/D}$$

where Re Pr is identified as the Peclet number. The Prandtl number is $\mu C_p/k$ and is a fluid properties modulus. Hence Peclet number becomes

$$\mathrm{Pe} = \mathrm{Re\ Pr} = \left[\frac{DV\rho}{\mu}\right]\left[\frac{C_p\mu}{k}\right] = \frac{DV\rho\ C_p}{k} \tag{87}$$

Temperature distributions for laminar flow have been determined for duct cross sectional shapes other than circular - usually by numerical analysis.

2.4.2 Circular Tube - Turbulent Flow

2.4.2.1 Reynold's Analogy

Since forced convection with turbulent flow does not lend itself to mathematical solution, experiment has been necessary. Considerable utilization of heat transfer and momentum analogies that are semi-empirical in nature has evolved.

Initially it was observed that radial profiles of velocity and temperature were similar for the turbulent flow of air in a pipe. If the profiles are assumed to be identical relationships between heat transfer and friction can be derived.

Non-dimensional temperature and velocity ratios are used

$$\frac{T_w - T}{T_w - T_m} \quad \text{and} \quad \frac{V}{V_m}$$

where subscript m refers to the mean and w to the wall.

If the profiles are identical

$$\frac{\partial}{\partial r}\left[\frac{T_w - T}{T_w - T_m}\right] = \frac{\partial}{\partial r}\left[\frac{V}{V_m}\right] \tag{88}$$

Next assume turbulent flow and that heat transfer in the laminar sublayer is by conduction only.

$$\left[\frac{q}{A}\right]_{r=r_o} = - k \left[\frac{\partial T}{\partial r}\right]_{r=r_o} ; \quad \left.\frac{\partial T}{\partial r}\right]_o = - \left.\frac{q}{kA}\right]_o \tag{89}$$

$$\tau_o = \mu \left.\frac{\partial V}{\partial r}\right]_{r=r_o} ; \quad \left.\frac{\partial V}{\partial r}\right]_o = \frac{\tau_o}{\mu} \tag{90}$$

for any r

$$\frac{\partial}{\partial r}\left[\frac{T_w - T}{T_w - T_m}\right] = - \frac{1}{T_w - T_m} \frac{\partial T}{\partial r} = \frac{1}{V_m} \frac{\partial V}{\partial r} \tag{91}$$

Now recall definitions

$$\left.\frac{q}{A}\right]_o \equiv h\,(T_w - T_m) \quad \text{defines film coefficient, h} \tag{92}$$

$$\tau_w = f \,\frac{\rho V_m^2}{2g} \quad \text{defines friction factor} \tag{93}$$

Substituting .92 and .93 into .91

$$\left[-\frac{1}{T_w - T_m}\right]\left[\frac{\partial T}{\partial r}\right]_o = \frac{1}{V_m}\left[\frac{\partial V}{\partial r}\right]_o \tag{91a}$$

$$\left[-\frac{1}{T_w - T_m}\right]\left[\frac{-\left(\frac{q}{A}\right)_o}{k}\right] = \frac{1}{V_m}\left[\frac{\tau_o}{\mu}\right] \tag{94}$$

$$\left[-\frac{1}{T_w - T_m}\right]\left[-\frac{h(T_w - T_m)}{k}\right] = \frac{1}{V_m}\left[\frac{f\rho V_m^2}{2g_c\mu}\right] \tag{94a}$$

$$\frac{h}{k} = f\,\frac{\rho V_m}{2\,g_c\,\mu} \tag{94b}$$

or

$$\left[\frac{h}{V_m\rho\, C_p}\right]\left[\frac{\mu\, g_c\, C_p}{k}\right] = \frac{f}{2} \tag{94c}$$

or

$$\text{St Pr} = \frac{f}{2} \tag{95}$$

$$\text{Pr} = \frac{\mu C_p}{k} = \frac{\left[\frac{\mu}{\rho}\right]}{\left[\frac{k}{C_p\rho}\right]} = \frac{\nu}{\alpha} = \frac{\text{momentum diffusivity}}{\text{thermal diffusivity}}$$

By assuming ν and α equal, i. e., Prandtl number equals one, we have the Reynolds analogy

$$\text{St} = \frac{f}{2} \tag{96}$$

2.4.2.2 Colburn Analogy

The Colburn analogy fits experimental data well

$$\text{St Pr}^{2/3} = \frac{f}{2} \tag{97}$$

A set of correlations typically reported to fit experimental data for Reynolds numbers greater than 30, 000 is

$$f = 0.046 \, Re^{-0.2} \tag{98}$$

$$St \, Pr^{2/3} = 0.023 \, Re^{-0.2} = \frac{f}{2} = j_H \tag{99}$$

St $Pr^{2/3}$ is sometimes identified as j_H, or the j factor for heat transfer.

2. 4. 2. 3 Martinelli Analogy - Eddy Diffusivities

Results of Martinelli's analysis of turbulent heat transfer in circular tubes is known as the Martinelli analogy. While we will not discuss those results here we will point out the starting equations in that analysis in order to introduce some additional terms.

For laminar flow

$$\frac{\tau}{\rho} = - \frac{\mu}{\rho} \frac{dV}{dr} = - \nu \frac{dV}{dr} \tag{70a}$$

For turbulent flow - write a defining equation.

$$\frac{\tau}{\rho} = - (\nu + \epsilon_M) \frac{dV}{dr} \tag{100}$$

where ϵ_M = eddy diffusivity for momentum that can vary with radius.

Heat transfer, laminar flow

$$\frac{\left[\frac{q}{A}\right]}{\rho C_p} = - \frac{k}{\rho C_p} \frac{\partial T}{\partial r} = - \alpha \frac{\partial T}{\partial r} \tag{81a}$$

For turbulent flow

$$\frac{q}{A\rho C_p} = - (\alpha + \epsilon_H) \frac{dT}{dr} \tag{101}$$

where ϵ_H = eddy diffusivity for heat.

For fully established velocity profile

$$\tau = \frac{r}{r_w} \tau_w \tag{69b}$$

Martinelli assumed the same linear distribution for rate of heat transfer across the tube as exists for shear. Coupled with a change of coordinates, $r = r_w - y$, the equations for turbulent flow become

$$\frac{\tau_w g_c}{\rho}\left(1 - \frac{y}{r_w}\right) = (\nu + \epsilon_M)\frac{dV}{dy} \tag{102}$$

$$\frac{q_w}{A_w \rho C_p}\left(1 - \frac{y}{r_w}\right) = (\alpha + \epsilon_H)\frac{dT}{dy} \tag{103}$$

A basic concept is that ϵ_M and ϵ_H are related. To simplify calculations ϵ_H/ϵ_M is taken to be unity in many works. Experimental investigations have shown ϵ_H/ϵ_M to vary between 1.0 and 1.6. Some experimental correlations relate ϵ_H/ϵ_M to Reynolds number and position in the pipe. Relationships for semi-empirical correlations may also involve Prandtl number.

Although not discussed here, reference textbooks on fluid dynamics and heat transfer show universal velocity profiles, based on experimental measurements, in terms of a dimensionless velocity versus a dimensionless position in the tube. Separate correlating equations apply for each of the three regions, i.e., laminar sublayer, buffer layer, and turbulent core. From velocity distribution correlations ϵ_M can be computed. Subsequently, if experimental data are available for the ratio of ϵ_H/ϵ_M, heat transfer can be computed. Several difficulties are involved, including accuracy of velocity data and data for the ratio of ϵ_H/ϵ_M. Also, variable fluid properties will need to be considered. In general, correlations finally used for equipment design will include a specification for evaluation of fluid properties. These include either mean temperatures or wall temperatures with multiplying factors involving ratios of wall to mean fluid temperatures. Also, quite commonly film temperatures are specified and are defined as the mean temperature plus some fraction of the difference between wall and mean fluid temperatures, e.g.

$$T_{0.4} = T_m + 0.4\,[T_w - T_m]$$

2.4.3 Other Considerations - Turbulent Heat Transfer

2.4.3.1 Roughness

In reactor thermal design roughness inherent in fabrication processes, and possibly changes in the surface characteristics with operating life, will have to be considered. Generally, effects of roughness on friction factor can be predicted from correlations of existing experimental data or can readily be measured using actual components. Effects on heat transfer are complex and no general correlations exist. Limited experimental data indicate the increase will be less than the increase in friction factor, probably in the order of one third of the increase in friction factor.

2.4.3.2 Entrance Effects

Near the entrances to a tube, the velocity and temperature profiles will not be fully developed, but will be changing with axial distance. The result is that friction and heat transfer will be large and decay to fully developed values. The decay in heat transfer coefficient will essentially be completed in a length equal to 30 tube diameters, i.e. $x/D = 30$, and in engineering calculations adequate accuracy usually results if the decay is assumed to be complete for x/D of 15 to 20. In general, for gas cooled reactors, L/D of the tube will be in the order of ten times these values, and the power distribution will be such that wall temperatures will be lower at the entrance than near the exit, with the result that consideration of entrance effects will not be critical. An exception that will be discussed later is that in which a high ratio of wall to fluid temperature occurs at the entrance.

2.4.3.3 Axial Variation of Wall Heat Flux

Variation of wall heat flux with axial distance will generally result in a small effect on turbulent heat transfer coefficients. General procedure in the ANP program was to neglect this effect in design studies and later verify that the effects were in fact small.

2.4.3.4 Non-Circular Ducts

Heat transfer correlations for circular ducts can generally be utilized for non-circular ducts with turbulent flow by utilizing an equivalent diameter

$$D_e = \frac{4\,A_{ff}}{P} \tag{104}$$

where

A_{ff} is flow area

P is heated perimeter.

However, if a non-circular duct is used, literature should be studied and an assessment made. Studies reported in the literature include annular, square, and rectangular ducts. Typical of items to be considered are effects of unequal heating from the walls of an annular duct.

2.4.3.5 High Temperature Gases

Many correlations for heat transfer reported in the literature originated from tests at moderate temperatures and moderate film temperature differences. Higher temperatures associated with gas cooled reactors require additional experimental data and accurate data for the properties of the fluid. As recent as ten years ago, heat transfer data for air at temperatures up to 2000°F was considered sufficiently inadequate for the ANP program that tests with flat plate simulations of the HTRE reactor concentric ring fuel elements were conducted. Secondary considerations included effects of in stream structure and plate interruptions, including plate misalignment. Recent literature includes reports and correlation of data with several gases for temperatures up to about 5000°R.

2.4.3.6 Accuracy of Heat Transfer Data

Accuracy of experimental data is a significant consideration in the thermal design of nuclear reactors. Even, with experimental data for conditions closely simulating the reactor, uncertainties of 5 percent or more will normally apply to the prediction of film temperature differences in nuclear reactors.

2.5 THERMAL RADIATION

2.5.1 Role in Nuclear Reactors

In ANP reactors thermal radiation was a lesser consideration than conduction and convection, but in detail was a necessary consideration. Generally, its role in solid core reactors is one of temperature leveling or limiting the temperature difference between two surfaces that can "see" each other. Examples are (1) adjacent rings in a concentric ring fuel element, (2) adjacent tubes in ceramic reactors not in contact, (3) core-reflector interfaces, and (4) surface of tube inner walls at different axial locations.

Since heat transfer by thermal radiation is proportional to temperature to the fourth power, radiation may assume a greater role in systems with higher temperature levels, e.g. reactors for rocket engines may consider absolute temperatures approaching values twice as high as ANP reactors. However, power densities and convective heat transfer rates will also be higher.

If after reactor shut-down cooling is supplied in quantities just sufficient to maintain temperature level, the relative importance of thermal radiation increases because power generation and convective heat transfer become a small fraction of full power values while radiation rates are maintained because of being temperature governed. Whereas, for ANP reactors coolant for removal of afterheat is in principle readily available, a significant premium may be placed on minimizing amount of propellant used for aftercooling in nuclear rocket engines. It follows that radiation and conduction may play significant roles in the transmission of heat generation after shutdown to the surface of the engine, and that thermal radiation will be the controlling mode for heat transfer from the external surface of the engine.

2.5.2 Basic Concepts

2.5.2.1 Emission of Thermal Radiation

Our discussion will be limited to radiation in which the quantity and quality of radiant energy emitted per unit area is dependent solely on the temperature of a given body, i.e. from thermal excitation. If we argue that thermal radiation results from temperature it may appear logical to assume that the quantity of radiant energy could be increased by increasing the amount of material or number of particles. However, it is the nature of materials to absorb their own radiation, and the radiation escaping from a slab of material increases until some limiting value is reached. Opaque substances, such as metals, have a high absorption rate. Hence the limiting radiation is achieved with thicknesses equal to only a few molecular layers, and the radiant effect has been regarded as surface phenomenon. Some substances, however, are transparent to thermal radiation, and require a considerable thickness before the radiation limit is reached.

It has been shown that the maximum value of energy that can be radiated per unit surface area is the same, at the same wave length and surface temperature, for all substances, whatever the degree of transparency. A body which emits this limiting amount of energy is termed a "black body" and its energy "black body radiation". Two fundamental laws are usually used to show the nature of black body radiation.

2.5.2.2 Stefan-Boltzmann Law

This law was first proposed by Stefan from experimental data and later proven to be theoretically correct by Boltzmann when based on thermodynamic reasoning. This law is

$$W_b = \sigma T^4 \tag{105}$$

where

W_b = total radiation (black body), Btu/ft^2-hr

T = absolute temperature, ^{0}R

σ = Stefan Boltzmann constant

σ = 0.1713×10^{-8} Btu/(ft^2) (hr) (^{0}R^4)

2.5.2.3 Planck's Law

From quantum theory Planck developed an equation which shows that the intensity of thermal radiation of wave length λ at any temperature varies from 0 at $\lambda = 0$ through a maximum and back to 0 at $\lambda = \infty$. The area under the curve of $W_{b\lambda}$, the intensity of radiation of wave length λ versus λ from 0 to ∞ is equal to the total energy radiated as given by the Stefan-Boltzmann Law, i.e.

$$W_b = \sigma T^4 = \int_0^{\infty} W_{b\lambda}\, d\lambda \tag{106}$$

Wein's displacement law states that the position for the maximum monochromatic intensity, $W_{b\lambda}$, is inversely proportional to temperature. A practical use of this law is the use of color scales for estimating temperatures. For temperatures of 1000^{0}F or less thermal radiation is emitted at wave lengths greater than for visible light (0.38 to 0.78 microns, $\mu = 10^{-6}$ meters).

With increasing temperatures some thermal radiation is emitted at lower and lower wave lengths, such that at about 1000^{o}F the visible color is dull red. As temperatures are increased further more of the visible spectrum is covered such that colors change from red, to cherry, to orange and finally to white when the whole visible spectrum is included, i.e. about 2400^{o}F.

2.5.2.4 Emissivity - Gray Body

Generally emission from the surface is less than that from a black body. A "gray" body is defined as one in which the emission at every wave length is in the same proportion to emission from a black body. Because in actuality many bodies are approximately gray, a factor known as "emissivity" is often convenient in engineering calculations, and is defined as the ratio of total energy emitted from a gray body to the total energy emitted by a black surface at the same temperature, i.e.

$$\epsilon = \frac{W_g}{W_b} = \text{emissivity.}$$

The emissivity, ϵ, is called the total hemispherical emissivity to differentiate it from monochromatic emissivity, ϵ_x, and from directional emissivity. ϵ_θ the ratio of radiating powers in a direction at an angle θ from the normal to the surface. The emissivity, ϵ, of a surface varies with temperature, roughness and, in the case of metals, with oxidation. Values range from in the order of 0.05 for polished metals at low temperature to values approaching 1.0. Emissivity can be very sensitive to surface condition, e.g. imperfection of polish or oxidation can yield values several times as great as for minimum values obtainable.

2.5.2.5 Absorption of Radiation

Radiation incident on a surface can be absorbed, reflected, or transmitted through the surface. Expressed as a fraction of the incident energy, the sum of the three must equal unity, i.e.

$$\rho + \alpha + \tau = 1 \tag{107}$$

where

ρ is reflectivity

α is absorptivity

τ is transmissivity

2.5.2.6 Kirchhoff's Law

Determination of experimental data and application to problems is simplified by a relationship between emission and absorption of radiation. The relationship is that $\epsilon = \alpha$ and is derived from Kirchhoff's law which states that energy absorbed by a body receiving black body radiation from a second body is equal to the energy that would be emitted by the surface of the first body if it were at the same temperature as the second body.

2.5.3 Radiation Between Gray Body and Black Surroundings

For a gray body radiating to empty space the energy radiated will be less than that for a black body by the emissivity, ϵ, i.e.

$$W = \sigma \epsilon T^4 \tag{108}$$

If other bodies are in the neighborhood and are at temperatures greater than absolute zero, radiations from them may in part be absorbed by the first gray body, and hence reduce its net heat loss. For black surroundings at temperature T_2 the gray body will absorb a proportion of the radiations from the surroundings equal to α, or by Kirchhoff's Law, equal to ϵ

$$W = \sigma \epsilon_1 T_2^4 \tag{109}$$

The net rate of energy loss is then

$$W = \sigma \epsilon_1 (T_1^4 - T_2^4) \tag{110}$$

2.5.4 Radiation Between Gray Bodies

In most practical problems we will be concerned with radiation between two bodies that in many cases can be approximately represented as two gray bodies. Here in addition to the rate of emission from the surface of a gray body we have to consider the fraction of the emitted radiation that is reflected from the gray surroundings and reabsorbed by the surface of the original body, and by the rate at which the original surface absorbs radiations from neighboring gray surfaces. To compute net radiation exchange, knowlege of size and emissivity of all the surfaces involved must be available in addition to the angle by which the various surfaces see each other. For many problems, effects of all the variables are combined into several coefficients. Generally, an "angle" or "configuration" coefficient and an "emissivity" coefficient are used.

The resulting computational equation is

$$q = \sigma F_A F_\epsilon A (T_1^4 - T_2^4) \qquad (111)$$

where A = area of one of two surfaces, ft^2

F_A = angle coefficient by which surface A "sees" the other surface

F_ϵ = the emissivity coefficient which takes into account the departure of both surfaces from perfect blackness

T = ^oR

q = total net energy transferred Btu/hr

The problem of computing the coefficients F_A and F_ϵ in real equipment, such as nuclear reactors may be difficult due to configuration complications. For simple configurations evaluation of these coefficients are available in the literature. Calculation procedure then involves the breaking down and approximation of actual configurations into several of the simpler shapes. In nuclear reactors such a breakdown may still leave surfaces across which temperature variations are so large that characterization of the surface by a single temperature will lead to unacceptable accuracy. Hence, further breakdown will be required just from a consideration of reasonable temperature representations.

In nuclear reactor thermal analysis we have already indicated that solution of three dimensional transient heat conduction problems is usually accomplished by using finite difference approximations with the aid of digital computers. If radiation is to be accounted for, we will find that, in the process of setting up node volumes to satisfy accuracy criteria for thermal conduction, sufficiently fine breakdown of surfaces for radiation calculations is already provided for by the exposed surfaces of nodes in contact with fluids or that are separated from other node surfaces by a gap. In such a model, one node surface may see many other node surfaces.

2.5.5 Angle and Emissivity Coefficients

We will here avoid any detailed discussion of the computation of the angle and emissivity coefficients, because these are treated in reference books and in the literature. One note is that in such references you will read about the Inverse Square Law, which is usually stated with reference to a model involving two imaginary spherical shells of radius r_1 and r_2, that surround an emitter of incremental area, dA. The law simply states that since radiant heat rays propagate along straight lines that the radiation intensity (radiation energy per unit area per unit time) received by spherical surface areas A_1 and A_2 are in the ratio of r_2^2/r_1^2.

A second comment is that you will be exposed to the Cosine Emission Law As you will anticipate, this law in concept states that the radiation intensity incident on a receiving surface is proportional to the projected surface area of the emitter onto the receiving surface.

Some angle and emissivity factors for simple configurations are

Surfaces Interchanging Radiation	Area A	F_A Angle Factor	F_ϵ Emissivity Factor
Parallel Planes - large area	Either	1	$\dfrac{1}{\dfrac{1}{\epsilon_1}+\dfrac{1}{\epsilon_2}-1}$
Small enclosed body 1 body 2 surroundings	A_1	1	ϵ_1
Concentric spheres or cylinders 1 inner surface 2 outer surface	A_1	1	For diffuse reflectivity $\dfrac{1}{\dfrac{1}{\epsilon_1}+\dfrac{A_1}{A_2}\left(\dfrac{1}{\epsilon_2}-1\right)}$ For specular reflectivity $\dfrac{1}{\dfrac{1}{\epsilon_1}+\dfrac{1}{\epsilon_2}-1}$

Diffuse reflectivity is by definition reflection of thermal energy equally in all directions. By specular reflectivity we mean that radiant reflection is directional, or specifically, the angle for reflection measured from the normal to the surface is equal to the incident angle also measured relative to the same normal.

It is to be noted in the above tabulation that both F_A and F_ϵ as shown are keyed to a particular area, i.e.

$$q = F_{A_1} F_{\epsilon_1} A_1 (T_1^4 - T_2^4) \qquad (111a)$$

If it is desirable to utilize A_2 instead of A_1 in the above equation, the resulting q must have the same value.

Hence,

$$F_{A_2} F_{\epsilon_2} A_2 = F_{A_1} F_{\epsilon_1} A_1 \qquad (112)$$

or

$$F_{A_2} F_{\epsilon_2} = F_{A_1} F_{\epsilon_1} \left(\frac{A_1}{A_2}\right) \qquad (112a)$$

2.5.6 Non-luminous Gases

Homopolar gases, oxygen, nitrogen, etc. are normally considered to absorb and emit negligible amounts of radiation. Compound gases emit and absorb radiations in only certain ranges of wave length, i.e. in particular band widths. Since all such radiation bands fall in the infra-red region, radiation of visible wave lengths will not be emitted and hence is termed non-luminous radiation. Gases having emission bands of significant energy content include carbon dioxide, carbon monoxide, the hydrocarbons, water vapor, ammonia, sulphur dioxide, and hydrogen chloride.

Radiation absorption and emission by non-luminous gases in finite thicknesses is found to depend on temperature and on partial pressure of the gas. If mixtures of two or more gases are present, radiation bands may overlap and each may be slightly opaque to radiations of the other, with the result that the sum for two gases together will be less than the sum of their separate radiations. Gaseous radiation was generally negligible in ANP reactors.

2.5.7 Luminous Clouds

Gases can carry particles of solid carbon compounds that become luminous. Radiation in such systems involves both gas radiation and surface radiation. Although gases seeded with particles of carbon or carbon compounds are considered for receiving heat from gaseous core reactors, they are not commonly considered to be of significant interest for solid core reactors.

2.5.8 Heat Transfer Coefficient Radiation

Typically, in high temperature gas-cooled reactors computational procedures, particularly as used in finite difference equations, will utilize the radiation heat transfer coefficient as identified in Section 1.0 in order to obtain equations linear in temperature. It follows that in successive iterations improved accuracy will be obtained if the radiation heat transfer coefficient is re-evaluated using surface temperatures from the previous iteration.

3. 0 DESIGN CONSIDERATIONS AND ANALYSES

3. 1 INTRODUCTION

In section 1. 0 we have indicated both the nature of the input to thermal design, and characteristics that evolve from the thermal design and serve as input for the reactor mechanical design. Basic concepts of heat transfer and fluid dynamics have been indicated in section 2. 0. Our objective in this section will be to identify and characterize thermal design considerations, to show typical problem formulations, and, finally, to indicate typical design relationships.

We recall that basic input for the thermal design includes pressures and temperatures into and out of the reactor, flow rates, and operating modes. Output from the thermal design includes requirements for flow area and coolant channel dimensions. Further items of interest are temperature and pressure distribution predictions for all operating modes.

Orientation will be primarily in terms of the active core, particularly fuel elements. This choice is made because generalizations evolve more readily than for other components, and because principles and procedures are similar to those for other components.

3. 2 TEMPERATURES - DEFINITION AND MAGNITUDES

Subsequent discussion will be oriented primarily toward a discussion of reactor core and fluid temperatures with secondary considerations of reactor pressure drop and/or "void" volume, temperatures of other components, and pressure drop in ducts or flow channels external to the reactor proper.

First, we can define temperatures and dimensionless ratios of temperature differences, that will provide some convenience in summing or multiplying effects. If all holes in our model, i. e., a right circular cylinder pierced by circular holes in a triangular array (like ANP ceramic reactors discussed in section 1. 0) were identical and the heat distribution around the holes was in all cases identical, our problem of predicting temperatures of the coolant hole could be basically reduced to a one-dimensional temperature problem, axial or longitudinal. Further, if axial conduction is negligible, we can examine the interior temperatures as a one-dimensional problem, radial, except for some angular heat conduction caused by the hexagonal external surface. Since we have assumed no exchange of heat among adjacent tubes or hexagonal elements, we can now characterize the behavior of the reactor core by the characteristics of this one tube. Typically, we visualize such a system and refer to the single element by expressions like "average tube" or "average channel." We talk in terms of surface or wall temperatures, and maximum temperatures within the solid - at the corner of the hexagon. Also, when considering thermal stress problems the temperature obtained by averaging over the cross sectional area will be of interest.

We can now compute the axial variation of surface temperature from a knowledge of convective heat transfer phenomena and a knowledge of the axial variation of heat generation. Also, the internal temperatures can be computed independently, except for the need to know temperature level for selecting a thermal conductivity value. Generally, the surface temperature will tend to be greatest at a fractional axial distance of 0.80 to 0.90. Wherever it occurs we will call that temperature the average channel-maximum surface temperature. Further, we will call the highest temperature within the solid at that axial location the average channel-maximum internal temperature. It is to be noted that the true maximum internal temperature can occur at a different axial location, that this simplification usually results in a negligible difference, but that one verifies this. It should also be noted that the difference between maximum internal temperature and surface temperature is proportional to the heat generation rate and hence will in general tend to be greatest at a fractional distance of 0.5 or less.

Typically, system designs are initiated by considering this average channel with a judicious assumption of permissible maximum surface temperature, i.e., it is used to derive relationships among flow, void volume, gas temperatures, pressures, and pressure drops for purposes of system studies such as maximization of thrust-to-weight. The elevation of this temperature above the temperature of the gas as it exits from the tube is a measure of the unfavorableness of the axial distribution of heat generation and is also influenced by system design parameters. The elevation of temperatures of actual tube surfaces above the maximum surface temperature of the average tube is a measure of the degree of design and fabrication control achieved.

During reactor design and development several characteristics of the reactor will be measured. These include distribution of heat generation using "zero" power critical experiments and flow distributions among holes as measured in mockups of external duct systems with reactor flow simulators (the duct systems may induce non-uniform flow among the tubes). Using the measured data, tube to tube variations of temperature can be calculated while accounting for exchange of heat among the tubes. These temperatures we will call maximum calculated surface and internal temperatures. The temperatures thus computed are quite representative of those expected in a reactor core fabricated without tolerances and one for which all measurements and correlations are known precisely. However, measurements and correlations are always uncertain at least by some small amount. Tolerances on specifications of hole diameter, wall thickness, density, fuel concentration, etc., are of course necessary for feasible fabrication methods. It is convenient to treat tolerances with uncertainty allowances and think of corresponding temperature effects occurring randomly. By knowing or assuming uncertainty and tolerance probability distributions, probabilities of any tube, including the one with the maximum calculated temperature, exceeding the calculated temperature by any specified amount can be computed. One can then select a temperature for which there is a low probability of that temperature being exceeded. That temperature is then called the maximum surface temperature, or maximum internal temperature. It should be observed that changing to higher thermal capacity gases, i.e., air to hydrogen, will result in higher power densities and hence, larger internal temperature differences. Other things being equal, allowances for calculated effects and uncertainties will tend to be proportional to the temperature elevation above the temperature of the gas entering the reactor.

Finally, we need to distinguish between temperature of the fluid exiting from the reactor core or fuel elements and the temperature of that fluid after it has mixed with flow that has by-passed the reactor core, possibly with a significantly lower temperature rise. The by-pass flow can include unwanted leakage due to imperfect seals and flow from components cooled by a flow in channels parallel to those in the reactor core. Even though generally this dilution of the reactor core exit gases will be small for systems in which all other components are cooled by the gas prior to its introduction into the reactor core, because of leakage possibilities, it is well to allow for this effect in our temperature definitions. Actually, in some systems a series cooling arrangement may prove impractical or undesirable. For example, in some ANP reactors cooling of other reactor components, shielding components, and turbomachinery components in series would have led to impractical ducting designs and unacceptable system pressure losses. As a result parallel cooling circuits were deemed acceptable even with a reduction of the reactor fuel element exit gas temperature by as much as 10 percent of the temperature rise in the fuel elements.

Let us now summarize our definitions of temperatures. Generally, we will be attempting to achieve a gas temperature from the reactor, i.e., to a turbine or to a rocket nozzle, that approaches the maximum temperature in the reactor. If, instead of thinking in terms of temperature levels, we think in terms of temperature elevation above the gas temperature entering the reactor, and further normalize that difference by dividing by the maximum temperature less the inlet gas temperature, we can think of a product of temperature difference ratios that is always less than one. The value of that product is then a measure of the extent to which the gas temperature for producing useful work, or effects, approaches the maximum temperature capability of the active core.

Temperature ratios in the product will generally include (ΔT's are shown to indicate elevation above inlet gas temperature)

$\frac{\Delta T_R}{\Delta T_C}$,	ratio of temperature from reactor to temperature of gas from the core
$\frac{\Delta T_C}{\Delta T_{w_{avg}}}$,	ratio of temperature of gas from core to wall temperature of average tube - accounts for film temperature difference required for convective heat transfer from wall to fluid
$\frac{\Delta T_{w_{avg}}}{\Delta T_{w_{calc}}}$,	ratio of temperature of wall of average tube to that of tube with highest calculated temperature
$\frac{\Delta T_{w_{calc}}}{\Delta T_{w_{max}}}$,	ratio of temperature of highest calculated wall temperature to that of statistically estimated maximum, accounting for tolerances and uncertainties
$\frac{\Delta T_{w_{max}}}{\Delta T_{i_{max}}}$,	ratio of statistically estimated maximum wall temperature to maximum estimated interior temperature

Note that the last term could be replaced by a product of terms to individually account for average, calculated, and statistically estimated effects.

Values for these parameters can be tabulated for typical ANP reactors and compared with a set of values chosen somewhat arbitrarily to yield a maximum fuel element temperature of 5000°F with a reactor discharge temperature of 4000°F and a reactor inlet temperature of 0°F. These latter temperature conditions may be typical of design objectives for nuclear rocket engines. The tabulation is

Temperature Ratio	ANP Reactors		Nuclear Rocket (Arbitrary)
	Metallic	Ceramic	
$\frac{\Delta T_R}{\Delta T_C}$	0.91	0.88	0.99
$\frac{\Delta T_C}{\Delta T_{w_{avg}}}$	0.85	0.81	0.92
$\frac{\Delta T_{w_{avg}}}{\Delta T_{w_{calc}}}$	0.90	0.93	0.95
$\frac{\Delta T_{w_{calc}}}{\Delta T_{w_{max}}}$	0.88	0.91	0.95
$\frac{\Delta T_{w_{max}}}{\Delta T_{i_{max}}}$	0.98	0.98	0.97
$\frac{\Delta T_R}{\Delta T_{i_{max}}}$	0.60	0.59	0.80

It is intended that the data in the above tabulation merely show typical percentage improvements in temperature ratios required relative to ANP values if gas temperatures approaching within 1000°F of maximum reactor temperatures of 5000°F are to be achieved. No correlation with existing or proposed designs is involved.

An obvious improvement that may be more easily achievable in nuclear rocket engines than in ANP reactors is the elimination of reactor core bypass flow. This is reflected by a $\Delta T_R / \Delta T_C$ that closely approaches unity. Even with further reduction of effects that cause local areas to operate at temperatures higher than average tubes, i.e., power distributions, tolerances, and uncertainties, the ratio of core gas temperature to the wall temperature of the average tube will have to be increased. This ratio is determined by the design of coolant passages, i.e., heat transfer area and other dimensional characteristics.

Discussions in subsequent sections of this report will follow an outline designed to show effects and analysis procedures pertaining to the several temperature ratios identified above.

3.3 GAS TEMPERATURES - CORE EXIT

Typical design procedure will involve the following steps.

a. Identify basic flow circuitry
b. Based on nuclear predictions, estimate heat generated in each component
c. From preliminary mechanical design studies, make estimate of temperature capabilities of the several components
d. Estimate temperature of coolant exiting from each component and the corresponding flow rate
e. Compute temperature required for the gas exiting from the active core
f. As detailed design of reactor and engine components, iterations of the above sequence may result in modifications to the original estimates

Computation of the required temperature of the gas as it exits from the active core is straightforward once the flow rates and temperatures are known for other components, i.e,

$$\left[W\,Cp_m\,\Delta T\right]_R = \left[W\,Cp_m\,\Delta T\right]_C + \sum_x \left[W\,Cp_m\,\Delta T\right]_x \qquad (113)$$

where x denotes a reactor component and the summation must include all flows, including unwanted leakage,

hence

$$\frac{\Delta T_R}{\Delta T_C} = \frac{\dfrac{\left[W\,Cp_m\right]_C}{\left[W\,Cp_m\right]_R}}{1 - \dfrac{\sum_x \left[W\,Cp_m\,\Delta T\right]_x}{\left[W\,C_{cm}\,\Delta T\right]_R}} \qquad (114)$$

If enthalpy tables are available, the computation is simplified. Typical data for ANP ceramic reactors are as follows:

Component	% Airflow	Exit Air Temperature, ^{o}F
Inner reflector	0.9	1240
Outer reflector	4.0	1120
Pressure pads	1.3	740
Radial springs	1.0	740
Guide tubes	1.5	1050
Aft-retainer	1.3	1025
Components cooled by reactor by-pass	9.9	1200

For an inlet temperature of 580°F these data yield a requirement that the core exit gas (80.1% of flow) temperature be approximately 1900°F for a turbine temperature of 1740°F.

Actually, the ratio $\Delta T_R / \Delta T_C$ must be further modified to account for heat transfer from the gas as it flows from the active core to the turbine or nozzle, i.e., heat transfer to the walls of ducts or thrust chambers.

3.4 AVERAGE TUBE - MAXIMUM SURFACE TEMPERATURE

We consider an average fuel tube with internal hole diameter that is invariant with axial distance. It is to be noted that other means of axial temperature shaping are possible, e.g. in ANP metallic reactors axial variations of hydraulic diameter was utilized in a stagewise manner.

Here we will investigate the effects of axial power distribution on the axial temperature distribution. Included will be cases of uniform heat flux, uniform wall temperature, and families of sinusoidal distributions.

We will use the following nomenclature:

T = fluid temperature
T_s = surface temperature

where both T and T_s vary with axial distance $\epsilon = x/L_c$

Subscripts

0	$\epsilon = 0$
1	$\epsilon = 1$
m	$\epsilon = \epsilon_m$, i.e. location of maximum surface temperature

3.4.1 Uniform Heat Flux

If the convective heat transfer coefficient, h, the fluid specific heat, C_p, and the wall heat flux are all assumed to be constant we have

$$q = hA\,[T_s - T]$$

or

$$T_s - T = \frac{q}{hA} = \text{constant} \qquad (115)$$

where

$A = PL$
P = perimeter of channel = πD

but $\quad A_{ff} = \frac{\pi}{4} D^2$ from flow area.

So $\quad P = \pi D = \frac{4A_{ff}}{D}$

or $\quad D = \frac{4A_{ff}}{P}$ commonly used definition of hydraulic diameter hence

$$A = 4\ A_{ff} \frac{L}{D}$$

$$T_s - T = \frac{q}{h\ A_{ff}\ 4 \frac{L}{D}} \tag{115a}$$

but

$$q = W\ C_p\ [T_1 - T_0] \tag{116}$$

letting $\frac{W}{A_{ff}} = G$ we have

$$T_s - T = \frac{G\,C_p}{h} \frac{[T_1 - T_0]}{4 \frac{L}{D}} = \frac{T_1 - T_0}{4\,St \frac{L}{D}} \tag{117}$$

$$\begin{aligned} T_{s1} - T_0 &= [T_1 - T_0] + [T_{s1} - T_1] \\ &= [T_1 - T_0] \left[1 + \frac{1}{4\,St \frac{L}{D}} \right] \end{aligned} \tag{118}$$

$$\frac{T_1 - T_0}{T_{s1} - T_0} = \frac{1}{1 + \frac{1}{4\,St \frac{L}{D}}} \tag{118a}$$

where

$$St = \frac{h}{G\ C_p}$$

3.4.2 Uniform Wall Temperature

Now ask if this ratio can be larger by letting T_s be a constant.

$$dq = h P dx [T_s - T]$$

$$= h \frac{4 A_{ff}}{D} dx [T_s - T]$$

$$dq = W C_p dT = h \frac{4 A_{ff}}{D} dx [T_s - T]$$

$$\frac{dT}{T_s - T} = \frac{h 4 A_{ff}}{W C_p P} dx = \frac{h}{G C_p} \frac{4dx}{D} = 4 \text{ St} \frac{dx}{D}$$

$$- \ln(T_s - T)\Big]_{T_0}^{T} = 4 \text{ St} \frac{x}{D}\Big]_0^{x} \tag{119}$$

$$\frac{T_s - T}{T_s - T_0} = e^{-4 \text{ St} \frac{x}{D}} \tag{120}$$

$$\frac{T_s - T_1}{T_s - T_0} = e^{-4 \text{ St} \frac{L}{D}} \tag{121}$$

$$\frac{T_s - T_1}{T_s - T_0} = \frac{T_s - T_0}{T_s - T_0} - \frac{T_1 - T_0}{T_s - T_0} = e^{-4 \text{ St} \frac{L}{D}} \tag{122}$$

$$\frac{T_1 - T_0}{T_s - T_0} = 1 - e^{-4 \text{ St} \frac{L}{D}} \tag{123}$$

3.4.3 Generalized Power Distribution

We define a power distribution function $g(\epsilon)$ such that

$$\int_0^1 g(\epsilon)\, d\epsilon = 1 \tag{124}$$

and further define a function $G(\epsilon)$,

$$G(\epsilon) = \int_0^{\epsilon} g(\epsilon)\, d\epsilon \tag{125}$$

We will understand that q'''_ϵ and $\frac{dq}{d\epsilon}$ are proportional to $g(\epsilon)$, and that if C_p is constant

$$\frac{T - T_0}{T_1 - T_0} = G(\epsilon) \tag{126}$$

and

$$\frac{dq}{dx} = \frac{q}{L}\, g(\epsilon) = \frac{W\, C_p}{L}\, [T_1 - T_0]\, g(\epsilon) \tag{127}$$

$$dq = h\, dA\, [T_s - T]$$

$$= h\, P\, dx\, [T_s - T]$$

or

$$T_s - T = \frac{\frac{dq}{dx}}{hP} = \frac{\frac{dq}{dx}}{h\,\frac{4\,A_{ff}}{D}} \tag{128}$$

$$= \frac{W\, C_p}{h\,\frac{L}{D}\, 4\, A_{ff}}\, [T_1 - T_0]\, g(\epsilon) \tag{129}$$

$$= \frac{G\, C_p}{h}\; \frac{1}{4\,\frac{L}{D}}\, [T_1 - T_0]\, g(\epsilon) \tag{129a}$$

hence

$$\frac{T_s - T}{T_1 - T_0} = \frac{g(\epsilon)}{4\, St\, \frac{L}{D}} \tag{130}$$

Summing (126) and (130) we obtain

$$\frac{T_s - T_0}{T_1 - T_0} = G(\epsilon) + \frac{g(\epsilon)}{4\, St\, \frac{L}{D}} \tag{131}$$

The maximum value of T_s will occur when

$$\frac{d}{d\epsilon}\left[G(\epsilon) + \frac{g(\epsilon)}{4\ \mathrm{St}\ \frac{L}{D}}\right] = 0$$

$$g(\epsilon) + \frac{\frac{d\ g(\epsilon)}{d\epsilon}}{4\ \mathrm{St}\ \frac{L}{D}} = 0 \tag{132}$$

Hence

$$\frac{T_1 - T_0}{T_{s_m} - T_0} = \frac{1}{G(\epsilon_m) + \frac{g(\epsilon_m)}{4\ \mathrm{St}\ \frac{L}{D}}} \tag{133}$$

We note that for uniform heat flux

$$g(\epsilon) = 1$$
$$G(\epsilon) = \epsilon$$

and that

$$\frac{T_1 - T_0}{T_s - T_0} = \frac{1}{\epsilon + \frac{1}{4\ \mathrm{St}\ \frac{L}{D}}} \tag{134}$$

Hence by inspection T_s reaches the maximum value at $\epsilon = 1$ and as before

$$\frac{T_1 - T_0}{T_{s_m} - T_0} = \frac{1}{1 + \frac{1}{4\ \mathrm{St}\ \frac{L}{D}}} \tag{135}$$

We conclude that in general if ϵ_m computed from equation (132) is greater than one that the actual T_{s_m} occurs at $\epsilon = 1$.

3.4.4 Sinusoidal Power Distribution

3.4.4.1 Evaluation of Constants

Nuclear reactors typically have axial power distributions that can be closely approximated by a sinusoidal function. If no end reflectors are used or if equally effective end reflectors are used the distribution is symmetrical about $\epsilon = 0.5$. In general, $g(\epsilon)$ is greater than zero at $\epsilon = 0$ and $\epsilon = 1$. Frequently, $g(0.5)$ is assumed to be two times $g(0)$ or $g(1)$. If we let

$$g(\epsilon) = C_1 \sin (C_2 \pi [\alpha + \epsilon]) \qquad (136)$$

then

$$g(0.5) = 2\, g(0)$$

or

$$\sin (C_2 \pi [\alpha + 0.5]) = 2 \sin (C_2 \pi [\alpha + 0]) \qquad (137)$$

from which

$$C_2 \pi (\alpha + 0.5) = \frac{\pi}{2}, \quad C_2 \pi \alpha = \frac{\pi}{6}$$

and

$$\frac{\alpha + 0.5}{\alpha} = 3$$

or

$$\alpha = 0.25 \qquad (138)$$

and

$$C_2 = \frac{1}{6\alpha} = \frac{1}{1.5} \qquad (139)$$

As we will demonstrate, maximum fuel temperatures can be reduced if the power distribution is forward peaked, i.e., if the maximum value of $g(\epsilon)$ occurs at $\epsilon < 0.5$. Such power distributions are attainable, e.g. by using a front reflector that is more effective than the rear reflector. We can then consider a family of sinusoidal power distributions characterized by variations of α greater than 0.25. To simplify we will later maintain $C_2 = 1/1.5$, which keeps the dimensionless length corresponding to half of a complete sine wave, i.e. from 0 to π, equal to 1.5. Hence, for $g(1)$ to be positive, $\alpha \leq 0.5$. An actual power distribution might be better represented by some other value of C_2, or alternately $g(\epsilon)$ might be represented by some other function.

For the general sinusoidal distribution we can proceed to evaluate C_1 by the requirement that

$$G(\epsilon) = \int_0^1 g(\epsilon)\, d\epsilon = 1$$

The integration yields

$$C_1 = \frac{C_2 \pi}{\cos (C_2 \pi \alpha) - \cos C_2 \pi (\alpha + 1)} \tag{140}$$

3. 4. 4. 2 Solution for Axial Distance for Maximum Surface Temperature

Recall that ϵ_m is determined as the value that satisfies

$$g(\epsilon) = - \frac{1}{4\, St \frac{L}{D}} \frac{d\, g(\epsilon)}{d\epsilon}$$

Performing the evaluation we find

$$\tan (C_2 \pi[\alpha + \epsilon_m]) = - \frac{C_2 \pi}{4\, St \frac{L}{D}} = - \lambda \tag{141}$$

$$\sin (C_2 \pi[\alpha + \epsilon_m]) = \frac{\lambda}{[\lambda^2 + 1]^{1/2}} \tag{142}$$

$$\cos (C_2 \pi[\alpha + \epsilon_m]) = \frac{-1}{[\lambda^2 + 1]^{1/2}} \tag{143}$$

3. 4. 4. 3 Maximum Surface Temperature

We recall that

$$\frac{T_1 - T_0}{T_{s_m} - T_0} = \frac{1}{G(\epsilon_m) + \frac{g(\epsilon_m)}{4\, St \frac{L}{D}}}$$

and obtain $G(\epsilon)$ by integrating

$$G(\epsilon) = \int_0^{\epsilon} g(\epsilon)\, d\epsilon$$

$$= \frac{C_1}{C_2\pi} \{\cos(C_2 \pi \alpha) - \cos(C_2 \pi [\alpha + \epsilon])\} \qquad (144)$$

Substituting we obtain

$$\frac{T_1 - T_0}{T_{s_m} - T_0} = \frac{\dfrac{C_2\pi}{C_1}}{\cos(C_2 \pi \alpha) + \left\{1 + \left[\dfrac{C_2\pi}{4\,\mathrm{St}\,\frac{L}{D}}\right]^2\right\}^{1/2}} \qquad (145)$$

or

$$\frac{T_1 - T_0}{T_{s_m} - T_0} = \frac{\cos(C_2 \pi \alpha) - \cos(C_2 \pi [\alpha + 1])}{\cos(C_2 \pi \alpha) + \left\{1 + \left[\dfrac{C_2\pi}{4\,\mathrm{St}\,\frac{L}{D}}\right]^2\right\}^{1/2}} \qquad (145a)$$

For values of 4 St L/D greater than those corresponding to $\epsilon = 1$, T_{s_m} will occur at $\epsilon = 1$, i. e.

$$\frac{T_1 - T_0}{T_{s_m} - T_0} = \frac{T_1 - T_0}{T_{s_1} - T_0} = \frac{1}{G(1) + \dfrac{g(1)}{4\,\mathrm{St}\,\frac{L}{D}}}$$

$$\frac{T_1 - T_0}{T_{s_m} - T_0} = \frac{1}{1 + C_1 \sin(C_2\pi [\alpha + 1])} \qquad (146)$$

Plots of maximum surface temperature parameter versus the heat transfer parameter are shown in Figure 3. 1 for the several cases discussed but only for $C_2 = 1/1.5$. As you may have anticipated the curves for the sine distribution are bracketed above by the curve for uniform temperature and below by the curve for uniform heat flux. Gains in the temperature ratio by increasing α, i. e., forward shifting the longitudinal power distribution are to be observed. For all cases the curves tend to

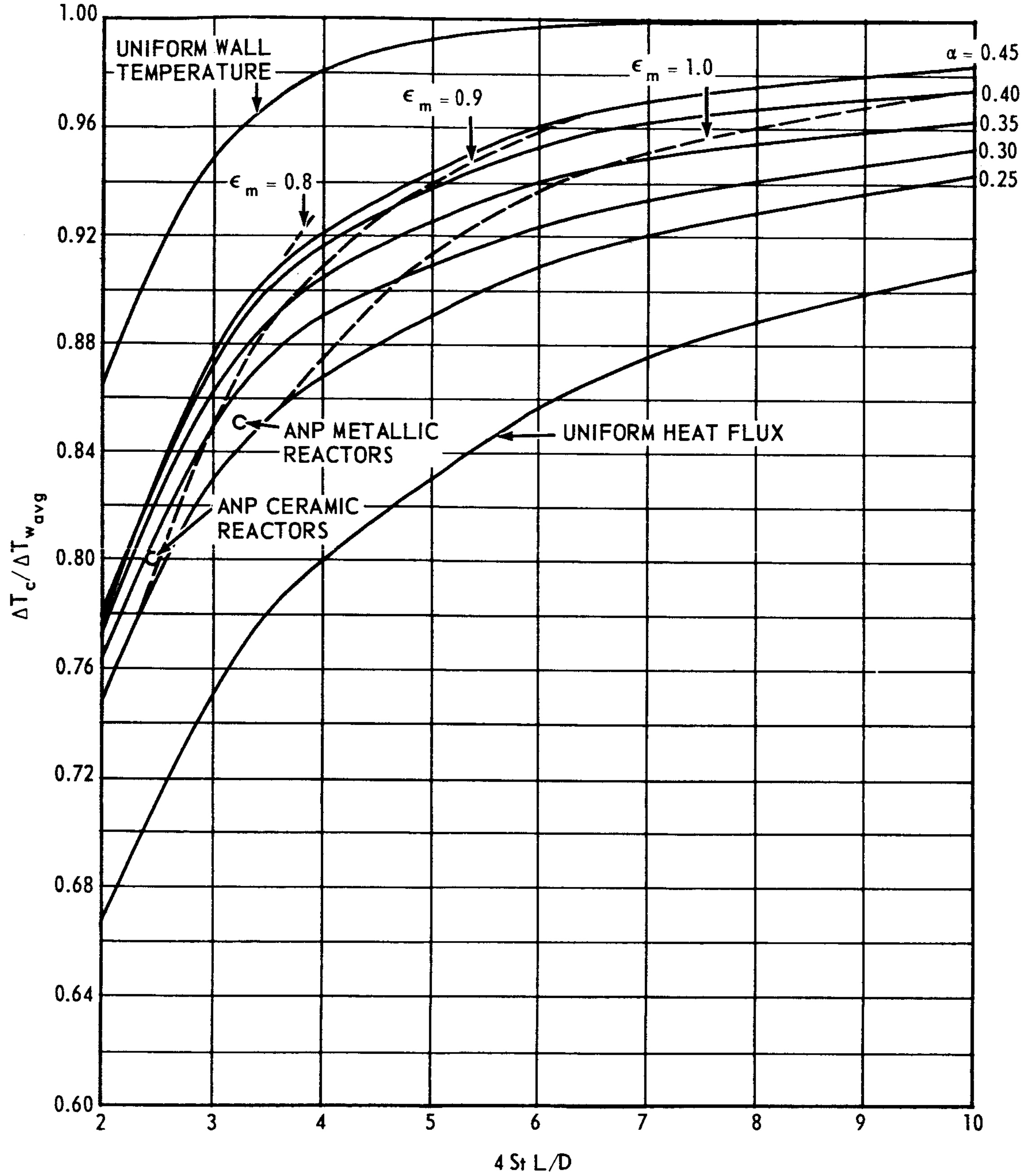

Fig. 3.1 — Wall temperature versus heat transfer parameter

rise sharply for values of 4 St L/D up to about 4 and then tend to rise much less rapidly. It appears that temperature ratios above 0.9 are achievable (recall earlier we indicated possible desire for a value of about 0.92). For a symmetrical distribution, $\alpha = 0.25$, it appears that a temperature ratio of 0.92 is achievable with a 4 St L/D of about 7. Further, if an α of 0.40 to 0.45 can be achieved we can almost halve the 4 St L/D. In anticipation that pressure losses or flow area will increase significantly with increases in 4 St L/D we view the shape of the curves and tentatively anticipate that 4 St L/D values of 5 or less will be desirable. It then follows that forward shifting of the power distribution to achieve α's of 0.35 or more becomes necessary if we are to achieve temperature ratios of about 0.92. We also note that ϵ_m for T_{s_m} is about 0.9.

Characteristic values for ANP gas cooled reactors are indicated on the plot. It is to be noted that the temperature ratio and 4 St L/D are significantly less than values we now anticipate. Reasons can be thought of in terms of system optimizations involving reactor size versus increased thrust achievable with higher air temperatures. Similar system optimizations are involved for a nuclear rocket engine and will finally fix the value of 4 St L/D.

3.4.4.4 Axial Variation of Surface Temperature

We will now turn to the question of axial temperature distributions. A heat transfer correlation used in the ANP program is

$$\frac{hD}{k_f} = 0.0205 \left(\frac{\rho VD}{\mu}\right)_f^{0.8} \left(\frac{C_p\mu}{k}\right)_f^{0.4} \tag{147}$$

or

$$Nu_f = 0.0205\,(Re)_f^{0.8}\,Pr_f^{0.4} \tag{147a}$$

where subscript f refers to a film average temperature,

$$T_f = \frac{T_s + T_b}{2}, \text{ and } T_b = T \tag{148}$$

As a common practice p is assumed invariant across the thermal boundary layer, and the perfect gas law is utilized to give

$$\rho_f = \frac{p}{RT_f} \tag{149}$$

$$p = \rho_b RT_b$$

$$\rho_f = \frac{\rho_b T_b}{T_f} \tag{150}$$

assuming R doesn't vary with temperature, then letting

$$\rho_b V = \frac{W}{A_{ff}} = G$$

$$\left(\frac{\rho V D}{\mu}\right)_f = \frac{GD}{\mu_f}\,\frac{T_b}{T_f} \tag{151}$$

we will now understand Re_f to mean DG/μ_f

Now

$$\frac{hD}{k_f} = Nu_f = 0.0205\,(Re)_f^{0.8}\left(\frac{T_b}{T_f}\right)^{0.8}(Pr_f)^{0.4}$$

$$h = 0.0205\,\frac{(Re_f)^{0.8}}{D}\left(\frac{T_b}{T_f}\right)^{0.8} Pr_f^{0.4}\;k_f$$

$$h = 0.0205\,\frac{G^{0.8}}{D^{0.2}}\,\frac{Pr_f^{0.4}\,k_f}{\mu_f^{0.8}}\left(\frac{T_b}{T_f}\right)^{0.8} \tag{152}$$

We will now examine the effect of variable fluid properties on the wall temperature. Assume that hydrogen property data can be approximated by

$$\frac{Pr^{0.4}\,k}{\mu^{0.8}} = AT^{0.27} \text{ from } 2000^{\circ} \text{ to } 4500^{\circ}R \tag{153}$$

hence

$$h = C\,\frac{G^{0.8}}{D^{0.2}}\,\frac{T_b^{0.8}}{T_f^{0.53}} \tag{154}$$

and

$$\frac{\left(\frac{dq}{dx}\right)}{\left(\frac{dq}{dx}\right)_m} = \frac{g(\epsilon)}{g(\epsilon_m)} = \frac{h(T_s - T_b)_\epsilon}{h(T_s - T_b)_{\epsilon_m}}$$

or
$$\frac{g(\epsilon)}{g(\epsilon_m)} = \left(\frac{T_{b_\epsilon}}{T_{b_{\epsilon_m}}}\right)^{0.8} \left(\frac{T_{f_{\epsilon_m}}}{T_{f_\epsilon}}\right)^{0.53} \frac{(T_s - T_b)_\epsilon}{(T_s - T_1)_{\epsilon_m}} \tag{155}$$

From which we anticipate that $g(\epsilon)$ will be most severely limited at $\epsilon = 0$.

If we require that $T_{s_0} = T_{s_m} = 5000^{\circ}R$ and recall that

$$(T_s - T_b)_{\epsilon_m} = (T_{b_1} - T_{b_0}) \frac{g(\epsilon_m)}{4\ St\ \frac{L}{D}}$$

and that

$$(T_{b_1} - T_{b_0}) = \frac{(T_{s_m} - T_{b_0})}{G(\epsilon_m) + \frac{g(\epsilon_m)}{4\ St\ \frac{L}{D}}}$$

we find that

$$(T_s - T_b)_{\epsilon_m} = \frac{(T_{s_m} - T_{b_0}) \ \frac{g(\epsilon_m)}{4\ St\ \frac{L}{D}}}{G(\epsilon_m) + \frac{g(\epsilon_m)}{4\ St\ \frac{L}{D}}} \tag{156}$$

Then, as an example, choose a value of $4\,St\,L/D$ equal 4 which as we will see later will assure a given void volume for a given reactor pressure ratio. By iterative computations we can then compute T_{b0} using our property relationship for several values of α. This computation yields values which for the assumptions made so far represent the minimum T_{b0} permissible:

α	T_{b0}, ^{o}R
0. 25	238
0. 30	306
0. 35	378
0. 40	456
0. 45	540

Hence, as an attempt is made to increase the ratio of $[T_1 - T_0]/[T_{s_m} - T_0]$ by increasing α, the minimum T_{b0} permitted increases. It then is of interest to examine the axial variation of surface temperature. If, for example, we examine $\alpha = 0.40$ we find

ϵ	$T_s(\epsilon)^{(1)}$	$T_s(\epsilon)^{(2)}$
0	5000	1435
0. 05	3660	1730
0. 10	3530	2030
0. 20	3610	2620
0. 40	4150	3720
0. 60	4690	4540
0. 80	4980	4960
1. 00	4870	4880

(1) $\dfrac{P_r^{0.4}}{\mu^{0.8}}k = AT^{0.53}$

(2) $h = h_{\epsilon_m}$

As we anticipated, the temperature at $\epsilon = 0$ is limiting, but we also observe that the surface temperature drops very rapidly as ϵ becomes greater than zero. Since T_0 could be less if it were not for the region close to $\epsilon = 0$, we ask whether the sharp increase as $\epsilon \rightarrow 0^+$ is real. We recall that in a thermal entrance region that the heat transfer coefficient, h, is high and decreases to a constant value in 10 to 20 x/D's. If St is in the order of 0. 003, for a $4\,St\,L/D$ of 4, L/D is in the order of 300. Hence, x/D of 10 to 20 corresponds to an ϵ of 0. 03 to 0. 07 which is the same magnitude as ϵ for the sharp drop aft of T_s. Additionally, axial conduction may lead to a reduction of surface temperature in this region. Also, nuclear design might possibly make possible a power distribution that decreases more rapidly than a sine distribution as $\epsilon \rightarrow 0^+$. A reduced D in that region will also decrease the surface temperature by increasing h, i. e., as D is decreased G increases inversely as D^2 and hence DG increases inversely to the decrease in D. Hence, several potential fixes exist, such that, depending on a more detailed investigation, surface temperatures in the region $\epsilon = 0.05$ to 0.10 might be limiting and lower T_0 could be permitted. As we will see later, tolerance considerations may provide a further restraint.

We conclude that achievement of ratios of $[T_1 - T_0]/[T_{s_m} - T_0]$ closely corresponding to those for the exponential power distribution, even with complete freedom to tailor the axial power distribution, and with variations of fluid properties in the direction indicated here are not possible unless the ratio of T_1/T_0 is significantly smaller than the ones considered here, i. e., 10 to 20. Inlet temperature, depending on system design may be of concern as a design problem, i. e., prior to entering the reactor core heat equal to 5 to 10 percent of heat added within the core will have to be added to the fluid if conditions assumed here actually apply.

Words of caution include the fact that the heat transfer correlation used in the above discussion, while applicable to ANP reactors, was not validated for situations like the ones here. Also, the hydrogen property data representation may involve significant approximation since a pressure dependency will in general need to be included. Our objective has been to merely illustrate the nature of problems that require somewhat detailed investigation.

3. 4. 4. 5 Approximation For Heat Transfer Coefficient

In the generation of data above the following can be extracted

ϵ	$h_\epsilon / h_{\epsilon = 1}$	Underestimate of T_S By Using $h_{\epsilon = 1}$
0. 8	0. 95	40
0. 9	0. 97	13
1. 0	1. 0	0

Since we observe that generally ϵ_m will be greater than 0. 8 and probably approach 0. 9, little error will be involved in finding ϵ_m and T_{s_m} by evaluating h at $\epsilon = 1$, or for that matter by basing T_f on T_{s_m} and T_{b_1}.

3.4.4.6 Summary Comment

1. We anticipate an interest in low values of 4 St L/D from a void volume - pressure loss consideration
2. If we are interested in, for example, a value of 0.92 for $[T_1 - T_0]/[T_{s_m} - T_0]$, an α of 0.40 is required to limit 4 St L/D to 4
3. Depending on T_0, T_s at $\epsilon = 0$ may equal or exceed T_{s_m}, but design fixes may permit lower T_0. If not, larger values of 4 St L/D are required - as high as 7 if α is restricted to 0.25
4. Instead of letting the dimensionless length corresponding to the angle 0 to $\pi = 1.5$, a preferable procedure may be to choose that length and α such that $g(\epsilon)$ closely equals actual power in the region $\epsilon = 0.9$ to 1.0 and at $\epsilon = 0$, or some slightly larger value if warranted by a more detailed investigation
5. Moderate increases in the maximum surface temperature parameter are reflected in significant increases in the heat transfer parameter and hence the coolant configuration becomes "finer", i. e., L/D increases almost directly with heat transfer parameter since St varies only as $Re^{-0.2}$ for turbulent flow. ANP reactors and probably most reactors for nuclear rocket engines are characterized by turbulent flow for normal operation.

3.5 AVERAGE TUBE-PRESSURE DROP AND FLOW AREA

3.5.1 Introductory Comment

We have seen that the maximum surface temperature for the average tube is closely related to the internal tube diameter for a given active core length, L. Choice of L will be dominated by nuclear design considerations.

Identification of the number of tubes, and hence, total flow area, will involve considerations of reactor pressure drop, reactor discharge pressure, reactor inlet and exit gas temperatures, and to a small extent, longitudinal power distribution. Pressure drop equations can be coupled to the surface temperature equations if appropriate heat transfer-momentum analogies can be identified.

3.5.2 Rearrangement of Pressure Drop Equation

The pressure drop equation by Fox presented earlier can be rearranged to give

$$4\left[\frac{f}{2}\right]\frac{L}{D} = \frac{\phi_1\left(M_2, \frac{p_1}{p_2}\right) - \left[1 - \frac{T_{01}}{T_{02}}\right]}{b\left[1 - \frac{T_{01}}{T_{02}}\right] + \frac{T_{01}}{T_{02}}} \qquad (157)$$

where

$$\phi_1 = \frac{\left[\left(\frac{p_1}{p_2}\right)^2 - 1\right] - 2M_2^2 \ln \frac{p_1}{p_2}}{2\gamma_2 M_2^2 \left[1 + \frac{\gamma_2 - 1}{2} M_2^2\right]} \qquad (158)$$

As indicated earlier, b can be readily evaluated utilizing the appropriate integral involving $g(\epsilon)$. Using the sinusoidal representation we can readily compute values of b, i.e.

α	b
0.25	0.50
0.35	0.54
0.45	0.58

For purposes of illustration let us assume $b = 0.56$ and $T_{01}/T_{02} = 0.10$

Then

$$\phi_1\left(M_2, \frac{p_1}{p_2}\right) = 0.9 + 0.6\left[4\left(\frac{f}{2}\right)\frac{L}{D}\right] \tag{159}$$

$$= 0.9 + 0.6\left[4\ St\ \frac{L}{D}\right]\left[\frac{\frac{f}{2}}{St}\right]_A \tag{159a}$$

where $\left[\frac{\frac{f}{2}}{St}\right]_A$ can be evaluated from the appropriate analogy, e.g. the value is unity for Reynold's Analogy.

3.5.3 Heat Transfer Momentum Analogies

Typical ANP relationships, analogies if you will, yield

$$\frac{\frac{f}{2}}{St} = \frac{K_f\ 0.023\ Re^{-0.2}}{K_h\ 0.0205\ Re_f^{-0.2}\ Pr_f^{-0.6}} \tag{160}$$

where K_f and K_h allow for increases of friction factor and heat transfer coefficients, respectively, due to roughness and other perturbing influences such as structure and interstage gaps in concentric ring fuel elements. Typical values of K_f/K_h used in ANP design studies were 1.15 and 1.65 for ceramic and metallic reactors, respectively. Although evaluation of Reynolds number in the friction relationship, in general will be based on temperatures other than the mean fluid temperature, the effect was small for ANP reactors and generally neglected. In any case, the ratio of the two Reynolds numbers raised to the 0.2 power will closely approach unity near the reactor exit. For gases $Pr^{0.6}$ will be in the order of unity e.g., approximately 0.8 for air. Hence for Prandtl number of unity we can anticipate values for f/2 divided by St of unity or more. With ratios of K_f/K_h indicated above and $Pr^{0.6} = 0.8$ we can expect values of about 0.9 for very smooth tubes, about 1.05 in ANP ceramic reactors, and about 1.50 with interrupted surfaces and transverse struts. The actual value is a detailed design consideration that may require experimental verification.

We have now established that $\phi_1(M_2, p_1/p_2)$ varies linearly with 4 St L/D. For many heat transfer surfaces, even if the ratio of f/2 to St is a function of Reynolds number, appropriate ranges of interest can be identified such that the effect becomes small.

3.5.4 Flow Area Relationships

Let us now assume that values of M_2 greater than 0.3 are not of significant interest. We will assume that γ_2 is in the order of 1.4 and simplify the expression for ϕ into an approximate relationship. Further, we will anticipate an interest in pressure ratios of 1.2 to 1.3. The first term in the numerator is then 10 to 15 times the second and so we will let the second term be zero.

Compressible flow relationships permit us to replace the denominator with $G^2 \, R \, T_2/g_c \, p_2^2$. Substitution and rearrangement yield

$$\frac{(\Delta p)^2 + 2 \, p_2 (\Delta p)}{G^2 \frac{RT_2}{g_c}} = 0.9 + 0.6 \left[4 \frac{f}{2} \frac{L}{D}\right] \tag{161}$$

or the specific flow area

$$\frac{A_{ff}}{W} = \frac{1}{G} = \frac{1}{p_2} \sqrt{\frac{RT_2}{g_c}} \left[\frac{\left[0.9 + 0.6 \left[4 \, St \frac{L}{D}\right] \left[\frac{\frac{f}{2}}{St}\right]_A \right]}{\left[\frac{\Delta p}{p_2}\right]^2 + 2 \left[\frac{\Delta p}{p_2}\right]} \right]^{1/2} \tag{162}$$

where $\Delta p = p_1 - p_2$

We observe that the specific flow does increase as 4 St L/D and, hence the surface temperature parameter, is increased, For example, if 4 St L/D is increased from 4 to 8 the specific flow area increases by about 35 percent, compared to only a few percent increase in the surface temperature parameter. Alternately an increase in p_2 of about 35 percent, or an increase in $\Delta p/p_2$ of about 60 percent ($\Delta p/p_2$ initially equal 0.3) is required to maintain the original flow area.

The parameter, Δp, plus other system pressure drops, will be proportional to the pumping power required. The reactor Δp will also be a significant parameter in the mechanical design of the reactor.

The effect of increasing 4 St L/D is to decrease Reynolds number because D will decrease. Decreases in G, i.e., increases in specific weight flow also cause Reynolds number to decrease. Hence, increases in 4 St L/D has a double effect in decreasing Reynolds numbers.

3.6 AVERAGE TUBE-INTERNAL TEMPERATURE DIFFERENCES

We have already derived the relationship for the temperature difference between the outer and inner surfaces of a hollow heat generating cylinder, and will now rearrange the equations with the substitution of some different parameters.

Recall that

$$\frac{4k(T_2 - T_1)}{q''' r_1^2} = 1 - \frac{r_2^2}{r_1^2}\left[1 - \ln\left(\frac{r_2^2}{r_1^2}\right)\right] \qquad (163)$$

In many nuclear reactors the internal surface of the fuel element will be coated or clad with a material of thickness t_{cl}. Although the internal heating rate will be relatively low, and in general, the thickness small relative to the fueled body, the temperature drop may be significant because of the high heat flux imposed at the outer surface.

For the clad we will utilize temperature equations for a slab, i.e., we will consider that the radius ratio is close to one. Hence

$$\Delta T_{cl} = T_1 - T_s = \frac{q'''_{cl} t_{cl}^2}{2k_{cl}} - t_{cl}\left[\frac{dT}{dr}\right]_{cl_1} \qquad (164)$$

where s is the inside surface of the clad that is in contact with the flowing gas and 1 is the outside surface of the clad.

Now

$$\left[\frac{dT}{dr}\right]_{cl_1} = -\left[\frac{Q}{A}\right]_1 \frac{1}{k_{cl}} \qquad (165)$$

Assuming that Q/A accounts for all heat generated in the fueled body

$$-\frac{q}{A} = \frac{q'''_F \pi \left[r_2^2 - r_1^2\right] dx}{2\pi r_1 \, dx} \qquad (166)$$

Hence

$$[T_1 - T_s]_{cl} = \frac{q'''_{cl}\, t^2_{cl}}{2k_{cl}} + \frac{t_{cl}\, r_1\, q'''_F}{2k_{cl}} \left[\frac{r_2^2}{r_1^2} - 1\right] \tag{167}$$

$$[T_2 - T_1]_F = \frac{q'''_F\; r_1^2}{4k_F} \left[1 - \frac{r_2^2}{r_1^2}\left[1 - \ln\left(\frac{r_2^2}{r_1^2}\right)\right]\right] \tag{168}$$

We now assume $T1_{cl} = T1_F$, i.e., no thermal resistance at the interface, we change identification of $T2$ to T_i (for internal), we add to eliminate T_1

$$T_i - T_s = \left[\frac{q'''\; r_1^2}{4k}\right]_F \left[1 - \frac{r_2^2}{r_1^2}\left[1 - \ln\left(\frac{r_2^2}{r_1^2}\right)\right] + 2\,\frac{t^2_{cl}}{r_1^2}\,\frac{k_F}{k_{cl}}\,\frac{q'''_{cl}}{q'''_F} + 2\,\frac{t_{cl}}{r_1}\,\frac{k_F}{k_{cl}}\left[\frac{r_2^2}{r_1^2} - 1\right]\right] \tag{169}$$

In subsequent manipulations we will assume the second term involving q'''_{cl}/q'''_F is negligibly small.

We will now relate q''' to flow conditions

$$q'''_F\,(\epsilon) = \frac{W\, C_{p_m}\,[T_1 - T_0]\, g(\epsilon)}{\pi\left[r_2^2 - r_1^2\right] L} \tag{170}$$

but

$$W = G\, A_{ff} = \frac{\pi}{4}\, D^2\, G \tag{171}$$

$$\left[\frac{T_i - T_s}{T_1 - T_0}\right] = \left[\frac{G\, D^2\, C_{pm}\, g(\epsilon)}{4k_F\,[4L]}\right] \phi_2 \tag{172}$$

where $\phi_2 = \phi\left(\frac{t_{cl}}{r_1}, \frac{r_2}{r_1}, \frac{k_F}{k_{cl}}\right)$

$$\phi_2 = -1 + \frac{\ln\left(\frac{r_2^2}{r_1^2}\right)}{\left[1 - \frac{r_1^2}{r_2^2}\right]} + 2\frac{k_F}{k_{cl}}\left[\frac{\frac{2t_{cl}}{D}}{1 + \frac{2t_{cl}}{D}}\right] \tag{173}$$

$$g(\epsilon_m) = C_1 \frac{\lambda}{[\lambda^2 + 1]^{1/2}} \tag{174}$$

where $\lambda = \dfrac{\frac{\pi}{1.5}}{4\,\mathrm{St}\frac{L}{D}}$

$$C_1 = \frac{\frac{\pi}{1.5}}{\cos\left(\frac{\pi}{1.5}\alpha\right) - \cos\left(\frac{\pi}{1.5}[\alpha + 1]\right)} \tag{175}$$

The denominator in the expression for $g(\epsilon_m)$ approaches unity as 4 St L/D increases, e.g., for 4 St L/D = 5 the value is about 1.04. The denominator in the expression for C_1 only varies from 1.73 to 1.58 as α varies from 0.25 to 0.45. Hence, we will approximate $g(\epsilon_m)$,

$$g(\epsilon_m) = \frac{2.7}{\left[4\,\mathrm{St}\frac{L}{D}\right]} \tag{176}$$

We can replace

$$\frac{D^2}{4[4\,L]} \text{ with } \frac{L\,\mathrm{St}^2}{\left[4\,\mathrm{St}\frac{L}{D}\right]^2} \tag{177}$$

We can replace G with $G_c\ A_c/A_{ff}$ where A_c is the frontal area of the core and G_c is the mass flow per unit of core frontal area. The frontal area of the core can be viewed as including,

A_{ff} = flow area
A_{cl} = clad area
A_F = fueled material area
A_s = area of structure, other components, and nonuseable void among components.

Let $A_{ff} + A_{cl} + A_F = A_T$, i.e., area of tubes

Then
$$\frac{A_{ff}}{A_c} = \frac{A_{ff}\,A_T}{A_T\,A_c} \tag{178}$$

Finally, for our assumption regarding $g(\epsilon)$,

$$\frac{T_i - T_s}{T_1 - T_0} = \left[\frac{3.4\,\frac{W_T}{D_c}\,St^2}{\left(4\,St\,\frac{L}{D}\right)^3}\right]\left[\frac{C_{p_m}}{k_F}\right]\phi_3 \tag{179}$$

where
$$\cancel{\phi_3 = \frac{L\,A_{ff}\,A_T}{D_c\,A_T\,A_c}\phi_2} \quad \phi_3\ \frac{L}{D_c}\,\frac{A_T}{A_{ff}}\,\frac{A_c}{A_T}\,\phi_2 \tag{180}$$

Some comments on the above are

1. The function ϕ_3 will be determined by nuclear and mechanical design considerations.
2. The value of 4 St L/D appears as a significant parameter in reducing this temperature ratio.
3. Increasing the core diameter decreases the temperature ratio.
4. Increasing the thermal conductivity of fueled material decreases the temperature ratio.
5. The Stanton number, St for a smooth tube varies to a small degree with Reynolds number. It can be increased by utilizing roughened surfaces or surfaces that increase the amount of turbulence. This might be desirable to reduce the L/D ratio, and hence the number of tubes, but as can be seen, would increase this temperature difference markedly.
6. Instead of this parameter controlling the design, temperature differences that bear on the thermal stress level, may be more limiting. For example, the pertinent temperature difference

might be the difference between a mean temperature and a surface temperature. Hence, a design relationship like the above might evolve, but would have some different expression for ϕ_2 and might be evaluated at a different combination of $g(\epsilon)$ and temperature level.

7. Our stated objective was to investigate ratio of $[T_{s_m} - T_0]/[T_i - T_0]$. We have evaluated $T_i - T_s/T_1 - T_0$. They are related by

$$\frac{T_{s_m} - T_0}{T_i - T_0} = \frac{1}{\left[\frac{T_i - T_{s_m}}{T_1 - T_0}\right]\left[\frac{T_1 - T_0}{T_{s_m} - T_0}\right] + 1} \tag{181}$$

Hence, if we want $[T_{s_m} - T_0]/[T_i - T_0]$ to be 0.98 and $[T_1 - T_0]/[T_{s_m} - T_0]$ to be about 0.92 $[T_i - T_{s_m}]/[T_1 - T_0]$ must equal 0.022, which is approximately the same value as for ANP reactors.

3.7 NON-AVERAGE TUBE TEMPERATURES

3.7.1 Effect of Non-Average Tube Power

We will compare an average tube with a non-average tube in which more than average heat is released to the fluid. If the flow rates were the same the temperature increase of the fluid as it flows through the tube would be in direct proportion to the heat release. This would be the behavior with an incompressible fluid.

With compressible flow as the temperature increases the ratio of pressure to density also increases. Typically, flow from all tubes of a reactor core exit into a common plenum, such that the pressure at the exit tends to be the same for all tubes. Hence, the density must decrease and for the mass flow, ρV, to remain constant the velocity, V, must increase. This means that the dynamic pressure, $[\rho V]V$ increases, and since pressure drop tends to be proportional to the dynamic pressure, the inlet pressure would have to be higher. In general, the flow also enters the reactor from a plenum, the same pressure drop is imposed on all tubes, and the mass velocity decreases. Hence, the temperature rise across the over-powered tube is increased by a greater percentage than the imposed change in heat release.

For conditions considered here, the mass flow change will be about 60 percent of the imposed power change, while the change in the temperature rise will be about 160 percent, i.e. if the heat release in the over-powered tube is one percent greater than for the average tube, the temperature rise will be 1.6 percent greater than average and the flow will be 0.6 percent less.

That the above effects are correct for turbulent flow can be shown by computational results from digital computer calculations for compressible flow, or can be estimated from approximate equations that can be derived by using pressure drop equations such as we used earlier. Such equations show that effects depend on the magnitude of

$$4\left[\frac{f}{2}\right]\frac{L}{D}$$

the power distribution parameter, b, the fluid temperature ratio, T_{o2}/T_{o1}, and upon m, the exponent applied to Reynolds number in typical relationships for friction factor, i.e.

$$f = \frac{C}{R_e^{\,m}} \qquad (182)$$

The values suggested above are of the correct magnitude for turbulent flow, wherein m is approximately 0.2 for smooth tubes. For rough tubes m will generally be less than 0.2 and the effects will be slightly less.

We can now think of temperature effects caused by tube characteristics that are either constant with axial distance, or that are averaged over the length. Consider that the non-average tube is characterized exactly as the average tube except for the total heat release. If we assume that even with heat exchange between adjacent tubes, heat release equal to 2 percent more than for the average tube is possible, we can write

$$\frac{[T(\epsilon) - T_o]_{avg}}{[T(\epsilon) - T_o]_{max}} = \frac{1}{1 + [0.02]\,[1.6]} = 0.97 \tag{183}$$

Actually, if the longitudinal power distribution is different this ratio will vary with axial distance fraction,

3.7.2 Film Temperature Difference

In addition to gross or full tube effects, local effects can cause the film temperature difference to be greater than for the average tube. These effects include differences in power and dimensions relative to those for the average tube. By utilizing a heat transfer correlation for turbulent flow like the one used in the ANP program and neglected effects of temperature dependency of fluid properties, we can write

$$dq = [P\,dx]\;h\;[T_s - T_b] \tag{184}$$

$$h = C_1\,G^{0.8}\,D^{0.8} \tag{185}$$

$$= C_1\,\frac{W^{0.8}}{A_{ff}^{\;0.8}}\;D^{0.8} \tag{186}$$

$$T_s - T_b = \frac{\frac{dq}{dx}}{Ph} \tag{187}$$

$$= \frac{\frac{dq}{dx}}{\frac{A_{ff}}{D}\;\frac{W^{0.8}}{A_{ff}^{\;0.8}}\;D^{0.8}} \tag{188}$$

$$= \frac{\left[\frac{dq}{dx}\right] D^{0.2}}{W^{0.8} \; A_{ff}^{0.2}} \tag{189}$$

$$= \frac{\frac{dq}{dx}}{W^{0.8} \; D^{0.2}} \tag{190}$$

Now consider

$$\frac{dq}{dx} = C_2 \, q''' \, A_F \tag{191}$$

$$= C_3 \, P \, g(\epsilon) \, A_F \tag{192}$$

where

P = tube power.

Finally,

$$T_s - T_b = \frac{P \, g(\epsilon) \, A_F}{W^{0.8} \; D^{0.2}} \tag{193}$$

wherein, several constants have been omitted.

We can now form the ratio

$$\frac{[T_s - T_b]_{avg}}{[T_s - T_b]} = \frac{[P \, g(\epsilon)]_{avg}}{P \, g(\epsilon)} \left[\frac{W}{W_{avg}}\right]^{0.8} \left[\frac{A_{F\,avg}}{A_F}\right] \left[\frac{D}{D_{avg}}\right]^{0.2} \tag{194}$$

Several things can be observed in the above equation. For a given mass flow ratio the temperature ratio is fairly insensitive to the diameter ratio. The film temperature difference is less sensitive to the mass flow ratio than is the effect on fluid temperatures discussed earlier.

3.7.3 Maximum Calculated Surface Temperature

Assume perfect dimensions and consider only power distribution effects. We observed earlier that the effect on weight flow was only about 60 percent of the imposed power effect. Approximately,

$$\frac{W}{W_{avg}} = \left[\frac{P_{avg}}{P}\right]^{0.6} \qquad (195)$$

and

$$\frac{[T_s - T_b]_{avg}}{[T_s - T_b]} = \left[\frac{P_{avg}}{P}\right]^{1 + [0.6][0.8]}$$

$$= \left[\frac{P_{avg}}{P}\right]^{1.5} \qquad (196)$$

Since approximately

$$\frac{[T_1 - T_0]_{avg}}{[T_1 - T_0]} = \left[\frac{P_{avg}}{P}\right]^{1.6} \qquad (197)$$

We can say that approximately

$$\frac{[T_{sm} - T_0]_{avg}}{[T_{sm} - T_0]_{mc}} = \left[\frac{P_{avg}}{P}\right]^{1.6} \qquad (198)$$

Finally, for $\frac{P}{P_{avg}} = 1.02$ (199)

$$\frac{[T_{sm} - T_0]_{avg}}{[T_{sm} - T_0]_{mc}} = 0.97 \qquad (200)$$

The above assumes that the maximum calculated temperature occurs at the same ϵ_m as the maximum temperature for the average tube and that the longitudinal power distributions are the same. Actually, as we observed in Section 1.0 there can be significant variations in axial power distributions. Consider the position $\epsilon = 0$. If $\frac{g(\epsilon)_{avg}}{g(\epsilon)}$ should be 0.9 and it is desired that the tube with this factor have a maximum calculated temperature at $\epsilon = 0$ equal to that for ϵ_m, it would be necessary that $g(0)_{avg}$ be 0.9 of the value required to yield a temperature equal to T_{sm} for the average tube. Effects of fluid dependent properties would have to be accounted for as an additional effect. As indicated earlier, radial variation of $g(\epsilon)$ near $\epsilon = 0$ may impose a restriction on selection of inlet fluid temperature and on the selection $g(\epsilon)$ for the average tube.

3.7.4 Maximum Surface Temperature

We now consider effects that are random, i.e. tolerances and uncertainties.

3.7.4.1 Full Tube Effects

We estimated that a measured excess of power of 2 percent relative to measured flow would give a temperature ratio of 0.97. In addition there may be an uncertainty in the measured value, say one percent, and in flow distribution of one percent. For both allow for possible temperature factor of 0.97.

In addition to power and flow effects, full tube effects due to hole diameter may influence the temperatures. Let us assume that tubes or groups of tubes may be undersize by about 0.5 to 1.0 percent and that the corresponding temperature parameter would be 0.97.

3.7.4.2 Local Effects

The primary additional effect to be considered is that represented by

$$\frac{g(\epsilon)_{avg}}{g(\epsilon)} \quad \frac{A_{F\,avg}}{A_F}$$

in the equation for $\frac{[T_s - T_b]_{avg}}{[T_s - T_b]}$

In the essence this grouping accounts for the actual number of fissions in a differential length of a tube relative to the same value for the average tube. Hence, it depends on the product of local neutron flux and number of fissionable atoms.

The local flux predictions may be uncertain, say by about 2 percent. The number of fissionable atoms locally depends on fabrication control, and may be thought of in terms of control on cross sectional area, density, fuel concentration, and enrichment. Let us assume that this whole grouping can be controlled within 10 percent and that the film temperature difference is about 20 percent. Our over-all temperature parameter would then be 0.98. Let us also lump heat transfer correlation, computational, and other uncertainties into another temperature parameter of 0.98, i.e. a 10 percent effect on film temperature difference.

3.7.4.3 Combined Effects

We will here perform a very crude summation of effects to indicate design procedures in a very general way.

Effect	Temperature Parameter	1 - Temperature Parameter
Full Tube		
Power & Flow	0.97	0.03
Hole Diameter	0.97	0.03
Local		
Power per Unit Length	0.98	0.02
Uncertainties, Heat Transfer, etc.	0.98	0.02
Combined Effect	0.90	0.05 (0.95)

In the first column the combined effect is simply the product of the individual factors. In the second column we took a simple statistical sum of incremental temperature effects, i.e. the square root of the sum of the squares. Normally, the first approach is considered far too pessimistic. The second approach is considered more realistic, but does involve many detailed questions, e.g. identification of mutually exclusive factors, and identification and handling of distributions. Appropriateness of that method has generally been verified by operation of reactors and in-pile tests of fueled assemblies. Because of difficulty of making accurate measurements of the local hot spot temperature, verification can never be absolute, i.e. experimental measurements may still leave uncertainties in the order of one percent.

In general, the approach in combing effects will be to arrive at a hot spot temperature prediction so defined that statistically only a few tubes can be predicted to exceed that temperature. In homogeneous reactors as discussed here, the temperature as predicted will be reduced by heat transfer to the immediate surroundings. For our purposes let us assume that the excess is reduced by about 1/3 and reason that the reduction will be even greater in areas that exceed the quoted hot spot temperature. Hence, instead of 0.95 for the temperature parameter we will take 0.97.

3.8 SUMMARY

In Section 3.2 we tabulated temperature ratios for typical ANP reactors. We than postulated temperatures for a nuclear reactor for use in a rocket engine, i.e. inlet gas temperature $0^{\circ}F$, exit gas temperature $4000^{\circ}F$, and fuel element hot spot temperature, $5000^{\circ}F$. In other words, we asked whether a ratio of gas temperature rise to the hot spot temperature less the inlet gas temperature could approach 0.80. In subsequent discussions we have found that we cannot provide a specific answer until nuclear, thermal, and mechanical design considerations and restraints are integrated into an over-all reactor design.

We can, however, tentatively conclude that our distribution of the difference between hot spot temperature and the exit gas temperature among the several temperature difference ratios is reasonable. No reactor thermal design problem, per se, has been identified that will preclude the achievement of the 0.8 value for the over-all ratio. Rather, we anticipate that the value of the over-all temperature ratio that will evolve in an actual reactor design will depend to a large extent on costs, i.e. cost of accurately measuring power and flow distributions, and costs of fabricating components, both accurately and with required operating reliability. Costs of obtaining higher temperature ratios will, of course, have to be weighed against worth of gains in system performance.

In the way of summary we will simply restate the temperature ratios we assumed initially and recall relationships with pertinent design parameters.

(1) $\frac{\Delta T_R}{\Delta T_C}$ We set as our goal a value of 0.99. Achievement of that high a value probably requires that all non-active core components be cooled by the fluid prior to its entrance into the active core. This factor also must account for unwanted leakage, e.g. one percent with no heat addition, or several percent with significant heat addition.

(2) $\frac{\Delta T_C}{\Delta T_{W_{avg}}} = \frac{T_1 - T_0}{[T_{sm} - T_0]_{avg}}$ Value of this parameter depends on power distribution, $g(\epsilon)$ and the heat transfer parameter, $4\ St\frac{L}{D}$. As an example we considered a sinusoidal power distribution with the amount of forward translation indicated by the value of a parameter, α , or more specifically α - 0.25. For values of α in the range of 0.40 to 0.45, i.e. g(1) in the range of 0.1 to 0.2, our objective for $\frac{\Delta T_C}{\Delta T_{W_{avg}}}$ of 0.92 can be obtained with $4\ St\frac{L}{D}$ values of about 5. For smaller values of α , i.e. less forward power shifting, the required value of $4\ St\frac{L}{D}$ increases rapidly. Assuming St is about 0.003, $\frac{L}{D}$ is in the order of 400 for a $4\ St\frac{L}{D}$ of 5, i.e. for a 40 inch long core the hole diameter would be 0.100 inch.

Increases of $4\ St\frac{L}{D}$ lead to a requirement for many small tubes which complicates fabrication problems. For example, a $4\ St\frac{L}{D}$ of 8 in a 20 inch long core would correspond to a hole diameter of only about 0.030 inch. We observe that as $\frac{\Delta T_C}{\Delta T_{W_{avg}}}$ is increased, the value of forward power peaking becomes increasingly important relative to the effect on the required $4\ St\frac{L}{D}$.

(3) $\frac{\Delta T_{W_{avg}}}{\Delta T_{W_{calc}}}$ This ratio is a measure of the success of radial temperature flattening efforts, and also must account for changes in radial power with operating life. Achievement of our tentative goal of 0.95 requires a match of tube power to flow of within about 3 percent. Successful achievement requires that local power anytime during the operating life, i.e. any control element postion, must be limited to 2 percent or less greater than average, and that temperature flattening techniques, i.e. fuel concentration, or hole size variation, be applied in many small radial increments.

(4) $\frac{\Delta T_{W_{calc}}}{\Delta T_{W_{avg}}}$ Achievement of higher values depends on reducing measurement and calculation uncertainties, and reducing fabrication tolerances. With moderate improvements relative to ANP accomplishments a value of 0.95 should be approachable.

(5) $\frac{\Delta T_{W_m}}{\Delta T_{C_m}}$ We found that the internal temperature difference within the wall is controlled by many parameters. One of the dominant areas is the void fraction that evolves in the the nuclear design. Another is the convective heat transfer parameter, $4\,St\,\frac{L}{D}$; we see that the temperature difference is reduced as $4\,St\,\frac{L}{D}$ is increased, i.e. as the core is more finely subdivided. Finally, we recognize that analogous relationship involving temperature differences that enter into thermal stress equations may be more controlling than the temperature difference.

BIBLIOGRAPHY

1. Carslaw, H.S. and Jaeger, J.C., "Conduction of Heat in Solids", London, England, Oxford University Press, 1959.

2. "Comprehensive Technical Report - General Electric Direct-Air-Cycle Aircraft Nuclear Propulsion Program", GE-ANPD, 1962.
   - APEX-904 Heat Transfer Reactor Experiment No. 1
   - APEX-905 Heat Transfer Reactor Experiment No. 2
   - APEX-906 Heat Transfer Reactor Experiment No. 3
   - APEX-907 XMA-1 Nuclear Turbojet
   - APEX-908 XNJ140E Nuclear Turbojet
     - Part A, Section 2, Precedent Design Studies
     - Part B, Section 4, Reactor
   - APEX-919 Aerothermodynamics

3. Eckert, E.R., "Heat and Mass Transfer", New York, McGraw-Hill Book Co, Inc., 1959.

4. "Gas-Cooled High Temperature Nuclear Reactor Design Technology", GE-ANPD, APEX-800, 1962.
   - Part A- 1. Introduction
     - 2. Influence of Performance Requirements on Power Plant Component Specifications
     - 3. Reactor Design
   - Part B- 4. Cellular Metallic Fuel Reactors
   - Part C- 5. Ceramic Reactors
   - Part E- 7. Shield Design

5. Glasstone, S., "Principles of Nuclear Reactor Engineering", Princeton, New Jersey, D. Van Nostrand Co., Inc., 1955.

6. Jakob, M., "Heat Transfer", Volume I, New York, John Wiley & Sons, Inc.

7. Kays, W.M. and London, A.L., "Compact Heat Exchangers", Palo Alto, California. The National Press, 1955.

8. Knudson, J.G. and Katz, D.L., "Fluid Dynamics and Heat Transfer", New York, McGraw-Hill Book Co., Inc., 1958.

9. Lapides, M.E. and Goldstein, M.B "Heat Transfer Source File Data", GE-ANPD, APEX-425.

10. McAdams, W. H., "Heat Transmission", New York, McGraw-Hill Book Co., Inc., 1954.
11. Prickett, W. Z., "General Reactor Sizing Techniques, Volume I, Aerothermodynamic Optimization", GE-ANPD, APEX-723A, 1961.
12. Schneider, P. J., "Conduction Heat Transfer", Cambridge, Mass., Addison-Wesley Publishing Co., Inc., 1955.
13. Shapiro, A. H., "The Dynamics and Thermodynamics of Compressible Fluid Flow", Volume I, New York, The Ronald Press Company, 1953.